Institut für Tierwissenschaften, Abteilung Tierzucht und Tierhaltung
der Rheinischen Friedrich-Wilhelms-Universität Bonn

Transcriptome analysis using RNA-Seq on response of respiratory cells infected with porcine reproductive and respiratory syndrome virus (PRRSV)

Inaugural-Dissertation

zur

Erlangung des Grades

Doktor der Agrarwissenschaften

(Dr. agr.)

der

Landwirtschaftlichen Fakultät

der

Rheinischen Friedrich-Wilhelms-Universität Bonn

von

Maren Julia Pröll

aus Bonn

Referent:	Prof. Dr. Karl Schellander
Korreferent:	Prof. Dr. Heinz-Wilhelm Dehne
Tag der mündlichen Prüfung:	12. September 2014
Erscheinungsjahr:	2014

Dedicated to my family

Meiner Familie

Transcriptome analysis using RNA-Seq on response of respiratory cells infected with porcine reproductive and respiratory syndrome virus (PRRSV)

The porcine reproductive and respiratory syndrome (PRRS) is one of the most important viral diseases of the swine industry worldwide (Balasuriya 2013). Its aetiological agent is the PRRS virus (PRRSV) (Balasuriya 2013, Conzelmann et al. 1993). The understanding of the genetic elements and functions, involved in the response to PRRSV and the comprehension of the changes in the global transcriptome profile post infection, remain still unclear.

Main objectives of this thesis are to characterize the global transcriptome profile of PRRSV infected lung DCs, by using the RNA-Sequencing (RNA-Seq), to improve the understanding of genetic components in the response to PRRSV as well as to determine the changes in the expression profile in different respiratory cells post PRRSV infection.

Six female 30 days old piglets of two different porcine breeds (Pietrain and Duroc) were selected, PAMs, lung DCs and trachea epithelial cells were isolated and infected with the European prototype PRRSV strain Lelystad virus (LV). Non-infected (0 h) and infected (3, 6, 9, 12, 24 hpi) lung DCs, PAMs and trachea epithelial cells as well as cell culture supernatants were collected. Non-infected and infected lung DCs of both breeds were used for RNA-Seq. The sequence alignment was done with the reference genome build Suscrofa 10.2 and with the complete genome of LV strain.

The transcriptome analysis of PRRSV infected lung DCs of Pietrain and Duroc resulted in an amount of 20,396 porcine predicted gene transcripts. The virus sequence alignment exhibited that the LV strain was able to infect lung DCs and to replicate there. Not only breed-differences post PRRSV infection in the virus growth, also breed-differences in the cytokine concentrations as well as in the detected mRNA expression profiles and in the differently expressed genes were identified. Beside these breed-dependent differences, cell-type dependent differences in the response to PRRSV were characterized. 37 clusters for Pietrain and 35 clusters for Duroc and important pathways were identified.

This thesis is the first comprehensive study that described the transcriptome profile of two different breeds post PRRSV infection, especially of infected lung DCs. The main findings of the investigations showed that the virus-host interaction was different for the various respiratory cell-types and that the gene expression trends proceeded contrarily for both breeds during the first time points after infection. Additionally, key clusters, key pathways and specific gene transcripts were identified.

Transkriptom-Analyse mittels RNA-Seq von respiratorischen Zellen nach deren Infektion mit dem Porcinen Reproduktiven und Respiratorischen Syndrom Virus (PRRSV)

Das Porcine Reproduktive und Respiratorische Syndrom (PRRS) ist eine der wichtigsten viralen Erkrankungen in der weltweiten Schweineindustrie (Balasuriya 2013). Das PRRS Virus (PRRSV) ist der ätiologische Erreger (Balasuriya 2013, Conzelmann et al. 1993). Die Einflussnahme von genetischen Elementen und Funktionen auf die Reaktion auf PRRSV sowie die Veränderungen im Transkriptomprofil nach einer Infektion sind noch unklar.

Hauptziele dieser Dissertation sind, das globale Transkriptomprofil von PRRSV infizierten Lungen-DCs mittels RNA-Sequenzierung (RNA-Seq) zu charakterisieren, das Verständnis über die Einflüsse von genetischen Komponenten auf die Reaktion auf PRRSV zu verbessern und die Veränderungen im Expressionsprofil von unterschiedlichen respiratorischen Zellen nach der Virusinfektion zu ermitteln.

Sechs weibliche, 30 Tage alte Ferkel von zwei unterschiedlichen Schweinerassen (Piétrain und Duroc) wurden ausgewählt. Aus deren Lungen wurden PAMs und DCs sowie Epithelzellen aus deren Trachea isoliert. Anschließend wurden diese Zellen mit dem europäischen PRRSV Stamm Lelystad Virus (LV) infiziert. Nicht-infizierte (0 h) und infizierte (3, 6, 9, 12, 24 hpi) Lungen-DCs, PAMs und Trachea-Epithelzellen wie auch deren Zellkulturüberstände wurden gesammelt. Zur RNA-Seq wurden nicht-infizierte und infizierte Lungen-DCs beider Schweinerassen eingesetzt. Das Sequenzalignment erfolgte mit dem Referenzgenombild Suscrofa 10.2 und mit dem kompletten Genom des LV Stammes. Die Transkriptom-Analyse von PRRSV infizierten Piétrain und Duroc Lungen-DCs erkannte 20.396 porcine Gentranskripte. Das Virus Sequenzalignment zeigte, dass der LV Stamm sowohl Lungen-DCs infizieren als auch sich dort replizieren kann. Nach der PRRSV Infektion konnten Rassenunterschiede festgestellt werden, sowohl beim Viruswachstum als auch in den Cytokinkonzentrationen sowie in identifizierten mRNA Expressionsprofilen und bei den unterschiedlich exprimierten Genen. Zudem konnten Reaktionsunterschiede auf PRRSV in den verschiedenen respiratorischen Zelltypen charakterisiert werden. Es wurden 37 Cluster für Piétrain, 35 für Duroc sowie wichtige Pathways identifiziert.

Diese Dissertation ist die erste umfassende Studie, die das Transkriptomprofil von PRRSV infizierten Lungen-DCs zweier unterschiedlicher Schweinerassen beschreibt. Als Hauptergebnisse zeigten die Untersuchungen, dass die Virus-Wirts-Interaktionen für die verschiedenen respiratorischen Zellen unterschiedlich verliefen und dass die Genexpressionstrends beider Rassen während der ersten Zeitpunkte nach der Infektion verschieden waren. Zusätzlich konnten Schlüssel-Cluster, Schlüssel-Pathways und spezifische Gentranskripte identifiziert werden.

Contents **page**

List of figures **page**

List of tables **page**

Appendix (List of tables) **page**

Appendix (List of figures) **page**

List of abbreviations

Acc no	Accession number
AM	Alveolar macrophages
APC	Allophycocyanin
APCs	Antigen-presenting cells
BAM	Binary Alignment/Map
BIC	Bayesian information criterion
bp	Base pair
CD	Cluster of differentiation
cDCs	Conventional DCs
CDPs	Common DC precursors
cDNA	Complementary DNA
CK	Cytokeratin
C_T	Comparative threshold cycle
CPE	Cytophathic effect
CTLs	Cytotoxic T cells
DAPI	4', 6'- diamidino-2-phenylindole
DCs	Dendritic cells
ddH_2O	Double-distilled water
DMEM	Dulbecco's Modified Eagle Medium
DMSO	Dimethyl sulfoxide
DNA	Deoxynucleic acid
dNTPs	Deoxyribonucleoside triphosphate
DPBS	Dulbecco's Phosphate-Buffered Saline
dpi	Days post infection
DTCS	Dye Terminator Cycle Sequencing
DTT	Dithiothreitol
Du	Duroc
E	Envelope glycoprotein
EDTA	Ethylenediaminetetraacetic acid
e.g.	For example

ELISA	Enzyme-linked immunosorbent assay
ER	Endoplasmic reticulum
F	Forward
FBS	Fetal Bovine Serum
FDR	False discovery rate
FITC	Fluorescein isothiocyanate
GM-CSF	Granulocyte macrophage-colony-stimulating factor
GP	Glycoproteins
H_2O	Water
HCl	Hydrochloric acid
hpi	Hours post infection
HSD	Honest Significant Difference
HSCs	Hematopoietic stem cells
IF	Immunofluorescence
IFA	Immunofluorescence assay
IgG	Immunoglobulin G
ISGs	IFN-stimulated genes
IM	Interstitial macrophages
kb	Kilobases
KCl	Potassium Chloride
KEGG	Kyoto Encyclopedia of Genes and Genomes
LPS	Lipopolysaccharides
LT	Low-Thoughput
LV	Lelystad virus
M	Matrix protein
MDDCs	Monocyte-derived DCs
MDPs	Macrophage and DC precursors
mg	Milligram
MHC	Major histocompatibility complex
min	Minute
MLV	Modified-live virus vaccines
ml	Millilitres

MOI	Multiplicity of infection
mRNA	Messenger RNA
MTT	Thiazolyl Blue Tetrazolium Bromide
N	Nucleocapsid protein
NaCl	Sodium chloride
NaOH	Sodium hydroxide
NCBI	National center for biotechnology information
NEAA	Non-Essential Amino Acids
ng	Nanogram
NGS	Next generation sequencing
no	Number
NSPs	Non-structural proteins
µg	Microgram
µl	Microliter
°C	Degree celsius
OD	Optical density
ORFs	Open reading frames
P	Primer
PAM	Pulmonary alveolar macrophages
PAMPs	Pathogen-associated molecular patterns
PCR	Polymerase chain reaction
pDCs	Plasmacytoid DCs
PE-Cy7	Phycoerythrin and a cyanine dye 7
PFU	Plaque-forming units
Pg	Picogram
pH	pH value
Pi	Pietrain
pp	Polyproteins
preDCs	Precursor DCs
PRRs	Pattern-recognition receptors
PRRS	Porcine reproductive and respiratory syndrome
PRRSV	Porcine reproductive and respiratory syndrome virus

qRT-PCR	Quantitative real-time reverse transcriptase polymerase chain reaction
QTL	Quantitative trait loci
R	Reverse
RBC	Red Blood Cell
RdRp	RNA-dependent RNA polymerase
RLRs	RIG-I like receptors
RNA	Ribonucleic acid
RNA-Seq	RNA-Sequencing
rpm	Rounds per minute
RT	Room temperature
RTC	Replication and Transcription Complex
SAGE	Serial Analysis of Gene Expression
SAM	Sequence Alignment/Map
sec	Second
Seq	Sequencing
Sn	Sialoadhesin
SNP	Single nucleotide polymorphisms
ss	Single-stranded
SSC	swine chromosome
TAE	Tris-acetate buffer
TCRs	T cell receptors
T_H1	Type 1 helper
T_H2	Type 2 helper
TIR	Toll/IL-1 receptor
TLRs	Toll-like receptors
UTR	Untranslated region
ZO-1	Zonula occludens protein
4PL	4 Parameters Logistic

A list of abbreviations of gene transcript and protein names are listed in the appendix (Table A1).

1 Introduction

In November 2013 the federal statistical office of Germany published a report about livestock status for Germany and listed 27,900 pig farms which keep in total 28,1 million animals, this is a growth of approximately 10 % in relation to the situation of 2001 (Statistisches-Bundesamt 2010, 2014). In parallel, the application of medications in animal production let to an increasing criticism because of the possible formations of multi-resistant germs (BMEL 2011, Niggemeyer 2012).

In 2006 growth promoters were legally prohibited in Europe. Nationwide vaccination of mycoplasma, of circovirus and partially of porcine reproductive and respiratory syndrome (PRRS) helped to improve the health status in fattening pigs. These processes reduced the risks of animal losses and allowed smaller applications of medications (Niggemeyer 2012). Higher densities in closed environments and the increasing herd sizes improved the possibility of transmission for airborne pathogens. Consequently in the modern swine production, respiratory diseases are the most serious disease problem (Brockmeier et al. 2002, reviewed by Sørensen et al. 2006).

One of the most important viral diseases of the swine industry worldwide is PRRS (Balasuriya 2013). Its aetiological agent is the PRRS virus (PRRSV) (Balasuriya 2013, Conzelmann et al. 1993). This syndrome costs the global swine industry significant production losses, leads to poor financial circumstances annually (Neumann et al. 2005, Pejsak and Markowska-Daniel 1997, reviewed by Zimmerman et al. 2012) and can become endemic in the major swine producing areas of Europe (Mateu et al. 2003, Zimmerman et al. 2012), Asia (Li et al. 2012, Tian et al. 2007), North and South America (Dewey et al. 2000, reviewed by Zimmerman et al. 2012). The massive outbreaks of PRRS in autumn and winter of 2009/2010 were reported in the paper “top agrar 10/2010” (Pabst 2010).

The development of these respiratory diseases is a multifactorial complex, including infectious agents, the host as well as environmental and management considerations and genetic factors (Brockmeier et al. 2002, reviewed by Sørensen et al. 2006). PRRSV infected pigs are ineffective in eliminating the virus and PRRSV can induce a prolonged viremia and a persistent infection (reviewed by Murtaugh et al. 2002). Unfortunately, the PRRSV genome changes and heterologous strains quickly arise, due to the high degree of genetic variability of PRRSV. Generally, the control remains problematic as the efficacy and universality of PRRS vaccination has not been established and no effective treatments against a largely uncontrolled disease are available (reviewed by Huang and Meng 2010,

reviewed by Kimman et al. 2009, reviewed by Mateu and Diaz 2008, Modrow et al. 2010, Palzer 2013).

PRRSV has a complex interaction with the immune system by replication and by strong modulations of the host immune responses in innate tissue cells such as macrophages, monocytes and dendritic cells (Genini et al. 2008, Loving et al. 2007, Miller et al. 2010, Xiao et al. 2010b). Researches have indicated that there are breed differences and genetic components, involved in the response to PRRSV infection. Variations in the host susceptibility of animals and in host resistance have been mentioned (Halbur et al. 1998, Petry et al. 2005). In their review Lunney and Chen (2010) summarized the influence factors on research of resistance/susceptibility to viral pathogens, including the route of infection, transmission, replication and the response of the innate and adaptive immune system. The development of breeding programmes, including host genetic improvement for disease resistance and tolerance may have an impact on the control and the reduction of PRRS (Flori et al. 2011b, Lewis et al. 2007, Lewis et al. 2009).

The above mentioned facts lead to the still important necessities: to improve pigs' health, to reduce economic losses, medical costs and treatments, to enhance breeding strategies for pigs with good parameters of immunity and production traits, to develop higher control and prevention strategies as well as more effective vaccines and to select disease resistant pigs. There are genetic components involved in determining how effective each pig will response to PRRSV infection. But a transcriptonal overview, related to understand the genetic influence on the immunological reaction to PRRSV infection, is needed. The knowledge about these factors is extremely important in order to increase the understanding of the immune response to PRRSV and to develop control and therapy strategies for this type of viral infection.

Accordingly, the main objective of this thesis was to investigate the transcriptome profile of respiratory cells of two different genetic breeds after PRRSV infection and to characterize gene expression changes of these cells. The aims in detail and the hypotheses of this thesis follow in chapter 2.4.

2 Literature review

2.1 Characterization of porcine reproductive and respiratory syndrome

2.1.1 Porcine reproductive and respiratory syndrome

In the late 1980s in the United States the first clinical outbreaks of porcine reproductive and respiratory syndrome (PRRS) have been reported and recognized as a mystery swine disease or swine infertility and respiratory syndrome (Benfield et al. 1992, López 2001, Wensvoort et al. 1991). In 1991 in the Netherlands the virus was subsequently isolated and named Lelystad virus (LV) (López 2001, Wensvoort et al. 1991). Fundamentally PRRS is characterized by high mortality of nursery piglets (Pejsak and Markowska-Daniel 1997) and leads to massive reproductive failures, including abortions, stillbirth (López 2001, Tizard 2013) and premature farrowings as well as to weak or mummified piglets (Balasuriya 2013, Modrow et al. 2010, reviewed by Zimmerman et al. 2012). In pigs of all ages, PRRS is associated with respiratory distress (López 2001, Tizard 2013), interstitial pneumonia in growing and finishing swines and it can cause decreased growth performance (Collins et al. 1992, Xiao et al. 2010b). The aetiological agent of PRRS, porcine reproductive and respiratory syndrome virus (PRRSV), is a single-stranded (ss) 15 kb positive-sense RNA virus with morphological and morphogenetic similarities to members of the arterivirus group (Conzelmann et al. 1993, Meulenberg et al. 1993). Arteriviridae are grouped together with the Coronaviridae and the Roniviridae in the order of the Nidovirales. All Nidovirales members are enveloped viruses like the equine arteritis virus and the lactate dehydrogenase-elevating virus (Balasuriya 2013, Modrow et al. 2010). The consequences of an infection can range from a persistent infection to an acute disease (reviewed by Snijder et al. 2013). Two distinct viral genotypes of PRRSV have been isolated and characterized recently, the European strain (LV) and the Norh American strain VR-2332 (Benfield et al. 1992, Collins et al. 1992, Modrow et al. 2010, Wensvoort et al. 1991). These two genotypes share morphological and structural similarities as well as about 55 - 70 % identity at the nucleotide level (Balasuriya 2013, Modrow et al. 2010).

2.1.2 Porcine reproductive and respiratory syndrome virus genome organization

The PRRSV ss positive-sense RNA genome consists of eight open reading frames (ORFs) (Conzelmann et al. 1993, Meulenberg et al. 1993). These ORFs encode the viral replicase and form six or seven 3´-coterminal nested subgenomic viral messenger RNA (mRNA) transcripts (mRNA1 - mRNA7) (Figure 1) (Meulenberg et al. 1993).

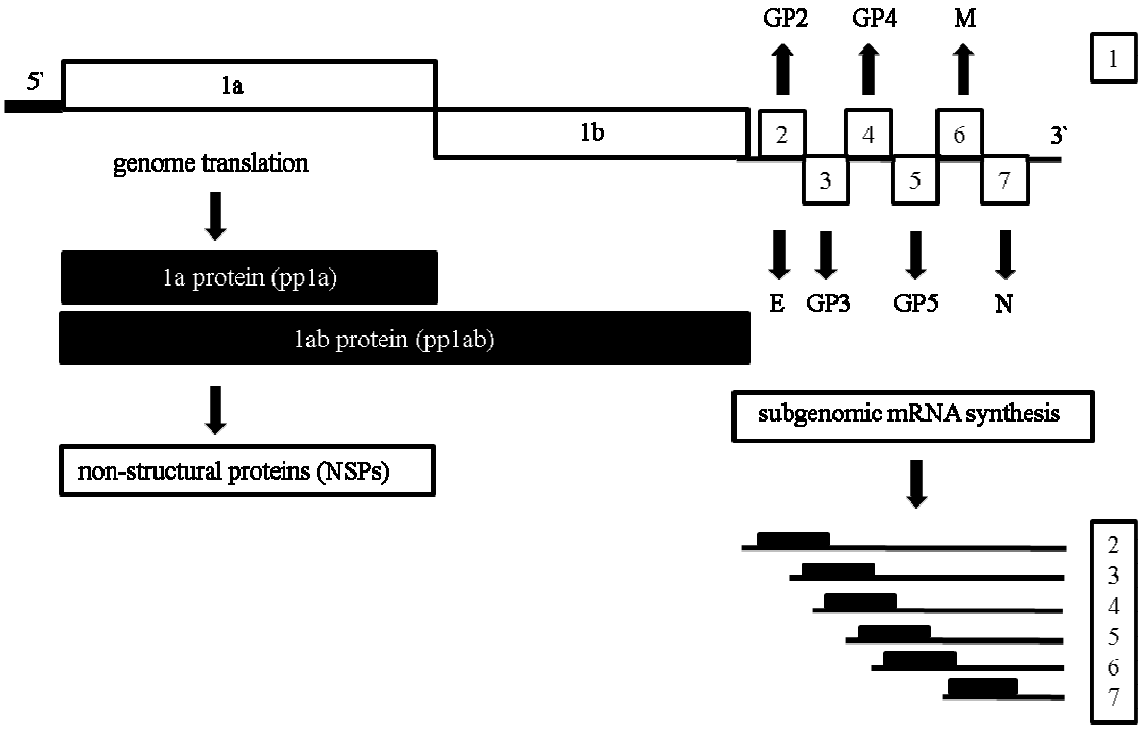

Figure 1: PRRSV genome organization from 5´ to 3´, schema modified and simplified, compare the reviews of Fang and Snijder (2010), Snijder and Meulenberg (1998)

ORF 1a and ORF 1b are located just downstream of the 5-untranslated region (UTR) and substantiate more than tow-third (approximately 80 %) of the viral genome (Meulenberg et al. 1993, Modrow et al. 2010). ORF 1a and ORF 1b encode two viral replicase polyproteins (pp) 1a and pp1ab (Figure 1). This synthesis and cleavage are the first steps of virus infection (Modrow et al. 2010, reviewed by Zimmerman et al. 2012). ORF 1a is translated by the genomic RNA, ORF 1b is expressed by a ribosomal frameshifting, engaging a large ORF 1ab polyprotein and resulting in products which are involved in the

virus transcription and replication. The viral pp1a and pp1ab are proteolytically processed in 12 functional non-structural proteins (NSPs). NSPs are involved in the genome replication and the subgenomic mRNA transcription (reviewed by Modrow et al. 2010, Snijder and Meulenberg 1998). ORF 1a encodes NSP2 (Allende et al. 1999) and is considered as an important region for monitoring genetic variation (Fang et al. 2004). NSP4 is the main protease and produces NSPs 3 - 12. All NSPs are fully conserved in the genomes of PRRSV (reviewed by Fang and Snijder 2010). The ORFs from 2 - 7 are situated at the 3´end of the genome (Meulenberg et al. 1993). ORF 2a, ORF 2b and ORFs 3 - 6 are characterized as membrane-associated proteins, encoding the viral structure proteins like glycoproteins (GP) 2a, GP2b, GP3, GP4, GP5 and the matrix protein (M) whereas the nucleocapsid protein (N) is encoded by ORF 7 (Conzelmann et al. 1993, Modrow et al. 2010, reviewed by Snijder and Meulenberg 1998) (Figure 1). N protein forms the principal component of the viral capsid (Modrow et al. 2010) and is localized in the host cell nucleus and in the nucleolus during replication (King et al. 2011, Rowland et al. 1999). The envelope glycoprotein (E) (Snijder et al. 1999) is translated by ORF 2a/2b. E is required for the production of ion-channel proteins (King et al. 2011). A schematic representation of the arterivirus genome organization is depicted in Figure 2.

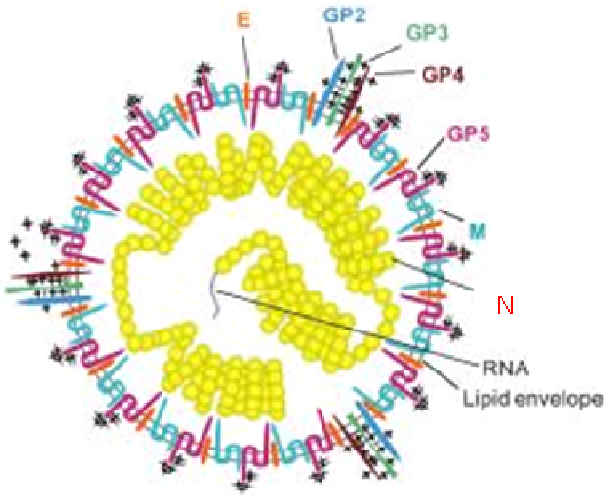

Figure 2: Schematic representation of arterivirus genome organization (King et al. 2011)

2.1.3 Virus cell tropism and viral replication cycle

Following the oronasal exposure, PRRSV replicates in the lung, in the tonsils and in the upper respiratory tract as well as in lymphoid tissues, in bronchiolar epithelium cells, in spleen, in thymus and in cells that are essential for the immune function (macrophages and dendritic cells (DCs)) (Brockmeier et al. 2002), in placenta (Karniychuk et al. 2011) and in spermatogenic epithelium, too (Sur et al. 1997). In vivo and in vitro PRRSV has a specific cell and tissue tropism. Predominantly the virus productive infection occurs in the monocyte/macrophage lineage (Duan et al. 1997, Pol et al. 1991, reviewed by Zimmerman et al. 2012) and results in their destruction (López 2001). That leads to increased susceptibility for secondary infections like bacterial pneumonia, septicaemia or enteritis (Balasuriya 2013, Tizard 2013). Beside these cells, PRRSV also infects monocyte-derived DCs (MDDCs) in vitro (Loving et al. 2007).

Several studies reported that PRRSV can be airborne transmitted over long distances (Dee et al. 2009) and enters into host cells of the respiratory tract. PRRSV infects cells after attachment to regions at the cell surface as well as to specific cellular receptors. Afterwards the virus invades the host via the receptor-mediated endocytosis route (Nauwynck et al. 1999). On the surface of porcine macrophages two specific PRRSV receptors for both virus strains have been identified: heparan sulphate glycosaminoglycans for the first binding (Delputte et al. 2002, Duan et al. 1998, Vanderheijden et al. 2003) and sialoadhesin (Sn) for the attachment and the internalization of the virus, via clathrin-mediated endocytosis (Delputte et al. 2002, Nauwynck et al. 1999, Vanderheijden et al. 2003).

The cluster of differentiation (CD) molecule CD163 is also known as a cellular receptor for PRRSV infection (Calvert et al. 2007, Van Gorp et al. 2008). The viral M protein and the viral N protein play an important role in attaching the virus to the target cells by heparin. Additionally, the disulfide-linked M-GP5 complexes can bind to heparin (Delputte et al. 2002). GP2 and GP4 are also viral attachment proteins and are able to bind to the receptor CD163 (Das et al. 2010).

After the standard entry process via a receptor mediated endocytosis, the viral nucleocapsid is released into the cytosol for replication (Kreutz and Ackermann 1996). The life cycle of PRRSV emerges only in the cytoplasm of infected cells (King et al. 2011, Modrow et al. 2010). Before the viral replication can proceed, the uncoating of the nucleocapsid has to pass (Vanderheijden et al. 2003). In the virus the RNA itself functions

as mRNA. PRRSV is a plus-strand RNA virus and these viruses carry their own RNA-dependent RNA polymerase (RdRp) for the replication of RNA in the viral genome. The enzyme region of PRRSV RdRp is located in NSP9 (reviewed by Fang and Snijder 2010, Modrow et al. 2010, Nedialkova et al. 2010). RdRp transcribes the viral plus-strand RNA into a minus-strand RNA which serves in turn as a template for the genomic plus-strand RNA (Gao et al. 2014, Nedialkova et al. 2010).

For positive stranded RNA viruses, the genome replication occurs in a membrane-associated viral Replication and Transcription Complex (RTC) (reviewed by Fang and Snijder 2010, Zhou et al. 2011b). NSP10 encodes the necessary RNA helicase motifs (Bautista et al. 2002). The viral replication cycle induces the generation of a nested set of 3′-coterminal subgenomic mRNAs (compare chapter 2.1.2, Figure 1) which serve as templates for the translation of the viral structural protein genes (King et al. 2011, Tijms et al. 2007). PRRSV assembles preformed viral nucleocapsids at the endoplasmic reticulum (ER). The viral nucleocapsids pass through the golgi network and exit the host cell via exocytosis (Dea et al. 1995, Modrow et al. 2010, reviewed by Snijder and Meulenberg 1998).

2.1.4 Virus transmission

PRRSV transmission within and between pigs and herds has been documented in studies, concerning direct and indirect routes of transmission (reviewed by Cho and Dee 2006, Wills et al. 1997). Rossow (1998) reviewed that PRRSV was isolated within different time points post infection from serum, semen, saliva, feces, urine, nasal swabs, oropharyngeal swabs and oropharyngeal scrapings. These porcine secretions and excretions form the direct routes of PRRSV infection. The indirect routes pass over fomites, transport vehicles, insects, avian and non-porcine mammalian species and over aerosols (reviewed by Cho and Dee 2006). PRRSV is a virus with the potential for airborne transmission, described by Kristensen et al. (2004). The transmission is possible over a short and a long distance (Dee et al. 2009, Mortensen et al. 2002). Additionally, the animal movement is one factor for disease spread (Dewey et al. 2000).

2.2 Immunology

The defence and the response of the body, collectively called the immune system, is a highly interactive and cooperative system. It consists of complex, interacting networks of biochemical and cellular reactions. The defence mechanisms can be passive (e.g. the skin as a natural barrier) or active (immune responses that involve a density of different effector mechanisms). Classically the immunity itself is separated in two pillars, referred to innate and adaptive host defence mechanisms (Abbas et al. 2012, Murphy et al. 2008).
The innate immune response is the first line of defence and immediately typically activated after the infection. It consists of physical barriers, phagocytic cells such as DCs, monocytes or macrophages and the production of various cytokines, chemokines and proteins with the task of protection, recruitment of cells through an inflammatory process and the activation of the adaptive immune system (Abbas et al. 2012, reviewed by Chase and Lunney 2012, Kindt et al. 2007). The adaptive immune system is antigen-specific and based on the function of T and B lymphocytes, cytokines and antibody production (Table 1). It results in an immunological memory (Murphy et al. 2008).

Table 1: Features of innate and adaptive immune response, table modified and simplified, compare Abbas et al. (2012)

Category	Cells	Components
Innate immune system	Macrophages	Physical and chemical barrier
	Dendritic cells	Mediators of inflammation
	Mast cells	Cytokines
	Granulocytes	Chemokines
	Natural killer cells	
Adaptive immune system	T lymphocytes	Antibody
	B lymphocytes	Memory cells
		T helper cell cytokines

2.2.1 Innate immune system

The innate immune system is a phylogenetical defence mechanism (reviewed by Medzhitov and Janeway 1997) and enables the pig to respond rapidly to an infectious agent and to provide the first phase of an effective protection (reviewed by Chase and Lunney 2012). This system is involved in the detection, recognition, killing and delivery of antigens to the next lymphoid tissue. The innate immunity is separated in the cellular arm that mainly involves phagocytes (Abbas et al. 2012, Tizard 2013) and in the humoral arm which consists of antimicrobial peptides, lysozyme and lactoferrin (Beutler 2004, Tizard 2013).

The detection of pathogens is mediated via host molecules with the term pattern-recognition receptors (PRRs). PRRs recognize microbial as well as viral components and are expressed on the cell surface within intracellular compartments or are secreted in blood and in tissue fluids. Pathogen-associated molecular patterns (PAMPs) represent a signature of pathogens and play a major role in the detection of invaders by PRRs (Abbas et al. 2012, Murphy et al. 2008, Tizard 2013).

The detection of invading pathogens and the recognition of specific patterns of pathogen components occur on the Toll-like receptors (TLRs). Among PRRs, the TLRs assume an important role in the activation of the immune responses (Kindt et al. 2007). For example viral DNA is recognized by TLR9 (Lund et al. 2003) and viral ssRNA by TLR7 (Diebold et al. 2004, Lund et al. 2004). Through adapter proteins like MyD88 (Medzhitov et al. 1998, Sun and Ding 2006), MAL (Fitzgerald et al. 2001) and TRIF (Yamamoto et al. 2003) TLRs transmit signals in the cytoplasma. These intracellular signalling pathways function as activators of host defence genes. A variety of pro-inflammatory molecules react, include the transcriptional activation of cytokines and chemokines as well as the synthesis of cell adhesion molecules and immunoreceptors. MyD88 and TRIF together initiate the expression of multitudinous cytokines through the activation of transcriptional factors like NF-$_K$B (reviewed by Janeway and Medzhitov 2002, Piras and Selvarajoo 2014, Tizard 2013).

RIG-I like receptors (RLRs) belong to the DExD/H box helicases family of proteins. RIG-I, MDA5 and LGP2 are RLRs members (reviewed by Schlee 2013). They play key roles in the detection of distinct molecular patterns of virus-derived nucleic acids (Gack 2014, Weber et al. 2013). The produced cytokines and chemokines are able to interact with other

immune cells and to induce the inflammatory and adaptive immune response. Cytokines and chemokines are working as mediators (Abbas et al. 2012).

2.2.2 Adaptive immune system

In contrast to the innate immune system, the adaptive one can generally make a response when it has been informed by the innate immune response and stimulated by pathogens (Alberts et al. 2008, reviewed by Reis e Sousa 2001). It enhances the efficiency of the innate immune mechanisms as well as the development of the immunological memory in order to respond promptly to the next encounter with pathogens. The adaptive immune system is mediated by antigen-specific T and B cells (Alberts et al. 2008, reviewed by Kaiser 2010, Kindt et al. 2007). B cells are capable to produce antibodies and to mature and differentiate into antibody-secretion plasma cells by recognizing extracellular antigens and by being activated by the signals of CD40, TLRs and other receptors (Abbas et al. 2012, Alberts et al. 2008, DeFranco et al. 2007). Naïve T cells are separated into two subsets (Figure 3): Type 1 helper (T_H1) and Type 2 helper (T_H2), whereas T_H1 secretes IFN-γ, T_H2 produces IL-4, IL-5, IL-10 and IL-13. T_H1 is mainly responsible for cellular immunity and T_H2 promotes the humoral immunity (Abbas et al. 2012, reviewed by Akira et al. 2001).

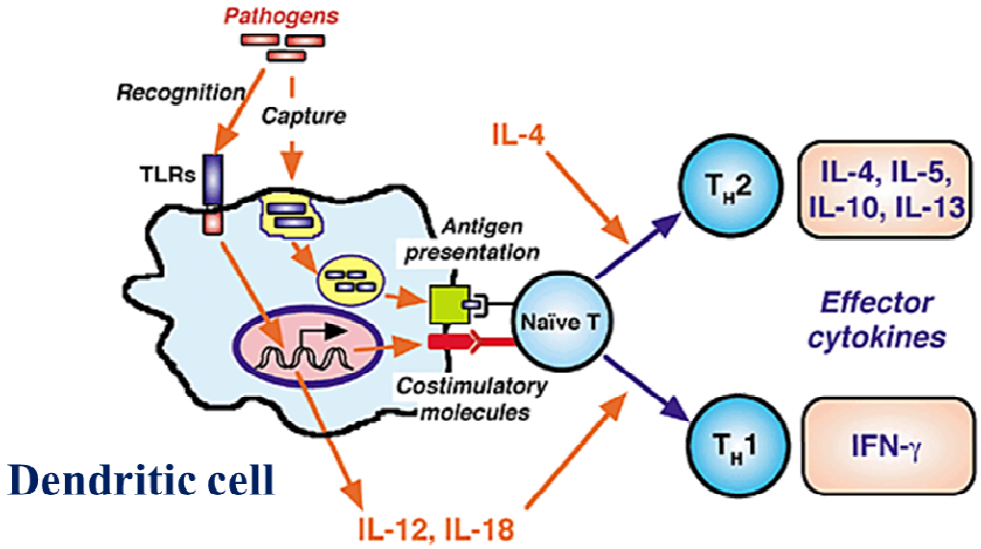

Figure 3: Recognition of pathogens by dendritic cells and stimulation of naïve T cells, picture modified, compare the review of Akira et al. (2001)

2.2.3 Immune cells, located in the respiratory system

The respiratory apparatus consists of lung and pleura, it comprises the nasal cavity, pharynx, larynx, trachea, bronchi, bronchioles as well as the alveoli (reviewed by Sørensen et al. 2006). The respiratory tract is one common route of infection with airborne microorganisms. If microorganisms cross the epithelial barrier and enter into the host tissues, local pulmonary immune cells will recognize the pathogens. The immune cells have to differentiate between the induction of a protective immune response against pathogens and the induction of tolerance of non-pathogens (Murphy et al. 2008).

Large populations of DCs are found in the tissues of the upper and lower respiratory tract and are present within the airway epithelium, submucosa and the associated lung parenchymal tissue (Abbas et al. 2012, Gong et al. 1992, Sertl et al. 1986). These DCs are the "gatekeepers" of the adaptive immune system (reviewed by Stumbles et al. 2003). Chemokines and their receptors control the migration of immune cells at basically any stage of an immune response (Kindt et al. 2007, Tizard 2013). Alveolar macrophages (AM) are abundant in the lung and have a special role there as well as in the alveolar space, where they are well placed to be the first line of defence against invasive pathogens (Figure 4) (Abbas et al. 2012, López 2001).

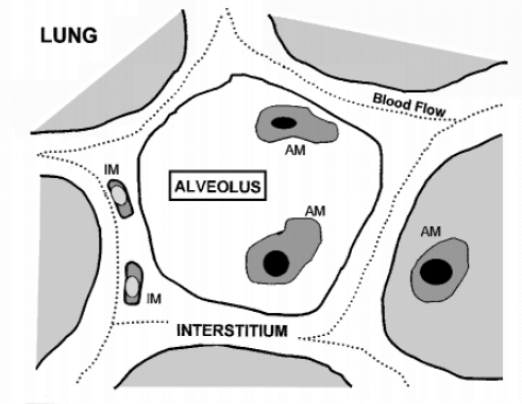

Figure 4: Location of macrophages in the lung, alveolar macrophages (AM) and interstitial macrophages (IM), modified and simplified, compare the review of Laskin et al. (2001)

2.2.4 Development of immune system cells

The cells of the immune system can be classified, according to their belonging to the innate or the adaptive immunity, but overlapping criteria are possible (MacPherson and Austyn 2012). The immune cells are originated in the hematopoietic stem cells (HSCs) of the bone marrow. HSCs are pluripotent (Abbas et al. 2012). The cell types which are developed from HSCs belong to the lymphoid as well as to the myeloid lineage. The myeloid lineage leads to monocytes and to some populations of macrophages as well as to common DC precursors (CDPs) (DeFranco et al. 2007, reviewed by Geissmann et al. 2010, Goldman and Prabhakar 1996), the lymphoid lineage generates T and B lymphocytes (Figure 5) (DeFranco et al. 2007, Goldman and Prabhakar 1996).

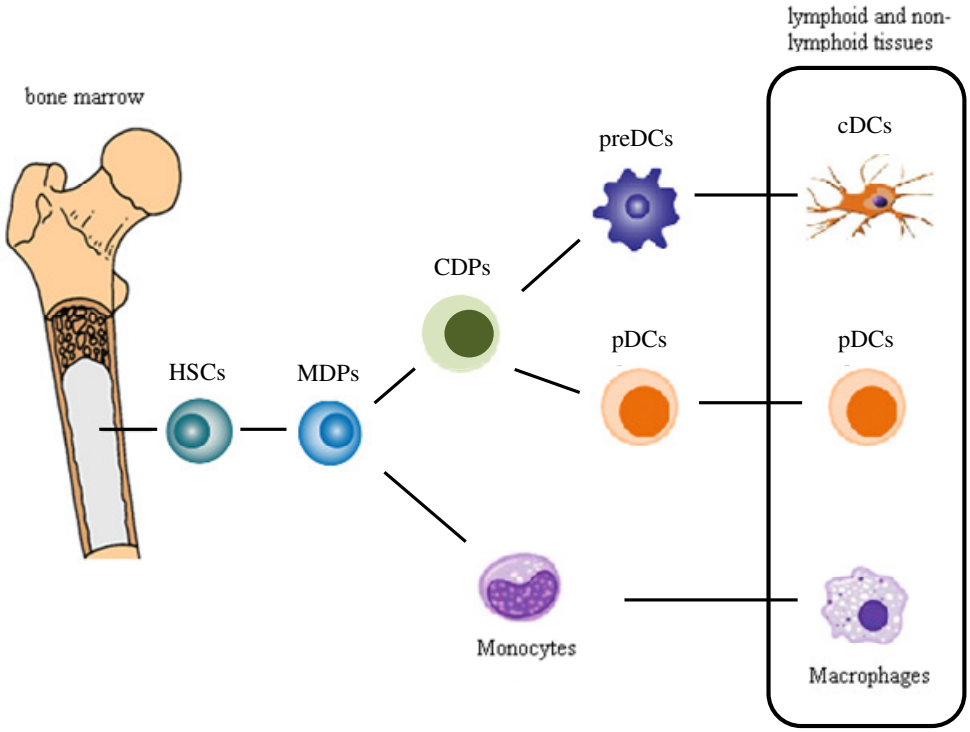

Figure 5: Pathway of immune cell development, modified and simplified, compare the reviews of Geissmann et al. (2010), Okwan-Duodu et al. (2013), as well as Tsunetsugu-Yokota and Muhsen (2013)

The first cells which develop from HSCs are called macrophage and DC precursors (MDPs). MDPs serve as templates for the generation of CDPs (Fogg et al. 2006, Liu et al. 2009b) and of monocytes (Fogg et al. 2006). One subset of the monocytes enters into the

peripheral blood and patrols there for 1 - 3 days, then it migrates into the tissues where it develops to macrophages. Another subset of monocytes rapidly shifts into inflamed tissues and can differentiate into MDDCs (Abbas et al. 2012). CDPs develop to precursor DCs (preDCs) or to plasmacytoid DCs (pDCs) and migrate through the blood and enter the peripheral tissues. Arrived in lymphoid or non-lymphoid tissues, preDCs differentiate into conventional DCs (cDCs) (DeFranco et al. 2007, reviewed by Geissmann et al. 2010, Murphy et al. 2008). The granulocyte macrophage-colony-stimulating factor (GM-CSF) and cytokines are candidates which are important in supporting these programs of proliferation and differentiation (Geissmann et al. 1998, Sallusto and Lanzavecchia 1994).

2.2.5 Dendritic cells

Dendritic cells (DCs) play crucial roles in linking the innate with the adaptive immunity, based on their rapid response to the presence of infection and they activate lymphocytes (Abbas et al. 2012, MacPherson and Austyn 2012). DCs are the most professional antigen-presenting cells (APCs) of the immune system. They are proficient at antigen processing with a high phagocytic activity in their immature cell stage, as mature DCs the endocytic capacity is reduced (Garrett et al. 2000, Murphy et al. 2008, Tizard 2013). DCs are divided into different categories: preDCs, cDCs (migratory DCs and lymphoid-tissue-resident DCs) and inflammatory DCs (compare chapter 2.2.4) (reviewed by Shortman and Naik 2007). In the blood stream circulating, preDCs enter into peripheral tissues as immature DCs (Figure 5), as mentioned in the review of Geissmann et al. (2010) and (Tizard 2013). DCs populations have been identified in a variety of tissues and organs: in all lymphoid organs, in lung, in upper and lower respiratory tracts (Abbas et al. 2012, Sertl et al. 1986), in blood, heart, kidney (Austyn et al. 1994, Murphy et al. 2008), spleen, liver (Chen et al. 2009, Mosayebi and Moazzeni 2011) and the urogenital tract (Bizargity and Bonney 2009). Immature DCs in tissues can be activated via their TLRs which signal the presence of pathogens, the damage of tissues or of cytokines which are produced during the inflammatory response. Through this process a modulation program of specific DCs surface receptors is initiated (reviewed by Banchereau and Steinman 1998, reviewed by Janeway and Medzhitov 2002, reviewed by Shortman and Liu 2002). In addition, DCs start with the migration towards secondary lymph nodes and launch the T and B cells' activation (Grayson et al. 2007, reviewed by Janeway and Medzhitov 2002). The effective interaction

of DCs with T cells can be largely attributed to the up-regulation of the co-stimulatory molecules such as CD80 and CD86 (Figure 3) (reviewed by Akira et al. 2001, reviewed by Janeway and Medzhitov 2002). The proteins of antigens are processed as peptide fragments and these are presented to T cells on the major histocompatibility complex (MHC) class I and II molecules which are located on the surface of DCs (Beutler 2004, reviewed by Guermonprez et al. 2002, reviewed by Janeway and Medzhitov 2002). This antigen-presentation and the induction of co-stimulatory molecules allow the activation of naïve T cells, so the adaptive immune response is started (reviewed by Janeway and Medzhitov 2002). Beside these antigen-specific functions, the secretion of cytokine mixtures is an important assignment of DCs (e.g. IL-12, type and TNF, IL-6, IFN-γ) (Abbas et al. 2012, reviewed by Akira et al. 2001, Tizard 2013).

2.2.6 Macrophages

Monocytes mature and become macrophages (compare chapter 2.2.4 and Figure 5) (Abbas et al. 2012). Macrophages are found in connective tissue, brain, lung, liver and spleen (Beutler 2004, reviewed by Gordon and Martinez 2010, Murphy et al. 2008). Laskin et al. (2001) described in their review an existing macrophages' subpopulation heterogeneity of liver and lung tissues. Macrophages are close to invasive pathogens and have the ability to migrate to local sites of injury and infections (Beutler 2004, reviewed by Gordon and Martinez 2010). An important function of macrophages is the recognition of pathogens and their phagocytosis as well as the killing and/or the neutralizing of inhaled particulate antigens without the assistance of the adaptive immune response. They express many different receptors and recognize pathogens via cell-surface receptors (reviewed by Gordon and Martinez 2010, Murphy et al. 2008, Tizard 2013). The tasks of macrophages are the production of inflammatory cytokines, the control of inflammation, due to the production of inhibitor molecules (reviewed by Nicod 1999). The involvement of alveolar macrophages plays a role in repairing and remodelling the lung. It is a common function of macrophages to repair damaged tissues (Abbas et al. 2012).

2.2.7 T cells and B cells

The adaptive immune system uses two fundamental types of naïve lymphocytes, the mature T and B cells. For T and B cells the originating cells are the HSCs (compare chapter 2.2.4 and Figure 5). The thymus is the organ for developing T cells, B cells are generated in the bone marrow (Alberts et al. 2008, reviewed by Martelli and Bierer 2003). These naïve lymphocytes migrate into the peripheral lymphoid organs and wait there to be activated by antigens (Abbas et al. 2012, Tizard 2013). After 1 to 3 months without any antigenic stimulation the naïve lymphocytes do not survive. But different cytokines, like IL-7, can transmit survival signals to naïve lymphocytes (Abbas et al. 2012, Kindt et al. 2007).

The activation of naïve T lymphocytes requires the recognition of peptide antigens, presented by MHC and by co-stimulatory molecules, expressed on the same APCs (Figure 3) (Abbas et al. 2012, Alberts et al. 2008).

The T cells recognize fragments of antigens on the surface of APCs via their T cell receptors (TCRs). This leads to the first steps of T cell activation. MHC I and II of APCs stimulate cytotoxic T cells (CTLs) and helper T cells, respectively (Alberts et al. 2008, Kindt et al. 2007). The second stimulation signal is sent by the co-stimulatory molecules CD80 and CD86 which are located on APCs with the effect of binding to CD28 on the T cell membrane. This whole process leads to a complete activation of T lymphocytes (Alberts et al. 2008, reviewed by Miller et al. 2008). Activated T lymphocytes migrate and reach the injured tissue and they help B cells in lymphoid organs (Alberts et al. 2008).

B cells are activated after contact with T cells and DCs. Next they migrate to various areas and respond by differentiating into plasma cells. These plasma cells produce antibodies that neutralize the initial pathogen (reviewed by Kaiser 2010, reviewed by Martelli and Bierer 2003). Helper T cells secrete cytokines which permit activation of macrophages, natural killer cells and eosinophils (Alberts et al. 2008, reviewed by Martelli and Bierer 2003). Memory cells can persist for months or years and provide optimal defence against pathogens. They respond quicker and to a lager extent to infections than naïve cells (Abbas et al. 2012).

2.3 Porcine reproductive and respiratory syndrome virus and the immune system

2.3.1 Virus-host interplay

The immune response to PRRSV is a multifactorial process and very complex. This is due to the facts that the interaction between the pig as a host and PRRSV depends particularly on the viral strain, the infection route, the age of the pigs, their immune status, genetic predisposition, previous infections and their vaccination status, on the viral co-infection and/or on the bacterial infections and on the pigs' environment (Brockmeier et al. 2002, Cho et al. 2006b, Cho et al. 2006a, reviewed by Murtaugh et al. 2002). In addition to the ability of the virus to escape or to modulate the host immune system and due to the ineffective elimination of the virus through the pigs, the understanding of the interactions between PRRSV and the host are difficult and complex (reviewed by Mateu and Diaz 2008, reviewed by Murtaugh et al. 2002). It has been documented that PRRSV modulates the host immune responses by inhibiting key cytokines and by inducing regulatory cytokines (Genini et al. 2008, Xiao et al. 2010b, Xiao et al. 2010a). Weesendorp et al. (2013) compared the responses of pulmonary alveolar macrophages (PAMs) and bone marrow-derived DCs to two European subtype 1 strains and to a virulent subtype 3 strain. In their study they revealed phenotypic modulations, differences in immunologically relevant cell surface molecules and a reduced specific immune response. Their results gave a hint to a decreased adaptive immune response.

The reason is still unclear why PRRSV is not efficiently controlled by the immune response. The complexity of the immune response to PRRSV leads the focus also on cell-based virus recognition mechanisms (reviewed by Zimmerman et al. 2006). Zhang et al. (2000) mentioned a relation between the genome replication of PRRSV and an altered gene expression of the host RNA helicase. In another study the results showed that TLR1, TLR2, TLR4, TLR6 were significantly enhanced in lungs tissue post infection with the classical North American type of PRRSV (Xiao et al. 2010a). Equally RIG-I and MDA5 represented a higher expression post infection. The exception was TLR3 which indicated no changes in this study (Xiao et al. 2010a).

Different studies underlined the importance of IFN in PRRSV infection. PRRSV counteracts the IFN production which has a high impact on the immune system (reviewed by Bonjardim 2005). This mechanism can be activated during the viral genome replication where the ssRNA virus duplicates into the double-strand RNA which interferes with the

type I IFN signalling pathway (Luo et al. 2008). The virus evokes an induction of INF-β but no expression of IFN-α mRNA in PAMs (Genini et al. 2008). In their study Loving et al. (2007) showed that MDDCs and lung DCs responded to a virus infection with an increased INF-β mRNA expression. But there was no altered gene expression of IFN-α in infected lung DCs as already researched by Genini et al. (2008). Loving et al. (2007) concluded that the usual type I interferon response is missing after PRRSV infection. Genini et al. (2008) also found an up-regulation of IL-10 in infected PAMs, this is documented, too, in the study of Xiao et al. (2010b). These authors described a varying innate immune response and an anti-apoptotic state after virus infection, in form of an up-regulation of anti-apoptotic genes like IL-10, MCL1, BFL-1, ADM and a suppressed expression of pro-apoptotic genes like p53, APR-1, IRF3.

Some viruses are able to repress apoptosis to have more time to exploit the cells for their viral replication. At the same time the virus is manipulating the innate defence mechanisms of the cells (Dimmock et al. 2007, Sieg et al. 1996, Xiao et al. 2010b, reviewed by Zhou and Zhang 2012). Beside these reported observations, in their review Zhou and Zhang (2012) described that the reason for the down-regulation of innate immune responses post PRRSV infection may be different expressions of cytokine patterns. Post PRRSV infection, alterations can occur in antigen presentation processes. Rodriguez-Gomez et al. (2013) wrote a review about the relation between APCs and PRRSV and the potential mechanisms which PRRSV uses to trigger the immune response. They suggested that T cells are ineffectively activated and they supported further analyses to understand the virus' strategies in order to improve powerful control processes.

A variety of strategies are utilized by PRRSV to induce ultimately prolonged viremia and to cause persistent infections. PRRSV encodes viral products, like NSP1α, NSP1β, NSP2, NSP4, NSP11 and N. These proteins have the capacity to evade the host immune response and to develop a strong inhibitory activity (Beura et al. 2010, Chen et al. 2010, Li et al. 2010, Wang et al. 2013).

2.3.2 Breed differences and genetic components in host response to virus infection

Breed differences and genetic components are factors that determine the response to PRRSV infection in pigs. Genetic variations in the host resistance/susceptibility of animals have already been reported (Halbur et al. 1998, Petry et al. 2005) and reviewed by Lunney and Chen (2010). Susceptibility to PRRS of different breeds was identified with an experimental PRRSV infection of Duroc, Hampshire and Meishan pigs by Halbur et al. (1998). They observed differences in the severity of lung lesions and the number of PRRSV-antigen-positive cells in the lungs of infected pigs. Petry et al. (2005) described the reduced rectal temperatures and the decreased viremia in a PRRSV infected Large White-Landrace synthetic line in comparison to an infected Hampshire-Duroc synthetic line. This research group indicated that the Large White-Landrace population is more resistant to PRRSV than the Hampshire-Duroc population. Breed differences were also detected between Pietrain pigs and Wiesenauer Miniature pigs after an in vivo PRRSV infection. The results of this study documented a shorter duration of viremia and a lower viral level for Wiesenauer Miniature pigs in comparison to Pietrain pigs (Reiner et al. 2010). Another in vitro study indicated that macrophages of different pig breeds (Large White, Duroc-Pietrain synthetic, Landrace, Duroc-Large White synthetic and Hampshire) were variable in their susceptibility to PRRSV (Vincent et al. 2005). Ait-Ali et al. (2011) observed transcriptional differences in infected PAMs between Pietrain and Landrace animals. They found a higher number of PRRSV-regulated transcripts in Landrace PAMs than in those of Pietrains. Additionally, they suggested that Landrace PAMs have a reduced PRRSV susceptibility and that further genetic analyses are necessary to understand and to encode PRRSV resistance.

Biffani et al. (2011) used PorcineSNP60 BeadChip in order to obtain possible breed-cluster effects on PRRS viremia. Four different breeds were examined in their study Large White, Landrace, Duroc and Pietrain. Their results did not lead to a significant breed-cluster effect but they identified the influence of environment and management on PRRS viremia. Further analyses with the same dataset were done, the focus lay on the host immune response in order to determine significant genetic variability. Results out of these studies had been published by Badaoui et al. (2013). They detected a low infection rate of Landrace animals in contrast to Large White, Duroc and Pietrain animals. The authors assumed a higher breed resistance to PRRSV infection of different breeds.

2.3.3 Genetic components of immune traits

In pigs, approximately 10,497 Quantitative trait loci (QTL) have been mapped for 658 different traits (http://www.animalgenome.org/cgi-bin/QTLdb/index, update: April 2014). 6453 QTL regions were identified for meat and carcass quality, 1032 for reproductive traits, 971 for productive traits and 1156 for the health as well as 885 for the exterior. The early work of Edfors-Lilja et al. (1998) was done for the identification of QTL, involved in the immune capacity of pigs like total and differential leukocyte counts, neutrophil phagocytosis, mitogen-induced proliferation and IL-2 production, virus-induced IFN-α production of mononuclear cells.

QTL regions, associated with health traits, are divided into distinct categories: blood parameters, disease susceptibility, immune capacity and pathogens. For the disease susceptibility other important sub-categories are listed in which PRRSV antibody titer and PRRSV susceptibility are performed (www.animalgenome.org/cgi-bin/QTLdb/index).

In the study of Boddicker et al. (2012) the relationship between the host response and PRRSV was described with a strong genetic component and QTL regions on swine chromosome (SSC) 1, 4, 7, 17, X were identified. On SSC4 and SSCX two major QTL regions were detected which had an effect on the response to PRRS. Lu et al. (2011b) identified QTL by a microsatellite marker supported study. They detected QTL regions that effected the expression of IFN-γ and of IL-10.

Uddin et al. (2011) found candidate genes in QTL regions which were involved in cytokines and TLRs reactions in response to different antigens. The research on QTL regions could help to understand the relations between the genetic basis and the innate immune traits. The improvement of the animals' health is along with the identification of candidate genes or markers for immune competence and disease resistance (Wimmers et al. 2009).

Until now genome-wide association studies and genome-wide transcriptional profiles were carried out with the emphasis on economically important traits, as growth, muscularity, meat quality as well as on other production traits (Do et al. 2014, Heidt et al. 2013, Karlskov-Mortensen et al. 2006, Ponsuksili et al. 2008). The identification of genomic regions, responsible for immune capacity traits in swine, is under progress (Lu et al. 2013, Uddin et al. 2011). Therefore the research focuses on immune-related QTL regions and single nucleotide polymorphisms (SNP) in context with the pig's health but without any antagonistic influence on production and growth traits (Flori et al. 2011a, Lu et al. 2013).

Beside these mapping approaches, the gene expression profiling of immune tissues provides informations about functional networks and functional candidate genes. Further characterizations of candidate genes help to achieve genetic markers for the selection of animals which have a better protection against infections (Adler et al. 2013).
Heritability estimations of pro-inflammatory cytokines (IL-1B, IL-8, TNF and IL-6) were obtained in the study of Flori et al. (2011a). This research group observed weak to moderate heritability for the above named cytokines. Heritability was estimated, regarding the effect of PRRSV from 0.12 to 0.15 for number born alive, number stillborn and number of mummies in infected sows (Lewis et al. 2009). In their review Murtaugh et al. (2010) mentioned an actual research gap, concerning the heritability of PRRSV resistance. With their results Boddicker et al. (2012) underlined the idea of an improvement of the host resistance to PRRS and presented a moderate heritability of 30 % for the traits viral load and body weight gain post experimental PRRSV infection.

2.3.4 Prevention and control strategies

In general, the objectives of PRRSV prevention are: to stop the entry of the virus into the herd, to control it and to limit the adverse effect of the virus in various stages of production. On the one hand a variety of modified-live virus vaccines (MLV) and inactivated vaccines are commercially available, on the other hand management and animal husbandry procedures have been developed for the protection of the animals (reviewed by Zimmerman et al. 2012). Huang and Meng (2010) discussed in their review the PRRSV vaccine development, they mentioned the limitations of current MLVs and of inactivated vaccines. The main problems with the MLVs are the shedding of the vaccine virus, the incomplete protection and the risk to raise persistent infections, followed by the reversion to virulence. The control with the current vaccines remains problematic because the universality of an efficient PRRS vaccination has not been established and the genetically diversified field strains are circulating worldwide (reviewed by Huang and Meng 2010).
Elimination methods were reviewed by Corzo et al. (2010), they mentioned serological testing, herd depopulation and repopulation, connected with increasing costs as well as herd closure and regional elimination. They described the idea of creating a voluntary regional program which could be a powerful tool to eliminate the virus from a region and

to avoid re-infections. This tool should contain all factors and knowledge about epidemiology, biosecurity practices and elimination methods (Corzo et al. 2010).

Another possibility to control and to reduce the impact of PRRS is the development of breeding programmes, including host genetic improvement for disease resistance and tolerance (Flori et al. 2011b, Lewis et al. 2007, Lewis et al. 2009). This challenging objective can be substantiated from previous studies where the possible role is explained which breed effect may have in determining host resistance/susceptibility (Halbur et al. 1998, Petry et al. 2005). Flori et al. (2011b) demonstrated that many immune parameters were genetically controlled, they requested that a related immune competence with the resistance to disease has to be achieved. As mentioned before (compare chapter 2.3.3) Boddicker et al. (2012) stressed the idea of an improvement of the host resistance to PRRS. The understanding of the genetic components, involved in the response to PRRSV, are still unclear. Additionally, the key mechanisms by which the virus interferes with the host immune system are still inexplicit, too (Genini et al. 2008, Xiao et al. 2010b).

2.4 Aims of the present study

The aims of the present study should be achieved by using the latest high-throughput sequencing technology. The hypotheses reflect probable results which must be verified or falsified by the findings of the present study.

Aims of the present study:

- The understanding and the examination of how genetic components are involved in the immune response to PRRSV infection

- The characterization of the changes in the global transcriptome profile after PRRSV infection

- The detection of expression profiles in different respiratory cell types (DCs, PAMs as well as trachea epithelial cells) post PRRSV infection

- The identification of candidate genes which have a high impact on the host disease response to PRRSV

Hypotheses:

1. After a short period (within 24 h) of infection with PRRSV remarkable transcriptional reactions can be observed in DCs of pigs.

2. These reactions have an essential influence on the following pigs' immune responses to PRRSV, especially on immune related genes and proteins.

3. Based on the different genetic background of Pietrain and Duroc pigs, their cellular immune reactions are different during PRRSV infection.

3 Material and Methods

3.1 Materials

During this experiment, various chemicals, kits, reagents and culture media, purchased from different manufacturers, were used. Beside, during data analysis multifarious software packages, tools and databases were utilized.

3.1.1 Materials for laboratory analysis

Manufacturer/Supplier	Chemicals
Agilent Technologies Deutschland GmbH, Böblingen	RNA 6000 Nano Kit, RNA 6000 Nano Reagents
AppliChem GmbH, Darmstadt	Ammonium chloride (NH_4Cl)
Beckman Coulter GmbH, Krefeld	GenomeLab™ DTCS Quick Start Kit
Bio-Rad Laboratories GmbH, Munich	iTaq™ Universal SYBR® Green Supermix
Carl Roth GmbH + Co. KG, Karlsruhe	Roti®-Histofix 4 % (pH 7), Thiazolyl blue, Ethidium bromide, Aceton, Methanol, Crystal violet, Formaldehyde 37 %, Acetic acid, Tris Base, 2-Propanol ≥ 99.5 %, Bromphenol blue, Ethylenediaminetetraacetic acid (EDTA), Thiazolyl Blue Tetrazolium Bromide (MTT), Xylencyanol, di-Sodium Hydrogen Phosphat 2 Hydrate (Na_2HPO_4•2 H_2O), Glycerol, Potassium dihydrogen phoshate (KH_2PO_4), Potassium chloride (KCl), Sodium hydroxide (NaOH), Potassium bicarbonate ($KHCO_3$), Hydrochloric acid (HCl) fuming 37 %
Eurofins, Ebersberg	Primer (Table 3 and Table 4)
FCM BioPolymer, Brussels, Belgium	Avicel® RC581
Fisher Scientific GmbH, Schwerte	Sodium chloride (NaCl)

Genaxxon bioscience GmbH, Ulm	DF Taq Polymerase S (DNA-free)
InvivoGen, USA	Lipopolysaccharide from E. coli O111:B4 (LPS-EB) Ultrapure
Life Technologies GmbH, Darmstadt (Life Technologies™, Invitrogen™, Gibco®, Molecular Probes®)	Dithiothreitol (DTT), Dulbecco's Modified Eagle Medium (DMEM), RPMI 1640 Medium GlutaMAX™, LHC-9 Medium, Gentamicine (10 mg/ml), Fetal Bovine Serum (FBS), Penicillin-Streptomycin 100 x concentrate (Penicillin 10,000 units/ml, Streptomycin 10,000 µg/ml), (10,000 U/ml), sterile calcium-magnesium free Dulbecco's Phosphate-Buffered Saline (DPBS), MEM Non-Essential Amino Acids 100 x (MEM-NEAA), Trypsin-EDTA, Fungizone® Antimycotic, RNase-Free DNase Set, SuperScript® II Reverse Transcriptase, OptiPRO™ SFM, 5 x First-Strand buffer, Vybrant™ Phagocytosis Assay Kit
PAA Laboratories GmbH, Cölbe	DPBS (1 x), DMEM, MEM, Penicillin-Streptomycin, Trypsin-EDTA
Promega GmbH, Mannheim	Olig(dt)15 Primer, Random Primers, RNasin® Plus RNase Inhibitor, 10 x PCR buffer
Qiagen GmbH, Hilden	RNase-Free DNase Set, AllPrep® DNA/RNA/Protein Mini Kit
Reagena, Toivala, Finland	REASTAIN® Quick-Diff Kit
R&D Systems Inc., Minneapolis USA	IL-12p40, IL-1ß, TNF-α, IFN-γ and IL-8 Immunoassay
Roche Diagnostics Deutschland GmbH, Mannheim	Liberase™ Research Grade
Sigma-Aldrich Chemie GmbH, Taufkirchen	2-Mercaptoethanol, Trypan Blue Solution (4 %), Histopaque®-1083, NaN_3 (10 mM), Sucrose, Mineral oil, Sodium Pyruvate, Dimethyl sulfoxide (DMSO) ≥ 99.9 %, Deoxynucleotide Set, 100 mM, Hepes (10 mM)

STARLAB GmbH, Hamburg	StarPure Agarose
USB, Ohio, USA	ExoSAP-IT
VWR International GmbH, Darmstadt	Ethanol absolute AnalaR NORMAPUR® ACS

3.1.2 Buffer, reagents and media

All solutions, used in these investigations, were prepared with double-distilled water (ddH_2O), pH was adjusted with sodium hydroxide (NaOH) or hydrochloric acid (HCl).

Agarose loading buffer		
Bromphenol blue	0.0625	g
Xylencyanol	0.0625	g
Glycerol	7.5	ml
ddH_2O added to	25	ml
Avicel		
Avicel	12	g
ddH_2O added to	500	ml
Crystal violet solution 2 %		
Crystal violet	5	g
Formaldehyde 37 %	25	ml
Ethanol 99,9 %	50	ml
ddH_2O added to	175	ml
dNTP solution		
dATP (100 mM)	10	µl
dGTP (100 mM)	10	µl
dTTP (100 mM)	10	µl
ddH_2O added to	400	µl
EDTA (0.5 M), pH 8.0		
EDTA	146.12	g
ddH_2O added to	1000	Ml

Sucrose 36 %

Sucrose	180	g
ddH_2O added to	500	ml

Staining Buffer

DPBS	196	ml
FBS (2 %)	4	ml
NaN_3 (10 mM)	130	mg
Hepes (10 mM)	476	mg

Tris-acetate-EDTA (TAE)

Acetic acid 100 %	571	ml
Tris Base	242	g
EDTA	100	ml
ddH_2O added to	1	ml

Red Blood Cell (RBC) lysis buffer, pH 7.4

NH_4Cl	4.14	g
$KHCO_3$	0.5	g
EDTA	0.037	g
ddH_2O added to	500	ml

Phosphate buffered saline (PBS), pH 7.4 (without Ca ++ and Mg ++)

NaCl	8	g
KCl	0.2	g
$Na_2HPO_4 \bullet 2\ H_2O$	1.44	g
KH_2PO_4	0.24	g

3.1.3 Equipment and consumables

Manufacturer	Equipment
Agilent Technologies Deutschland GmbH, Böblingen	2100 Bioanalyzer
B. Braun Melsungen AG, Melsungen	Surgical Disposable Scalpels, Certomat® MV, Meliseptol®
BD Biosciences, Heidelberg	Cell Strainer 40 µm, Cell Strainer 70 µm, BD Falcon™ 96-well imaging plate, FACSCanto flow cytometer
Beckman Coulter GmbH, Krefeld	GenomeLab™ GeXP Genetic Analysis System, Optima™ L-80XP Ultracentrifuge, SW28Ti Beckman Coulter rotor, Open-Top Thickwall Polycarbonate Tube capacity 38 ml, CEQ 8000 Genetic Analysis
Bio-Rad Laboratories GmbH, Munich	MyCycler™Thermal Cycler, Gel Doc™ XR, Electrophoresis, Power Pac™ Basic
BioTek Instruments GmbH, Bad Friedrichshall	Synergy™ 2
BRAND GmbH + Co. KG, Wertheim	Accu-jet® pro pipette controller, Pipettes (0.5 - 10, 2 - 20, 20 - 200, 100 - 1000 µl)
Carl Roth GmbH + Co. KG, Karlsruhe	Rotilabo® Filter 0.22 µm, Multi® Quick Rack Transfer System, Petri dishes, 25 Mµlti® MIKRO ULTRA G 0.1 - 10 µl, SafeSeal® Tubes 2.0 ml, SafeSeal®Tubes 1.5 ml, Mµlti®-Ultra Tubes 0.65 ml
Carl Zeiss Jena GmbH, Jena	Axio Cam MRC5, Televal 31 5x/0.12 Microscope, TELAVAL31
Corning, USA	Cell Culture Flask (75 cm², 175 cm²), Deck Works™ Pipet Tips (10, 200, 300, 1000 µl)
Engelbrecht Medizin- und Labortechnik GmbH, Edermünde	Objectslide 76 x 26 mm

Eppendorf AG, Hamburg	Pipettes (0.5 - 10, 2 - 20, 20 - 200, 100 - 1000 µl), Centrifuge (5810R, 5424, 5416, 5415R), epDualfilter T.I.P.S®, Heating block Thermomixer comfort,
Fisher Scientific UK Ltd, Loughborough	Memmert CO_2 incubator
GFL Gesellschaft für Labortechnik mbH, Burgwedel	Water-bath 1083
Gilson, Inc., USA	Pipettes (0.5 - 10, 2 - 20, 20 - 200, 100 - 1000 µl)
Greiner Bio-One GmbH, Frickenhausen	Cell Scrapers , Aspirations Aspirating Pipette, serological Pipettes (1, 2, 5, 10, 25 ml), Cell Culture Flask
HERMLE Labortechnik GmbH, Wehingen	Universal High speed Centrifugation (Z 300 K, Z 300, Z 200 M/H, Z 233 MK, Z 323 K)
Kaltis Europe GmbH, Niederweningen, Switzerland	-80 °C/Typ499
KNF Neuberger GmbH, Freiburg	Mini LaboportVacuum Pump
Labomedic GmbH, Bonn	Cryo-tube Cryo.S™, Pipette tips, Pasteur pipette, Coverslip, Sterillium
Life Technologies GmbH, Darmstadt (Applied Biosystems®)	StepOnePlus™ Real time PCR System, MicroAmp® Fast Optical 96-well Reaction Plate with Barcode, 0.1 ml
Merck KGaA, Darmstadt (Merck Millipore)	Millipore apparatus, Milli-Q® Biocel, Stericup and Steritop Vacuum Filter Cups (500 ml)
Nikon GmbH, Düsseldorf	Microscopes ECLIPSE TS100, Digital Camera System for Microscopy Digital Sight Series DS-Fi1
Paul Marienfeld GmbH & Co. KG, Lauda-Königshofen	Counting chambers
PEQLAB Biotechnologie GmbH, Erlangen	Nano Drop 2000c

Pharmazeutische Handelgesellschaft mbH, Garbsen - Berenbostel	T61, Ketamin
SANYO North America Corporation, USA	Ultra-Low Temperature FREEZER MDF-U73V
SARSTEDT AG & Co., Nümbrecht	Centrifuge tubes (15 ml, 50 ml), Sample tube (5 ml, 75 x 12 mm), Cryotubes, Aspiration 2 ml
STARLAB GmbH, Hamburg (CytoOne®)	Tissue culture flask (25 cm², 75 cm²), Cell culture plates (6 well, 24 well, 96 well), X-Clear Advanced Polyolefin StarSeal
Systec GmbH, Wettenberg	Autoclave V120
Taylor-Wharton Germany GmbH, Husum	Liquid Nitrogen LS 750
Thermo Eectron Corporation, Waltham, MA	Fluorescence microplate reader
Thermo Fisher Scientific Biosciences GmbH, St. Leon-Roth	NanoDrop 8000, Safety Cabinet HERAsafe® and HERAcell® 240
Tuttnauer Europe B.V., Netherlands	ELV FullyAutomaticAutoclave 3870
VWR International GmbH, Darmstadt (Axygen®)	PCR®StripTubes
ZVG Zellstoff Verarbeitung AG, Niederbipp (zetClean®)	Wiper Bowl

3.1.4 List of software programs and statistical packages

Programs (software), homepages and statistical packages	Source of the programs (software, homepage) and statistical packages
bedtools	http://bedtools.readthedocs.org/en/latest/
Bioconductor packages:	http://www.bioconductor.org
biomaRt	
DESeq package	
GSEABase	
Gostatspackage	
Ismeans	
org.Ss.eg.db	
BLAST program	http://blast.ncbi.nlm.nih.gov/Blast.cgi
Bowtie 2	http://bowtie-bio.sourceforge.net/bowtie2/index.shtml
cutadapt	http://code.google.com/p/cutadapt/
D-NetWeaver	https://cbim.urmc.rochester.edu/software/d-netweaver/
ELISA Software	http://elisaanalysis.com
Entrez Gene	http://www.ncbi.nlm.nih.gov/sites/entrez?db=gene
Fastqc	http://www.bioinformatics.babraham.ac.uk/projects/fastqc/
Microscope Software	Axio Vision from Carl Zeiss
National center for biotechnology information (NCBI)	http://www.ncbi.nlm.nih.gov/http://www.ncbi.nlm.nih.gov/gene
Primer design	Primer3; http://primer3.ut.ee/
R statistical computing and graphics software	http://www.r-project.org/
Tophat	http://tophat.cbcb.umd.edu
SAMStat	http://samstat.sourceforge.net/
Samtools	http://samtools.sourceforge.net/samtools.shtml
seqtk	https://github.com/lh3/seqtk

3.2 Methods

3.2.1 Experimental animals

For time-course experiments six female 30 days old piglets of two different porcine breeds (Pietrain and Duroc) were selected from the teaching and research station of Frankenforst, University of Bonn, Germany. The three Pietrain piglets as well as the three Duroc piglets were selected from one litter. The pigs were free from all major pig diseases (PRRSV, porcine circovirus type 2, porcine parvovirus) and were exposed to the same unique environmental conditions. At the age of 28 days the piglets were weaned and placed in collective pens. The animals were vaccinated, following a specific vaccination schedule. The breeding sows are inoculated with Procilis® PRRS (Intervet) live vaccine three times per year, this happens independently of the sows' status. Additionally, the sows are vaccinated against porcine parvovirus and swine erysipelas three times per year. According to these procedures, the newborn piglets receive a passive immunity by consuming protecting antibodies of the mother's colostrum. The piglets themselves are vaccinated against mycoplasma at day three and ten of life.

3.2.2 Preparation of cells

In this study PAMs, lung DCs and trachea epithelial cells were isolated from the six 30 days old piglets. The animals were humanely euthanized with a doses of ketamin and afterwards T61 (Pharmazeutische Handelsgesellschaft mbH), adjusted to the individual body weight through the vena cava cranialis, due to the permission of the Veterinary and Food Inspection Office, Siegburg, Germany in order to investigate the animals scientifically. After the animals had been euthanized at the research station, their thorax were opened and the lungs in total, inclusive with the trachea were carefully removed and transported on ice to the institute. The complete trachea was placed in a 50 ml tube with sterile calcium-magnesium free Dulbecco's Phosphate-Buffered Saline (DPBS), supplemented with 1 % Penicillin-Streptomycin 100 x concentrate (Penicillin 10,000 units/ml, Streptomycin 10,000 µg/ml) and 1 % Fungizone® Antimycotic and also transported on ice.

Pulmonary alveolar macrophages

As mentioned before, the thorax of the piglets was opened and the lungs were removed softly, cleaned of blood by washing them with sterile DPBS and transported on ice. At the laboratory the PAMs were isolated by lung lavage of the major airways with sterile DPBS, as described by Wensvoort et al. (1991) but with few modifications. Sterile DPBS (50 - 100 ml) was poured into the lungs for 3 times and gently massaged, to spread the liquid before the lavage fluid was collected in a sterile bottle. The recovered lavage fluid was filtered by using sterile gauze and the cells were pelted by 1000 rpm for 10 min at 4°C. All centrifugation cycles were gradually slowed down to prevent any turbulence. After the centrifugation the supernatant was carefully and completely removed and the isolated cells were treated with 5 ml Red Blood Cell (RBC) lysis buffer solution to prevent a contamination with red blood cells. The following incubation period with RBC lyses buffer took 5 min at room temperature (RT). The reaction of lysis buffer was stopped with 15 - 20 ml sterile DPBS and a cell pellet was produced. This process was repeated as often as required until all red blood cells were completely removed. The viability of the cells was determined on the basis of trypan blue dye exclusion. The final cell suspension was diluted in 10 % trypan blue in sterile DPBS and the cells were counted with a hemocytometer. Then the cells were finally cultured in Roswell Park Memorial Institute 1640 medium (RPMI 1640 Medium, GlutaMAX™) containing 10 % Fetal Bovine Serum (FBS) and 1 % Penicillin-Streptomycin 100 x concentrate, 1 % Fungizone® Antimycotic, 1 % Sodium Pyruvate and 1 % MEM Non-Essential Amino Acids 100x (MEM-NEAA 100 x) in a humidified 5 % CO_2 atomosphere at 37°C.

Dendritic cells

Dendritic cells (DCs) were isolated as described by Loving et al. (2007) but with several modifications.

Before isolating the swine lung DCs, the lungs were washed with sterile DPBS. By lung lavage, PAMs were removed to minimize cell contamination (Grayson et al. 2007). To isolate lung DCs, different pieces of the lavaged, perfused lungs were cut and minced in ice cold sterile DPBS in a sterile petri dish. The tissue was minced with scissors and scalpels and poured in 50 ml tubes with sterile DPBS, supplemented with 2.5 mg Liberase and 20 µl DNase I. For an incubation period of 2 h the tissue-enzyme-mixture was kept in

a 37°C pre-heated shaking water-bath. Following the incubation time, the composite was filtered through a 70 µm BD cell strainer, the enzyme activity was stopped by inflicting DCs culture medium which consisted of RPMI-1640 supplemented with 10 % FBS, 1 % Gentamicin, 1 % Penicillin-Streptomycin 100 x concentrate, 1 % Fungizone® Antimycotic and 1 % Sodium Pyruvate. Next the cells were pelleted by 1500 rpm for 5 min at 4°C and the supernatant was carefully and completely removed. To prevent a contamination with red blood cells, the RBC lysis buffer process was done before the cells were seeded into the flasks. This process and the viability detection are described before (compare page 32).

Trachea epithelial cells

The trachea was transported to the laboratory on ice in a 50 ml tube, supplemented with a mixture of sterile DPBS, 1 % Penicillin-Streptomycin 100 x concentrate and 1 % Fungizone® Antimycotic. Before starting to collect the trachea epithelium, the trachea was cleaned from blood and other tissue particles with sterile DPBS. Then the trachea was placed in a sterile petri dish, opened with a scalpel and the inner trachea surface was removed by peeling off the skin with forceps. This inner epithelium was split into small pieces and placed into 6 well plates. After a 1 - 4 min surface drying process the trachea epithelial cell medium was added drop by drop. The mixture 1:1 of RPMI-1640 and LH-9 medium, supplemented with 1 % FBS, 1 % Penicillin-Streptomycin 100 x concentrate and 1 % Fungizone® Antimycotic. Every three days the medium was carefully removed and fresh medium was added to each well. After a period of seven days the tissues were taken out and the trachea epithelial cells grew to a monolayer. At this time point the FBS concentration was increased to 10 %.

3.2.3 Cell characterization

Cell characterization by flow cytometry analyses

In the 1970s flow cytometry and cell sorters were developed in order to characterize single-cells, due to their physical and chemical properties. It is a laser-based method and measures the single-cells in liquid suspension by passing them through an electronic detection apparatus (Kamentsky et al. 1965, Shapiro 2003).

Cell characterization by flow cytometry analyses on isolated lung DCs and PAMs was performed as follows: The surface antigens antibodies were used singly and labelled with fluorescein isothiocyanate (FITC), allophycocyanin (APC), phycoerythrin and a cyanine dye 7 (PE-Cy7) as displayed in Table 2. The cells were harvested, washed with sterile DPBS and the cell numbers were counted. Afterwards 1 x 10^6 cells were incubated under dark conditions with 10 µl of conjugated antibody to CD11c, CD86, CD163 and 20 µl of CD40 for 30 min at 4°C. The cells were stained, according to the antibodies manufacturers' recommendations. After two washing cycles, using the flow cytometry staining buffer, the cells were pelleted and finally resuspended within 400 µl flow cytometry staining buffer. The cell characterization was performed, using the FACSCanto flow cytometer (BD Biosciences), the analyses were executed, using *FlowLogic*® software (BD Biosciences; Germany) in order to enumerate the cell population, based on cell surface marker.

Table 2: Antibodies, used for flow cytometry analyses

Antibody	Isotype	Clone	Fluorescence	Company
CD86	IgG1	37301	APC	R&D Systems, cat. FAB141A
CD40	IgG1	G28.5	FITC	NOVUS Biologicals®, cat. NB100-77786
CD11c	IgG	N418	PE-Cy7	eBioscience, cat. 25-0114
CD163	IgG1	2A10/11	FITC	Abdserotec, cat. MCA2311F

Cell characterisation by immunofluorescence assay

For the immunofluorescence (IF) microscopy trachea epithelial cells were seeded on glass slides and on the following day washed with DPBS. Before the cells were incubated with a primary mouse monoclonal antibody against pan-cytokeratin (mouse-monoclonal, Abcam, C-11, cat. ab7753) and zonula occludens (ZO-1 Mid) (rabbit polyclonal, Invitrogen, cat. 40-2200) diluted 1:400 in DPBS overnight at 4°C, the cells were fixed on the glass slides with aceton-methanol. A cyanine 3-labeled donkey-anti-mouse serum and cyanine 2-labeled donkey-anti-rabbit serum (Dianova, Hamburg, Germany) were applied as secondary antibodies. Nucleus were tagged in blue through the counterstaining with 4', 6'-diamidino-2-phenylindole (DAPI). All photographic illustrations were done by using corresponding microscopic settings with 207 a Motic Axiovision microscope (Zeiss) (Eckerle et al. 2014).

Cell staining

REASTAIN® Quick-Diff Kit (Reagena, Toivala, Finland) was used for the cell element staining. Lung DCs and PAMs were seeded on glass slides. Before the cells were dipped 5 - 10 times for 1 sec into the REASTAIN Quick-Diff FIX solution the slides were air-dried. Afterwards the slides were dried again and then quickly immersed into the REASTAIN QICK-DIFF RED solution 15 times for 1 sec. Once more the slides were dried and then placed into the REASTAIN QUICK-DIFF BLUE solution 15 times for 1 sec. Subsequently the slides were rinsed with a 1:20 prepared buffered water solution and air dried afterwards. The stained cells were imaged under the microscope (Nikon) and are listed in appendix (Figure A1 and Figure A2).

3.2.4 Porcine reproductive and respiratory virus propagation

The European prototype PRRSV strain LV and MARC-145 cells were donated by Prof. Dr. Nauwynck from the Department of Virology, Parasitology and Immunology, Ghent University in Belgium.
All experimental works in connection with PRRSV were done in the Institute of Virology, University of Bonn Medical Centre. The MARC-145 a stable, mycoplasma-free cell line, a highly permissive clone of African Monkey kidney cell line MA104, was utilized in these experiments for PRRSV propagation. Cells were cultured in DMEM containing 10 % FBS, 1 % Penicillin-Streptomycin 100 x concentrate and 1 % Gentamicine in a humidified 5 % CO_2 atmosphere at 37°C. Next the cells were inoculated with PRRSV at about 1 - 2 days after seeding (approximate time to a doubling of the population). Cell cultures were examined daily for the appearance of a cytophathic effect (CPE). The CPE was assayed, using the light microscope after 5 - 6 days post infection (dpi). The culture supernatants of 5 - 6 dpi were collected and used to determine the virus growth with the plaque titration method.

Plaque assay for detection of viral particles

For the measurement of virus infectious units the plaque assay is a very widely used approach (Dimmock et al. 2007, Herzog et al. 2008, Matrosovich et al. 2006).
To quantify the virus titer the culture supernatant was collected. Briefly, 200 µl of virus in 10-fold serial dilution was added in duplicates to a monolayer of Marc-145 cells in a 24 well plate. After 1 h of incubation at 37°C in 5 % CO_2 atmosphere, the viral inoculum was aspirated and the cells were washed twice with sterile DPBS. After that 500 µl of Avicel overlay (Avicel® RC58, FCM BioPolymer, Belgium) with MEM medium, supplemented with 5 % FBS, was added to each well. Avicel overlays were made by mixing 2.4 % Avicel solution with an equal volume of 2 × MEM medium. After 4 days of incubation the cells were fixed with a solution of 4 % formaldehyde for 30 min, afterwards the plate was air dried for 10 - 20 min before proceeding to the next steps. Next the plate was stained with 500 µl/well of 2 % crystal violet solution for 15 min, then removed and the plate was washed carefully with ddH_2O. As a result in the cell monolayer round clear areas named plaques were counted visually and the virus titer in plaque-forming units per ml (PFU/ml) was calculated.

Purification of viral particles by ultracentrifugation

The purification of viral particles and the improvement of virus titer were performed by ultracentrifugation, as described by (Delputte et al. 2002) but with few modifications. Briefly, viral supernatants from infected MARC-145 cells were cleared from cell debris 6 dpi by centrifugation at 1000 rpm for 10 min. Afterwards 35 ml viral supernatant was placed cautiously on 10 ml of a 36 % sucrose cushion in each plastic ultracentrifugation tube (Open-Top Thickwall Polycarbonate Tube capacity 38 ml, Beckman Coulter). The layered plastic tubes were admitted in pre-cooled rotor tube holder for ultracentrifugation at 32,000 rpm for 3 h at 4°C by using the SW28Ti Beckman Coulter rotor and the pre-cooled Beckman Coulter Optima™ L-80XP Ultracentrifuge. After centrifugation the liquid was removed and the virus pellets were resuspended in 350 µl cold sterile DPBS. Next the virus was reposed for 2 h at 4°C, then the resuspension was repeated, before storing the virus in cryo-tubes at -80°C. The infectious dose of the virus stock was calculated by the plaque titration as previously described.

3.2.5 Virus infection of experimental cells

Lung DCs, PAMs and trachea epithelial cells were seeded in 24 well plates at approximately 2.5 x 10^5 cells per well and incubated until the monolayer was confluent. Before infecting the cells, they were washed with 100 µl sterile DPBS and infected at a multiplicity of infection (MOI) of 0.01. The MOI was determined as the ratio between PFU of virus stock, used for the infection, and the number of cells (Hewitt et al. 2006). Virus inoculum in 200 µl OptiPRO™ SFM was added to each well, 200 µl OptiPRO™ SFM without virus was done in non-infected wells at time point 0 (0 h). Within 1 h of incubation at 37°C in 5 % CO_2 the virus bound to but did not enter into the cells. The viral inoculum was aspirated and the cells were washed again with sterile DPBS. Subsequently 500 µl/well of cell culture medium was added, the medium had been especially prepared for each cell type. The experimental design I is depicted in Figure 6. The infection of Pietrain and Duroc lung DCs, PAMs and trachea epithelial cells was performed individually for each animal. The sample collection – harvesting of cells and supernatants - was done before the infection at time point 0 (0 h, non-infected samples) and at 3, 6, 9, 12, 24 hours post infection (hpi).

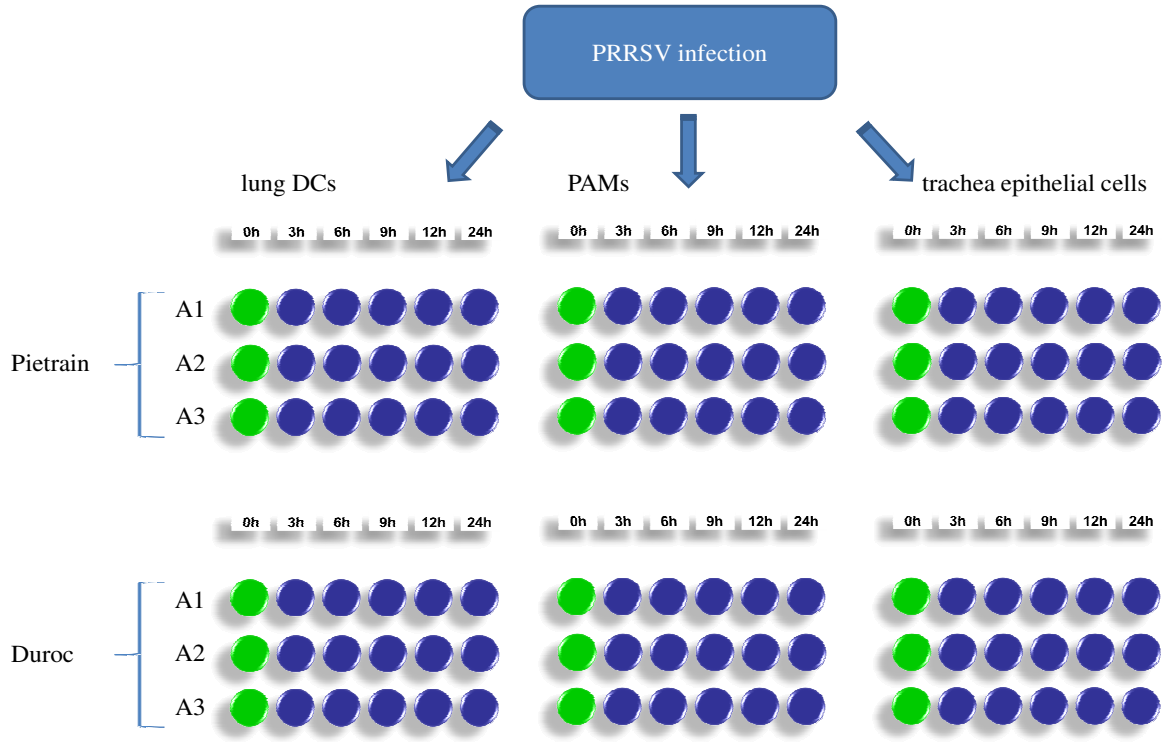

Figure 6: Experimental design I for PRRSV infection: Pietrain (n=3, animal A1, A2, A3) and Duroc (n=3, animal A1, A2, A3) lung DCs, PAMs and trachea epithelial infected with LV; sample collection: non-infected cells (green circle) at 0 h and infected cells (blue circle) at 3, 6, 9, 12, 24 hpi

3.2.6 Measurement of cell viability

The viability was determined with MTT (Thiazolylblau 3-(4.5-Dimethylthiazolyl-2)-2.5-diphenyl-2H-tetrazoliumbromid) assay in untreated samples after 6 and 12 h and in virus treated cells at 6 and 12 hpi. The MTT assay is a frequently used and easily reproducible method to measure the cell viability in different types of cell cultures (Stockert et al. 2012). For the assay 5 mg/ml MTT was dissolved in sterile DPBS, yielding a yellowish solution. Lung DCs, PAMs and trachea epithelia cells were seeded in doubles in 96 well plates, infected with PRRSV at a MOI of 0.01. After 1 h of incubation at 37°C in 5 % CO_2 the viral inoculum was aspirated and fresh specific cell medium was added. Additionally, 25 µl of MTT-solution were added for an incubation time of 2 h at 37°C in 5 % CO_2, during this procedure the blue dye reaction (Formazan dye) was performed. At the end of the incubation period the medium was removed and 100 µl of 4 % formaldehyde solution in DPBS, for fixing the cells, was added to each well and incubated for 30 min at RT.

Afterwards the formaldehyde was carefully removed and 100 µl Isopropanol (2-Propanol) was added to each well and placed on the shaker for 10 min. This mechanism eluted the blue dye from the cells. The absorbance of this converted dye was quantified by measuring at a wavelength of 562 nm λ_1 and at λ_2 630 nm on the plate reader Synergy™ 2 (BioTek Instruments). The calculation of relative cell viability (%) was based on the subtraction of blank optical density (OD) values from all other OD values and the relative cell viability was evaluated by the following formula: (viable cells) % = (OD treated sample)/(OD untreated sample) x 100.

3.2.7 Estimation of phagocytosis activity

Phagocytosis activities of lung DCs, PAMs and trachea epithelial cells were performed with the Vybrant™ Phagocytosis Assay kit (Molecular Probes®). The fundamental principle is based on the detection of the intracellular fluorescence, emitted by the ingestion of particles, as well as on the effective fluorescence quenching of the extracellular probe by trypan blue (Wan et al. 1993). For this assay cells were cultured in a 6 well plate and harvested by using cell scrapers. After two washing cycles with sterile DPBS the cells' density was adjusted to 10^6 cells/ml. Five negative controls, five positive controls and four experimental samples were performed and placed in a BD Falcon™ 96-well imaging plate. The experimental samples (Pietrain and Duroc lung DCs and PAMs) were supplemented with 50 µl of the Lipopolysaccharide from E. coli O111:B4 (LPS-EB) Ultrapure (Invivo Gen) at 5 µg/ml in RPMI-1640 medium as well as trachea epithelial cells with 50 µl of the Lipopolysaccharide from E. coli O111:B4 (LPS-EB) Ultrapure (Invivo Gen) at 1 µg/ml in RPMI-1640 medium. Afterwards the experimental plate was transferred for a 4 h incubation period at 37°C with 5 % CO_2 to allow the cells to adhere on the micro plate surface. Accordingly to this incubation period, the RPMI-1640 medium was removed and 100 µl of fluorescent BioParticle suspension was added to each well. After a 2 h incubation period at 37°C in 5 % CO_2, the BioParticle suspension was aspirated from all wells, 100 µl trypan blue suspension was added to each well and incubated for 1 min at RT. Immediately, the trypan blue suspension was aspirated and the fluorescence measurement was done with a fluorescence microplate reader (Thermo Eectron, Waltham; MA, USA) using ~ 480 nm excitation and ~ 520 nm emission. The relative phagocytosis effect (%) was calculated on the basis of the net experimental reading and the net positive reading.

3.2.8 Phenotype analysis with cytokine assays

The concentrations of IL-12p40, IL-1ß, TNFα, IFN-γ and IL-8 in cell culture supernatants were measured, using commercially available porcine specific Enzyme-linked immunosorbent assay (ELISA) kits (R&D System, Minneapolis, MN, USA), as specified by the manufacturer's instructions. The cytokines secretion differences of PRRSV infected cells (lung DCs, PAMs, and trachea epithelial cells) were determined at 9 hpi. The OD values were detected, using the plate reader Synergy™ 2 (BioTek Instruments) by 450 nm. Standard and samples dilutions were added in duplicate wells. The concentrations (pg/ml) of IL-12p40, IL-1ß, TNFα, IFN-γ and IL-8 of cell culture supernatants of lung DCs, PAMs and trachea epithelial cells were generated by an interpolation of a standard curve run on each plate. The analyses were performed with a 4 Parameters Logistic (4PL) curve program (http://elisaanalysis.com/). A regression formula was used for the calculations which included the cytokine standard curve parameter.

3.2.9 RNA isolation

The experimental design II for RNA isolation is demonstrated in the following Figure 7. Total cellular RNA was extracted for two different purposes, on the one hand for the RNA-Sequencing (RNA-Seq) and on the other hand for the quantitative real-time PCR analyses. For the RNA-Seq the RNA isolation included infected (3, 6, 9, 12 and 24 hpi) pooled Pietrain (pool n=3) and pooled Duroc (pool n=3) lung DCs as well as non-infected (0 h) pooled Pietrain (pool n=3) and non-infected pooled Duroc (pool n=3) lung DCs (Figure 7). The quantitative real-time PCR analyses were done in two isolated schemes: on one side total cellular RNA of pooled Pietrain (pool n=3) and of pooled Duroc (pool n=3) samples (lung DCs, PAMs, trachea epithelial cells) were extracted, on the other side the RNA of non-pooled (lung DCs, trachea epithelial cells) samples were isolated (Figure 7).

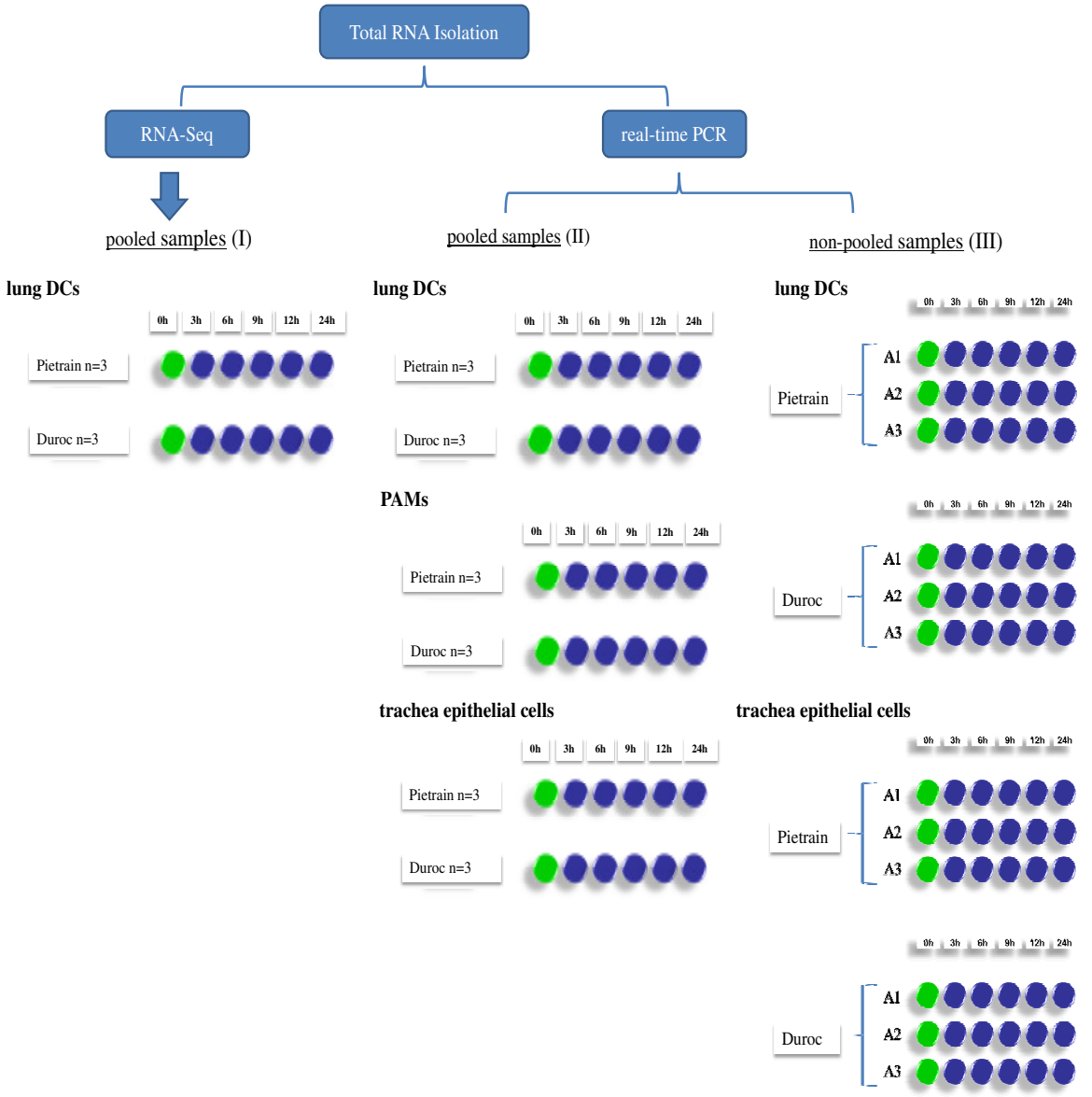

Figure 7: Experimental design II for total RNA isolation: RNA isolation for RNA-Seq of pooled Pietrain and Duroc lung DCs (I); RNA isolation for real-time PCR of pooled Pietrain and Duroc lung DCs and pooled Pietrain and Duroc PAMs (II) as well as of non-pooled lung DCs and non-pooled trachea epithelial cells (III) of Pietrain animals (A 1, 2, 3) and Duroc animals (A 1, 2, 3); non-infected cells (green circle) at 0 h and infected cells (blue circle) at 3, 6, 9, 12, 24 hpi

Preparatory work for total cellular RNA isolation

At six different time points (0 h, 3, 6, 9, 12, 24 hpi) the medium was completely removed and stored in -80°C for future assays and analyses. The cells were harvested, by adding 50 µl of trypsin to the cells for an incubation time of 3 - 5 min at 37°C in 5 % CO_2. Within this incubation time the adherent cells dissociated from the wells and appeared rounded in the suspension. To stop the trypsinization process, 100 - 150 µl of cell culture medium was added, mixed with the trypsin cell solution and replaced in a new collection tube for centrifugation at 1000 rpm for 5 min. The liquid was removed and 200 µl Lysis Buffer (AllPrep® DNA/RNA/Protein Mini Kit, Qiagen) was added to each cell pellet, mixed and the lysed cells were stored at -80°C. After all infection time points had been collected, the RNA isolation was continued. The total cellular RNA isolation was done with the AllPrep® DNA/RNA/Protein Mini Kit, according to the manufacturer's recommendations with slight modifications of chemical volumes, depending on the decreased specimens insert of 300 µl. Nearly all centrifugation steps were performed in a benchtop microcentrifuge at 10,000 rpm, the exceptions are mentioned in the text. The lysed samples were precisely unfreezed, homogenized by vortexing the tube for 1 min and then shortly down centrifuged.

Pooled RNA isolation of lung DCs for RNA-Sequencing

After the first preparation process, 100 µl of each lysed lung DCs were pooled together in one AllPrep DNA spin column and centrifuged for 30 sec. Each AllPrep spin column included the amount of lung DCs of one breed for one infection time point (compare experimental design II, Figure 7). The AllPrep DNA spin column was placed in a new collection tube and stored for further isolation at 4°C. The flow-through of the AllPrep DNA spin column was used to continue the RNA isolation, mixed with 200 µl 96 % ethanol absolute AnalaR NORMAPUR® ACS, transferred to a RNeasy spin column and centrifuged for 15 sec. The resulting flow-through was placed in a new tube and freezed by -80°C for following protein purification steps. The RNeasy spin column was reassembled in the collection tube, 450 µl RW1 Buffer was added, followed by a centrifugation step of 15 sec. Next the RNeasy spin column was washed twice with RPE Buffer: the first time with 350 µl, the second time with 250 µl. Then the RNeasy spin column was placed into a new collection tube and centrifuged at full speed for 1 min. Finally the RNeasy spin

column was transferred in a fresh 1.5 ml elution tube, provided with the kit. RNA was eluted with a total of 30 µl of RNase-and DNase-free water, also provided with the kit and centrifuged for 2 min. The total cellular RNA quality and quantity was measured by Nanodrop 8000 spectrophotometer (Thermo Fisher Scientific) and an Agilent Bioanalyzer with RNA 6000 Nano Kit (Agilent Technologies Inc, CA, USA), respectively. 5 µl of the isolated RNA samples were sent to GATC Biotech (Konstanz, Germany) for transcriptome analyses by RNA-Seq.

RNA isolation for quantitative real-time PCR of non-pooled samples

The total cellular RNA of non-pooled lung DCs and of non-pooled trachea epithelial cells (compare experimental design II, Figure 7) was isolated, using AllPrep® DNA/RNA/Protein Mini Kit (Qiagen), as described above and according to the manufacturer's recommendations with reduced usage of chemical volumes because of a decreased samples insert of 100 µl. The reduction included following volumes: 125 µl ethanol absolute AnalaR NORMAPUR® ACS, 300 µl RW1 Buffer, 200 µl and 150 µl RPE Buffer. Finally the total cellular RNA was measured by Nanodrop 8000 spectrophotometer (Thermo Fisher Scientific) and the complementary DNA (cDNA) was synthesized.

RNA isolation for quantitative real-time PCR of pooled samples

The total cellular RNA of pooled infected and of pooled non-infected lung DCs, PAMs and trachea epithelial cells (compare experimental design II, Figure 7) was extracted for all time points (0 h, 3, 6, 9, 12, 24 hpi). The RNA isolation process was similar to the RNA extraction of lung DCs for RAN-Seq and the cDNA was synthesized as described below.

cDNA synthesis of pooled and non-pooled total cellular RNA

The synthesis of cDNA, using SuperScript® II Reverse Transcriptase (Invitrogen™) was done with a final reaction volume of 20 µl and contained: cellular RNA, ddH_2O, 0.5 µl Olig(dt)15 Primer, 0.5 µl Random Primers, 0.7 µl RNasin® Plus RNase Inhibitor (Promega) as well as 0.3 µl SuperScript® II Reverse Transcriptase, 1 µl dNTPs, 2 µl DTT 0.1 M and 4 µl 5x reaction Buffer. Before adding the enzymes, the reaction mixture was

heated to 70°C for 5 min and placed directly on ice for 1 min. The cycling was performed at 25°C for 5 min, 42°C for 90 min and 72°C for 15 min. The synthesized cDNA was stored at -20°C until they were used for quantitative real-time reverse transcriptase polymerase chain reaction (qRT-PCR).

3.2.10 RNA-Sequencing

The TruSeq RNA Sample Preparation Kit (Illumina) (Figure 8) was used to sequence 12 lung DCs RNA samples (compare experimental design II, Figure 7) by GATC Biotech AG (Konstanz, Germany). The RNA was sequenced, using Illumina HiSeq 2000 with 100 bases single-read mode. The RNA-Seq library consisted of two pools, each included six samples. The whole RNA-Seq library was analyzed on two lanes of the same flow-cell. Before starting with the Illumina TruSeq RNA Sample Preparation Kit, 10 µl of RNase- and DNase-free water was added to the lung DCs RNA, to reach a total volume of 15 µl, followed by quality measurement with Agilent 2100 Bioanalyzer. The optimal processing for the 12 samples was done with the Low-Thoughput (LT) Protocol, selected from the TruSeq™ RNA Sample Preparation Guide. The following Figure 8 represents the whole processing of sample preparation, done by GATC Biotech (Konstanz, Germany). In essential it includes the purification of poly-A containing mRNA molecules, the mRNA fragmentation, the random primed first strand cDNA synthesis, followed by the second strand cDNA synthesis, the adapter ligation and the pooling of tagged libraries to two pools, each one consisting of six libraries. For sequencing Illumina Truseq PE Cluster Kit V3 and Illumina TruSeq SBS V3 Kit were used. The base calling, data filtration and sorting were done by CASAVA Pipeline Version 1.8.0. After the analyses of the samples on HiSeq 2000, FastQ files were produced, consisting of sequences and quality scores.

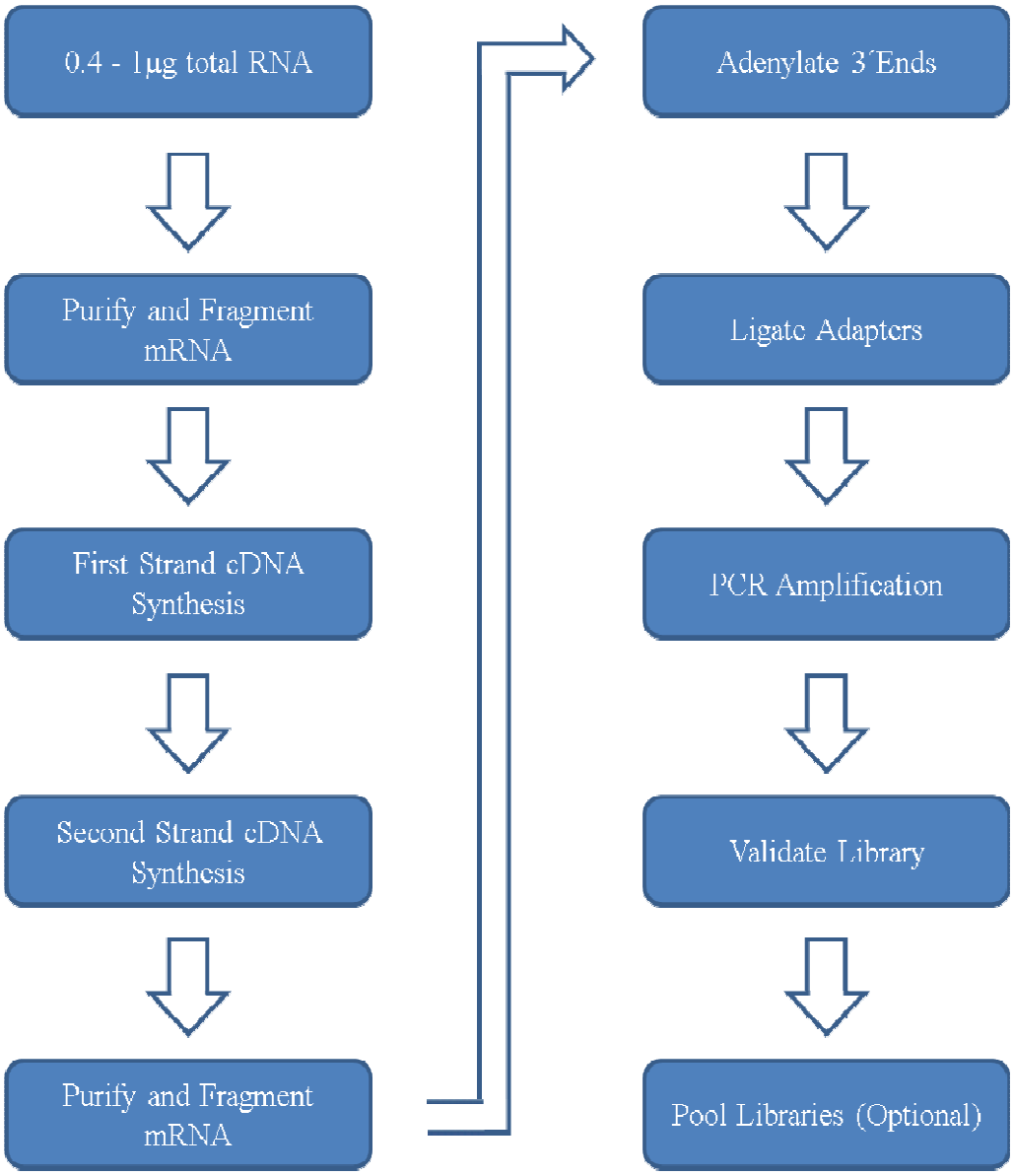

Figure 8: Workflow out of the LT TruSeq RNA Sample Preparation protocol

3.2.11 Validation of selected candidate genes by quantitative real-time polymerase chain reaction

The validation of the RNA-Seq data and the analyses of the expression profiles of selected candidate genes were performed by qRT-PCR. The expression abundances of these ten genes were determined for all six time points (0 h, 3, 6, 9, 12, 24 hpi) and in all three cell lines. Therefore non-pooled samples of lung DCs and non-pooled trachea epithelial cells as well as pooled samples of PAMs were investigated (compare experimental design II, Figure 7). All PCR primers (Table 3) were designed, using Primer3 online software (http://primer3.ut.ee/), and additionally proofed with Basic local Alignment Search Tool (http://blast.ncbi.nlm.nih.gov/Blast.cgi) to ensure specificity. Afterwards a PCR amplification product of each primer was validated by sequencing, using CEQ 8000 Genetic Analysis (Beckman Coulter). Each qRT-PCR reaction consisted of a sample in form of 2 µl cDNA (50 ng/µl), forward (F) and reverse (R) primers as well as 10 µl of iTaq™ Universal SYBR® Green Supermix (Bio-Rad Laboratories GmbH). The final reaction volume was 20 µl per well with RNase-and DNase-free water. The cycling conditions were conducted with the following program: 50°C for 2 min, 95°C for 10 min and 40 cycles of 95°C for 15 sec followed by 60°C for 1 min. A melting curve test was done, before verifying the presence of gene-specific peaks and the absence of primer dimer. The validation was performed with the use of qRT-PCR on the StepOnePlus™ Real time PCR System (Applied Biosystems®). The comparative threshold cycle (C_T) method was used to quantify the levels of mRNA abundance. The results were normalized with the expression level of two reference genes: Glyceraldehyde-3-phosphate dehydrogenase (GAPDH) and hypoxanthine phosphoribosyltransferase 1 (HPRT1).

Table 3: Primers and their sequences of ten selected candidate genes

Acc no[1]	Gene	P[2]	Sequence (5'-3')
HQ013301	Glyceraldehyde-3-phosphate dehydrogenase (GAPDH)	F[3]	GCTGGTGCTGAGTATGTCGT
		R[4]	CAAGCAGTTGGTGGTACAGG
NM_001032376	Hypoxanthine phosphoribosyl-transferase 1 (HPRT1)	F[3]	AACCTTGCTTTCCTTGGTCA
		R[4]	TCAAGGGCATAGCCTACCAC
NM_213779	Chemokine (C-C motif) ligand 4 (CCL4)	F[3]	CTCTCCTCCAGCAAGACCAT
		R[4]	CAGAGGCTGCTGGTCTCATA
NM_214087	CD80 molecule (CD80)	F[3]	TCAGACACCCAGGTACACCA
		R[4]	GACACATGGCTTCTGCTTGA
NM_214222	CD86 molecule (CD86)	F[3]	TTTGGCAGGACCAGGATAAC
		R[4]	GCCCTTGTCCTTGATTTGAA
NM_001001861	Chemokine (C-X-C motif) ligand 2 (CXCL2)	F[3]	ATCCAGGACCTGAAGGTGAC
		R[4]	ATCAGTTGGCACTGCTCTTG
NM_001003923	Interferon, beta 1, fibroblast (IFNβ1)	F[3]	ACCTGGAGACAATCCTGGAG
		R[4]	AGGATTTCCACTTGGACGAC
NM_001252429	Interleukin-6 (IL-6)	F[3]	GCTTCCAATCTGGGTTCAAT
		R[4]	GGTGGCTTTGTCTGGATTCT
NM_214113	Janus kinase 2 (JAK2)	F[3]	GACAGGAAATCCTCCCTTCA
		R[4]	TCACCTCCACTGCAGATTTC
NM_001097431	MHC class I antigen 1 (SLA-1)	F[3]	AGAAGGAGGGGCAGGACTAT
		R[4]	TCGTAGGCGTCCTGTCTGTA
NM_001113695	SLA-DRA MHC class II DR-alpha (SLA-DRA)	F[3]	ACTGGAACAGCCAGAAGGAC
		R[4]	AGAGCAGACCAGGAGGTTGT
NM_001044580	Signal transducer and activator of transcription 3 (acute-phase response factor) (STAT3)	F[3]	ATGCTGGAGGAGAGAATCGT
		R[4]	AGGGAATTTGACCAGCAATC

Acc no[1]= Accession number; P[2]= Primer, F[3]= Forward, R[4]=Reverse

3.2.12 Cytokine expression profile by quantitative real-time polymerase chain reaction

The expression profile of five selected cytokines was performed by qRT-PCR. Primers and their sequences are represented in Table 4. The process flow of primer design and qRT-PCR reactions proceeded as described above (compare chapter 3.2.11). The expression of these five genes was done for all six time points (0 h, 3, 6, 9, 12 and 24 hpi) and for all three cell lines. The analyses were performed with pooled samples of lung DCs, pooled PAMs and pooled trachea epithelial cells, as shown in experimental design II (compare chapter 3.2.9, Figure 7).

Table 4: Primers and their sequences for cytokine expression profiling

Acc no[1]	Gene	P[2]	Sequence (5'-3')
HQ013301	Glyceraldehyde-3-phosphatedehydrogenase (GAPDH)	F[3]	GCTGGTGCTGAGTATGTCGT
		R[4]	CAAGCAGTTGGTGGTACAGG
NM_001032376	Hypoxanthine phosphoribosyl-transferase 1 (HPRT1)	F[3]	AACCTTGCTTTCCTTGGTCA
		R[4]	TCAAGGGCATAGCCTACCAC
NM_213948	Interferon, gamma (IFN-γ)	F[3]	AGCTCCCAGAAACTGAACGA
		R[4]	AGGGTTCAAAGCATGAATGG
NM_001005149	Interleukin-1 beta (IL-1ß)	F[3]	GTACATGGTTGCTGCCTGAA
		R[4]	CTAGTGTGCCATGGTTTCCA
NM_214013	Interleukin 12B (natural killer cell stimulatory factor 2, cytotoxic lymphocyte maturation factor 2, p40) (IL-12p40)	F[3]	TCTCGACACGTGGAGATCAG
		R[4]	TTCACTCCAGGAGGAGCTGT
NM_213867	Interleukin 8 (IL-8)	F[3]	TAGGACCAGAGCCAGGAAGA
		R[4]	CAGTGGGGTCCACTCTCAAT
NM_214022	Tumor necrosis factor (TNF-α)	F[3]	CCACCAACGTTTTCCTCACT
		R[4]	CCAAAATAGACCTGCCCAGA

Acc no[1]= Accession number; P[2]= Primer, F[3]= Forward, R[4]=Reverse

3.2.13 Statistical analyses

The workflow of the next generation sequencing analysis and of the quantitative real-time PCR analysis is depicted in Figure 9. The intermediate steps will be explained in a short form.

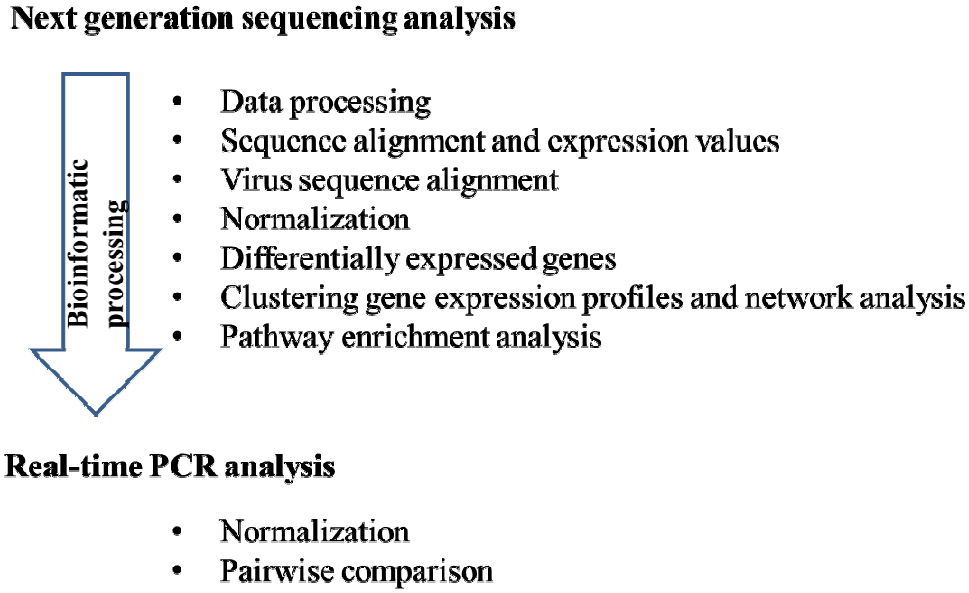

Figure 9: Workflow of statistical analyses

3.2.13.1 Next generation sequencing analysis

Data processing

FastQ Files were unzipped and the quality control check of the high throughput sequence data was performed with the supporting Java tool FastQC (http://www.bioinformatics.babraham.ac.uk/projects/fastqc/) (Wolf 2013). Next all overrepresented adapter sequences were trimmed by the use of the software cutadapt (http://code.google.com/p/cutadapt/) (Martin 2011). For this process the error rate was fixed at 5 % and at a 80 % overlapping rate. Additionally, based on the first quality control output, the first 15bp of the raw sequence data was removed by the usage of the tool seqtk (https://github.com/lh3/seqtk). Afterwards the quality control check by FastQC was repeated in order to monitor the sequence quality improvements of the previous steps. Further, the software cutadapt was used once more to remove the reads which were lower

than 50bp in length and to trim the read bases with Phred score less than 20 (-q20). After these filter steps a quality control was performed again with FastQC.

Sequence alignment and expression values

After the quality control the raw reads were mapped to the reference genome. The reference genome build, used here, was the current release of the porcine genome build, Susscrofa 10.2 (http://www.ncbi.nlm.nih.gov/assembly/304498/). The process was done with TopHat (http://tophat.cbcb.umd.edu), an efficient read-mapping algorithm, designed to align reads and to make substantial use of Bowtie 2 (http://bowtie-bio.sourceforge.net/bowtie2/index.shtml) (Langmead et al. 2009, Trapnell et al. 2009). All reads that did not map to the genome were set aside as unmapped reads. With the tool SAMStat (http://samstat.sourceforge.net/) all statistics were generated for mapped and unmapped reads. During the whole analysis Sequence Alignment/Map (SAM) files and Binary Alignment/Map (BAM) files were stored and Samtools (http://samtools.sourceforge.net/samtools.shtml) were used to generate BAM files from SAM files (Li et al. 2009). To calculate the expression set, read count matrix of all 12 samples, coverageBed utility of the BEDTools toolset (http://bedtools.readthedocs.org/en/latest/) (Quinlan and Hall 2010) plus gene feature information of Entrez Gene ID (http://www.ncbi.nlm.nih.gov/gene) were used.

Virus sequence alignment

The presence of the virus sequence in all 12 samples was detected by using the mapping tool Bowtie 2. To reach an alignment, the complete genome of the LV strain (GenBank: M96262), the whole transcript reads and the unmapped reads were compared.

Normalization

Normalization enables accurate comparisons of expression levels between and within samples. DESeq Bioconductor package and R, an open-source-interpreted computer language, were used to normalize the count data. The calculation based on a DESeq estimated size factor and a size factors function (Anders and Huber 2010).

Differentially expressed genes

After normalization, transcripts were filtered which had shown a read value of zero at every time point (0 h, 3, 6, 9, 12 and 24 hpi) for both breeds, they were excluded from further analysis. The analysis was continued, using the adjusted expression set. Differentially expressed gene transcripts were determined by the utilization of DESeq Bioconductor package (package chapter 3.2, "Working partially without replicates") and R. Pairwise comparisons of expression were done between PRRSV infected cells (3, 6, 9, 12, 24 hpi) and non-infected cells at time point zero, to detect differentially expressed gene transcripts. Significant differences between the time points were achieved by $p \leq 0.05$ and a false discovery rate (FDR) of 10 %.

Clustering gene expression profiles and network analysis

The normalized reads were used for further cluster and network analyses with the D-NetWeaver Software which was developed by the University of Rochester Center for Biodefense Immune Modeling (https://cbim.urmc.rochester.edu/software/d-netweaver/). This software offers a data visualization feature and creates clusters of individual genes into groups when the expression patterns of these genes are similar during the time course experiment. For this study the approach operated in different steps; step I: nonparametric mixed-effects model with mixture distribution for clustering, step II: nonparametric mixed-effects smoothing each module. The gene expression data modelling over time utilized mclust algorithms which were provided in a R package. It started with the modulation of 'mean curves' for each cluster of genes by a smoothing spline. Bayesian information criterion (BIC) represented the final number of clusters (Lu et al. 2011a, Ma et al. 2006, Ma and Zhong 2008). The numbers of clusters per breed were visualized in a dynamic network model.

Pathway enrichment analysis

The pathway enrichment analysis of clustered RNA-Seq gene transcripts was carried out, using a hyper geometric gene set enrichment test in R. The functional annotation analysis was done for all clusters of Pietrain and Duroc. In this process overrepresented gene sets were defined by Kyoto Encyclopedia of Genes and Genomes database (KEGG;

http://www.genome.jp/kegg/) and were tested by using Fisher's exact test. A gene-set was considered as significant if $p \leq 0.05$.
A "Top 10 List" of pathways was established, including all pathways which reached the statistical ranking ($p \leq 0.05$) and clusters with read counts over 20. Read counts lower than 20 were excluded from further analyses. The second criteria for the selection of pathways for the “Top 10 List” was the frequency of occurrence per breed.

3.2.13.2 Real-time PCR analyses

Normalization

The gene expression data of lung DCs, PAMs and trachea epithelial cells which were already analyzed under paragraph 3.2.11 and 3.2.12, were normalized against Ct values of the reference genes GAPDH and HPRT1.

Pairwise comparison

According to this calculation, the relative expression was determined and further statistical analyses were done by the ANOVA pairwise comparison method in R. The Tukey Honest Significant Difference (HSD) method was used to control the Type I error rate across the multiple comparisons. The pairwise comparison was utilized for all time points of one breed and for the comparison of Duroc and Pietrain.

4 Results

4.1 Cell characterization

4.1.1 Cell characterization by flow cytometry analyses

The phenotypic evaluation of the collected lung DCs and PAMs was carried out, using a flow cytometric analysis with cell surface markers such as CD11c, CD80, CD86, CD40 for lung DCs and CD163 for PAMs. The results of the flow cytometric analysis are arranged in the following histograms (Figure 10). The expression on lung DCs was of CD11c 83 %, of CD86 29 % (Figure 10, B), of CD80 14 % and of CD40 64 % (Figure 10, B). The expression of CD163 on the surface of PAMs was 27 % (Figure 10, B).

The lung DCs exhibited the phenotypic characteristics of immature DCs, including high CD11c and low CD80/86 expression.

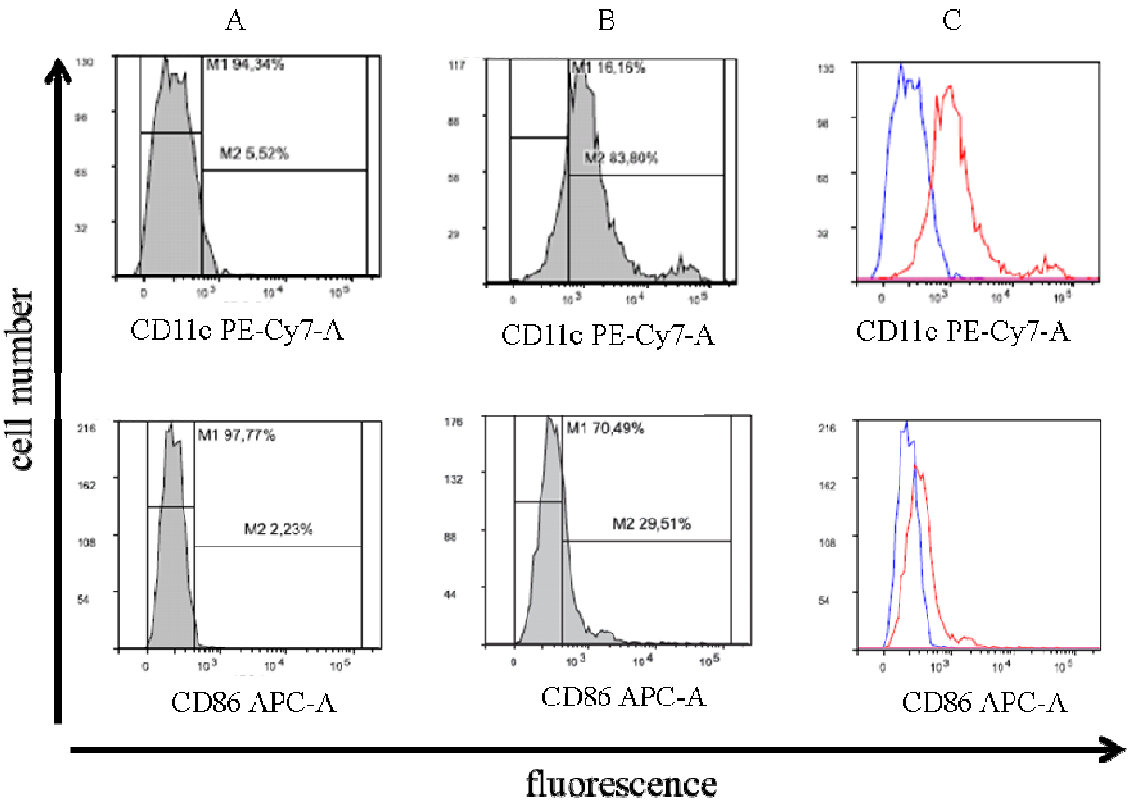

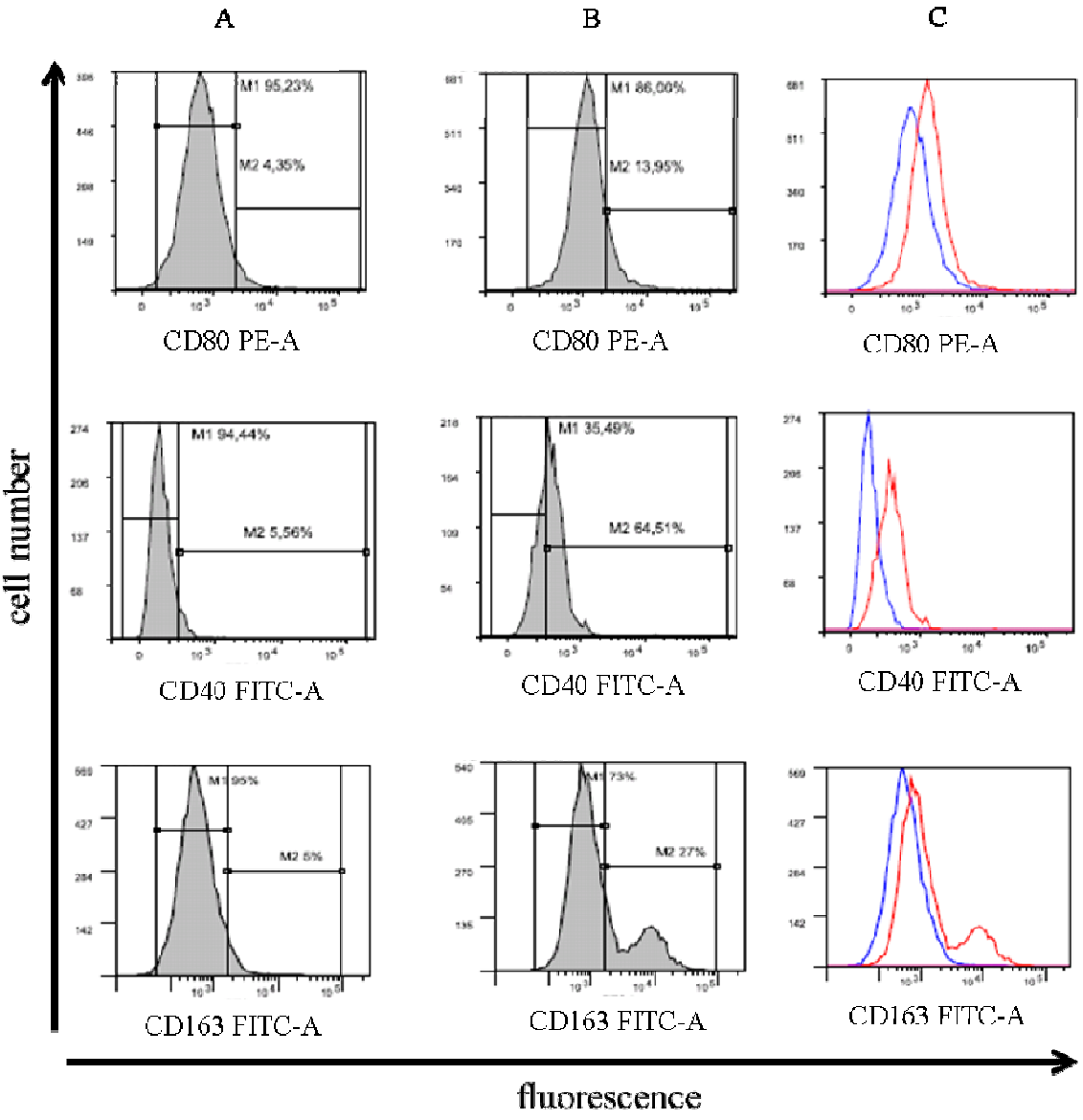

Figure 10: Staining of cell surface molecules on lung DCs and PAMs for flow cytometric analyses. The cell numbers are listed at the y-axis and the fluorescence on the x-axis. The first row (A) includes cells without staining and the second row (B) includes cells which were stained with the above mentioned cell surface markers. The last row (C) includes the measured fluorescence of both detections, first of cells without antibodies (blue-line histogram) and second of cells, stained with antibody (red-line histogram)

4.1.2 Cell characterization by immunofluorescence assay

Trachea epithelial cells were characterized with specific cell markers with immunofluorescence assay (IFA), according to their cell properties such as the expression of cytokeratin (CK) as well as of tight junction proteins zonula occludens protein (ZO-1). The nucleus was counterstained in blue by DAPI. In Figure 11 the IF staining of trachea epithelial cells are displayed.

The trachea epithelial cells (A, B, C) were positive for both of these specific epithelial markers.

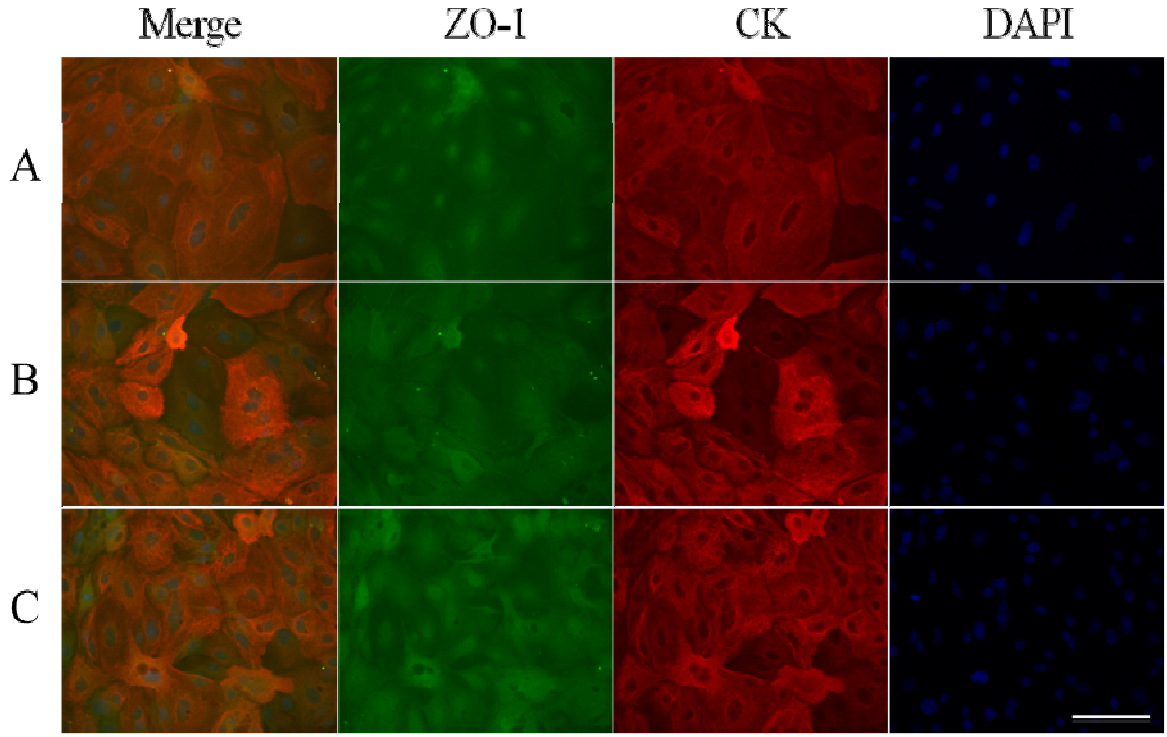

Figure 11: IF staining of trachea epithelial cells with zonula occludens protein (ZO-1), cytokeratin (CK) and DAPI. First the cell markers are merged together, next each marker is presented separately, the last pictures show the stained nucleus

4.1.3 Cell viability and phagocytosis activity

In the following subparagraphs the results of lung DCs, PAMs and trachea epithelial cells are presented. The investigations were done in the above mentioned respiratory cell lines of two different pig breeds, Duroc and Pietrain.

The viability of infected PRRSV lung DCs (Figure 12, A), PAMs (Figure 12, B) and trachea epithelial cells (Figure 12, C) was determined by MTT assay. The relative viability, indicated in percentage (%), was defined by the relationship between infected cells at 6 hpi and 12 hpi and non-infected samples at 6 h and 12 h. The relative cell viability of infected lung DCs was lower at 12 hpi in comparison to those at 6 hpi. The relative cell viability of virus infected PAMs was 84 % at all time points. Trachea epithelial cells showed a higher degree of viability at 6 hpi than at 12 hpi. At time point 6 hpi 69 % and at 12 hpi 61 % of relative cell viability were detected.
PRRSV infected lung DCs and trachea epithelial cells represented a lower relative cell viability at 12 hpi than at 6 hpi.

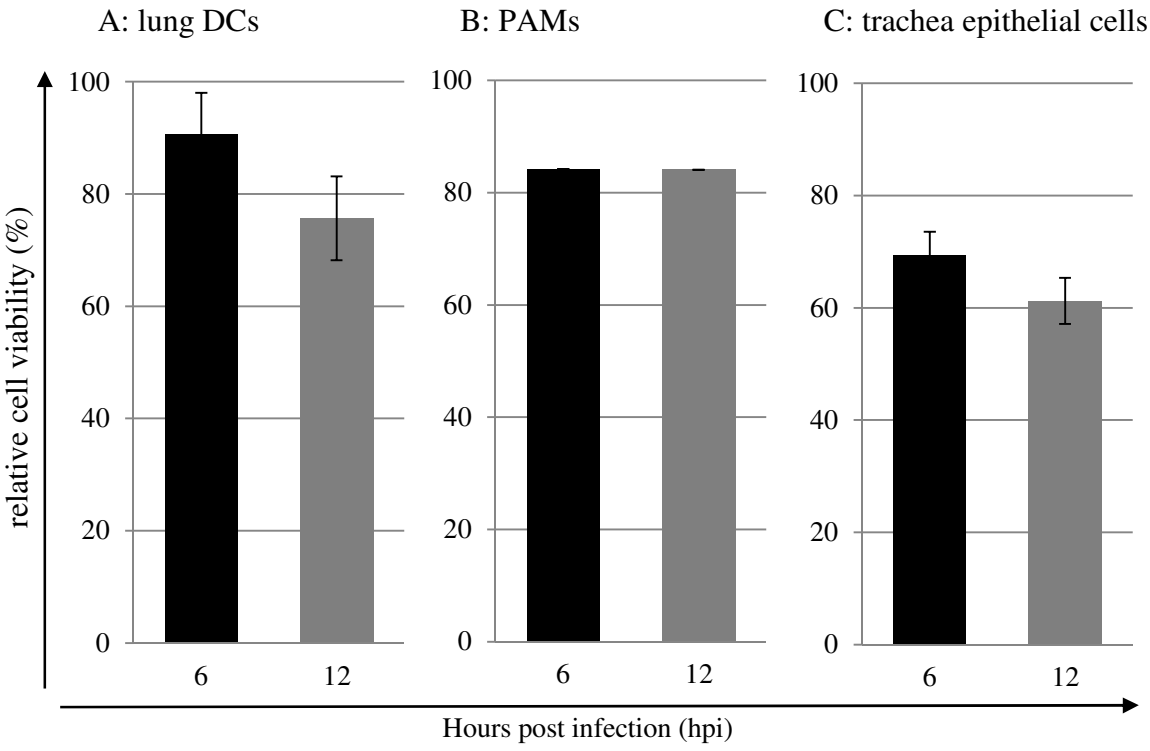

Figure 12: Relative cell viability of infected lung DCs (A), PAMs (B) and trachea epithelial cells (C) at 6 hpi and 12 hpi

The relative phagocytosis effect of lipopolysaccharides (LPS) stimulated lung DCs and PAMs (Figure 13) and trachea epithelia cells (Figure A3) was indicated in percentage (%). For the calculation of the relative phagocytosis effect net experimental reading and net positive reading were used.

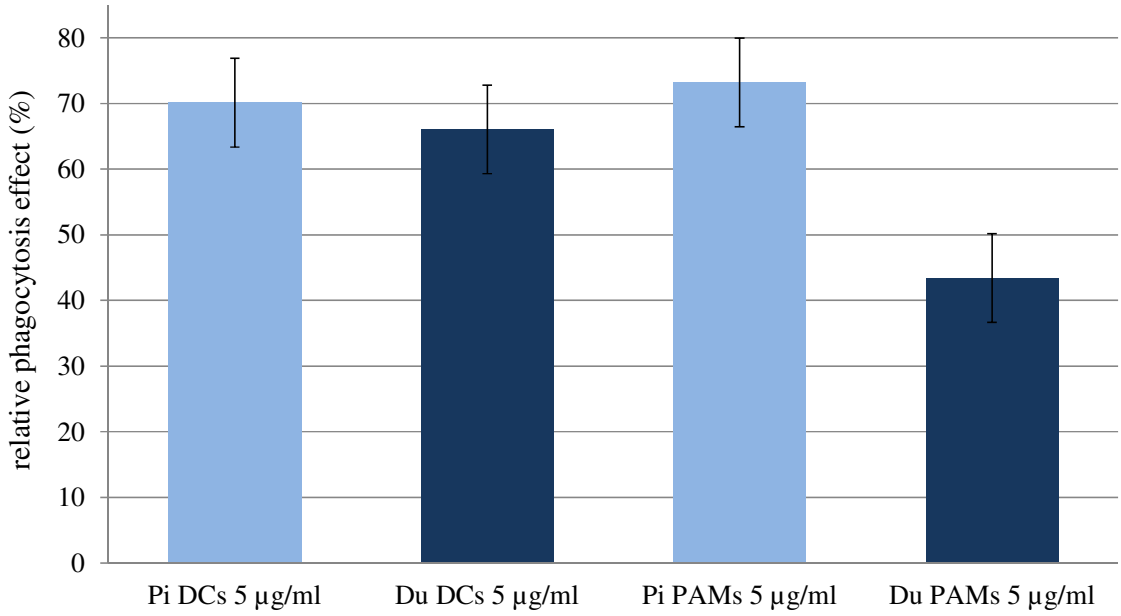

Figure 13: Relative phagocytosis effect (%) of LPS (dose: 5 µg/ml) infected Pietrain (Pi) and Duroc (Du) lung DCs and PAMs

Pietrain infected lung DCs presented a higher relative phagocytosis effect of 70 % after a dose of 5 µg/ml LPS in comparison to Duroc lung DCs (66 %). Comparing the relative phagocytic effect of LPS infected PAMs (Figure 13), the Pietrain samples revealed a much higher effect (73 %) after an infection dose of 5 µg/ml of LPS than Duroc PAMs (43 %).
The relative phagocytosis effect of infected trachea epithelia cells (79 %), is arranged in the appendix (Figure A3).
In general, strong breed differences were detected by the investigation of the relative phagocytosis effect of LPS infected lung DCs and PAMs.

4.2 Cytokines secretions in relation to the cytokine gene expression profiles

The cytokine concentrations of five (IFN-γ, IL-8, IL-1β, IL-12p40 and TNF-α) various cytokines in cell culture supernatants were measured. The cytokines secretion differences of PRRSV infected cells (lung DCs, PAMs, and trachea epithelial cells) at 9 hpi were determined. The levels of IFN-γ, IL-8, IL-1β and TNF-α are shown in Figure 14.

The levels of the cytokines IFN-γ (Figure 14, A) and TNF-α (Figure 14, B) were between 0 and 40 pg/ml and the levels of IL-1β (Figure 14, C) and IL-8 (Figure 14, D) ranged between 0 and above 8000 pg/ml. Pietrain lung DCs obtained an IFN-γ concentration of 32.99 pg/ml and Duroc lung DCs of 12.11 pg/ml. A difference was visible between infected trachea epithelial cells where concentrations of 15.15 pg/ml for Pietrain and 7.88 pg/ml for Duroc were detected. Very similar cytokine levels were recognizable for Pietrain and Duroc PAMs.

The cytokine levels of TNF-α were located in similar concentrations for all analyzed samples. The IL-1β concentration of Pietrain lung DCs increased to a level of 2532.90 pg/ml. In comparison, Duroc lung DCs reached a maximum IL-1β concentration of 104.65 pg/ml. A threefold high IL-1β concentration was observed in Duroc PAMs with 302.78 pg/ml in contrast to Pietrain PAMs where a concentration of 110.73 pg/ml was achieved.

For the cytokine IL-8 strong differences were detected, comparing Pietrain PAMs (a concentration of 113.33 pg/ml) and Duroc PAMs (a concentration of 3982.00 pg/ml). The other levels of IL-8 cytokine did not deviate strongly from each other. Regarding the 4PL curve analysis, there was no IL-12p40 concentration data detectable.

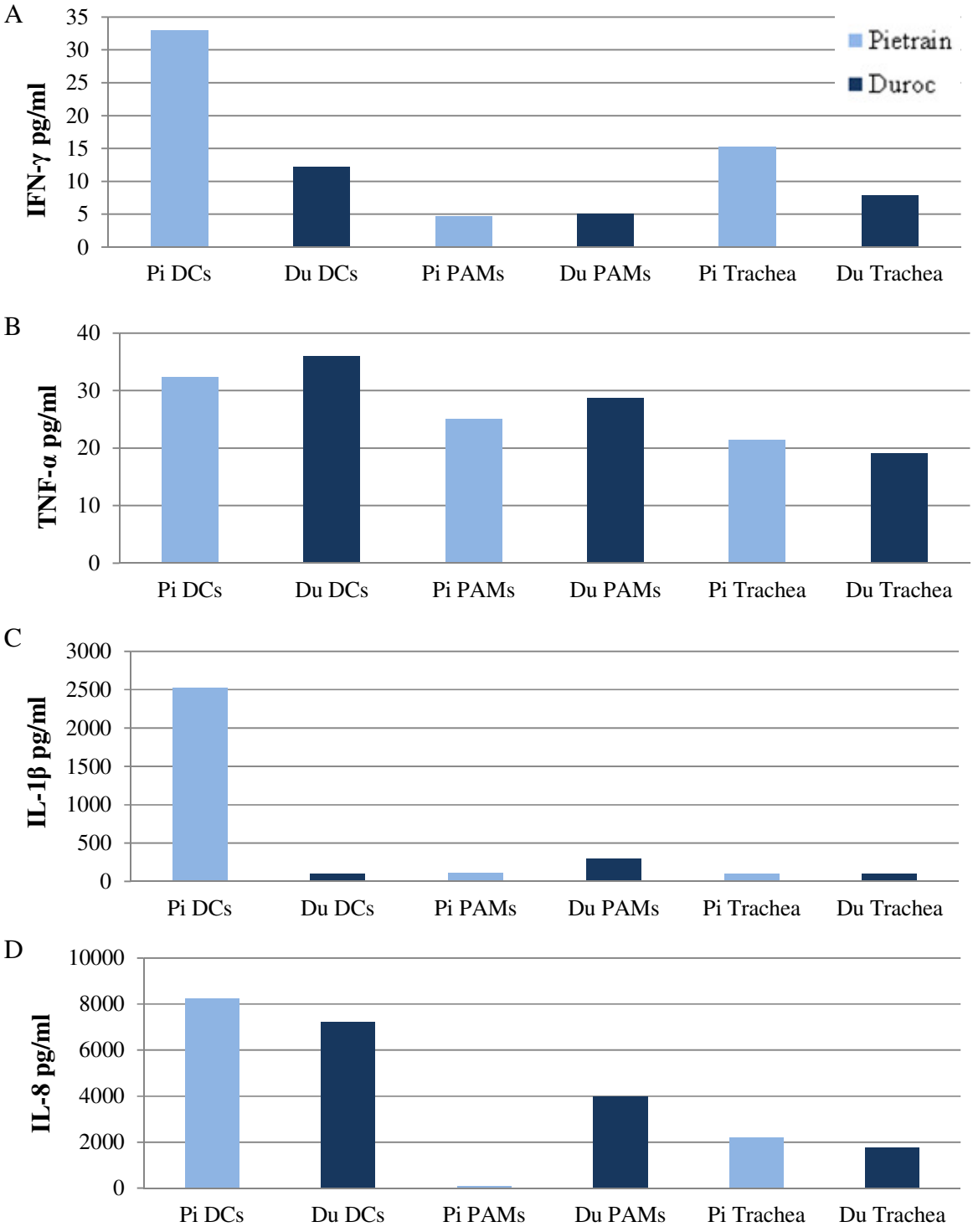

Figure 14: Levels of cytokines in cell culture supernatant at 9 hpi in lung DCs, PAMs and trachea epithelial cells of Pi and Du. The concentrations (pg/ml) of IFN-γ (A), TNF-α (B), IL-1β (C) and IL-8 (D) were measured with commercial porcine ELISA kits

In order to investigate the cytokine profiles of PRRSV infected lung DCs, PAMs and trachea epithelial cells in detail, the expression of IFN-γ, IL-1β, IL-8, TNF-α and IL-12p40 mRNA was quantified by quantitative real-time PCR. Only the analysis of IFN-γ in all respiratory cells and the analysis of IL-1ß in trachea epithelial cells failed, due to the small amount of detected expression data. The results of the expression analyses of IL-1β and IL-8 of pooled Pietrain and Duroc lung DCs, PAMs and trachea epithelial cells (compare experimental design II, Figure 7) are shown in the following Figure 15 and Figure 16.

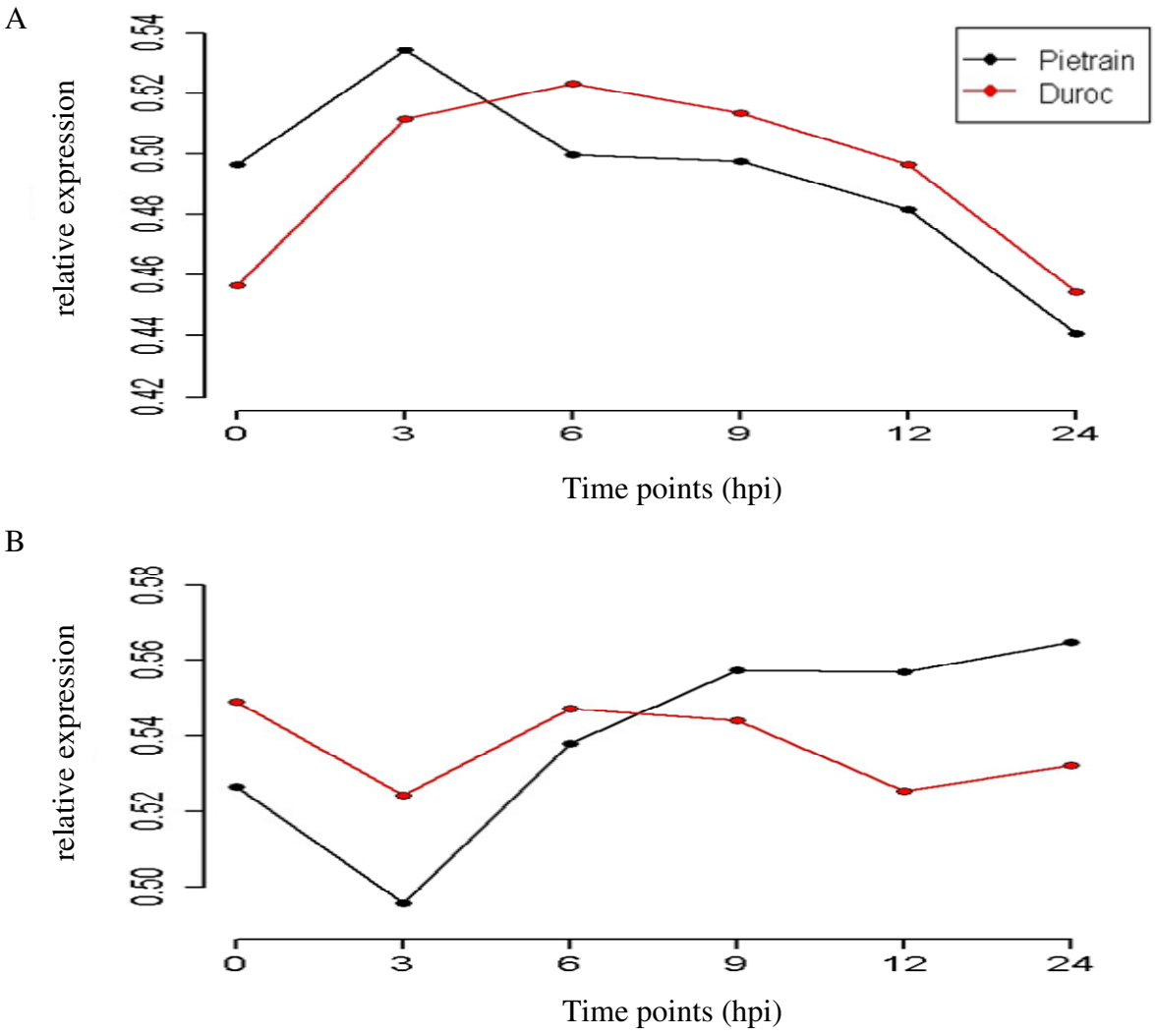

Figure 15: Gene expression levels of IL-1ß in non-infected (0 h) and infected (3, 6, 9, 12, 24 hpi) lung DCs (A) and PAMs (B) of Pietrain and Duroc

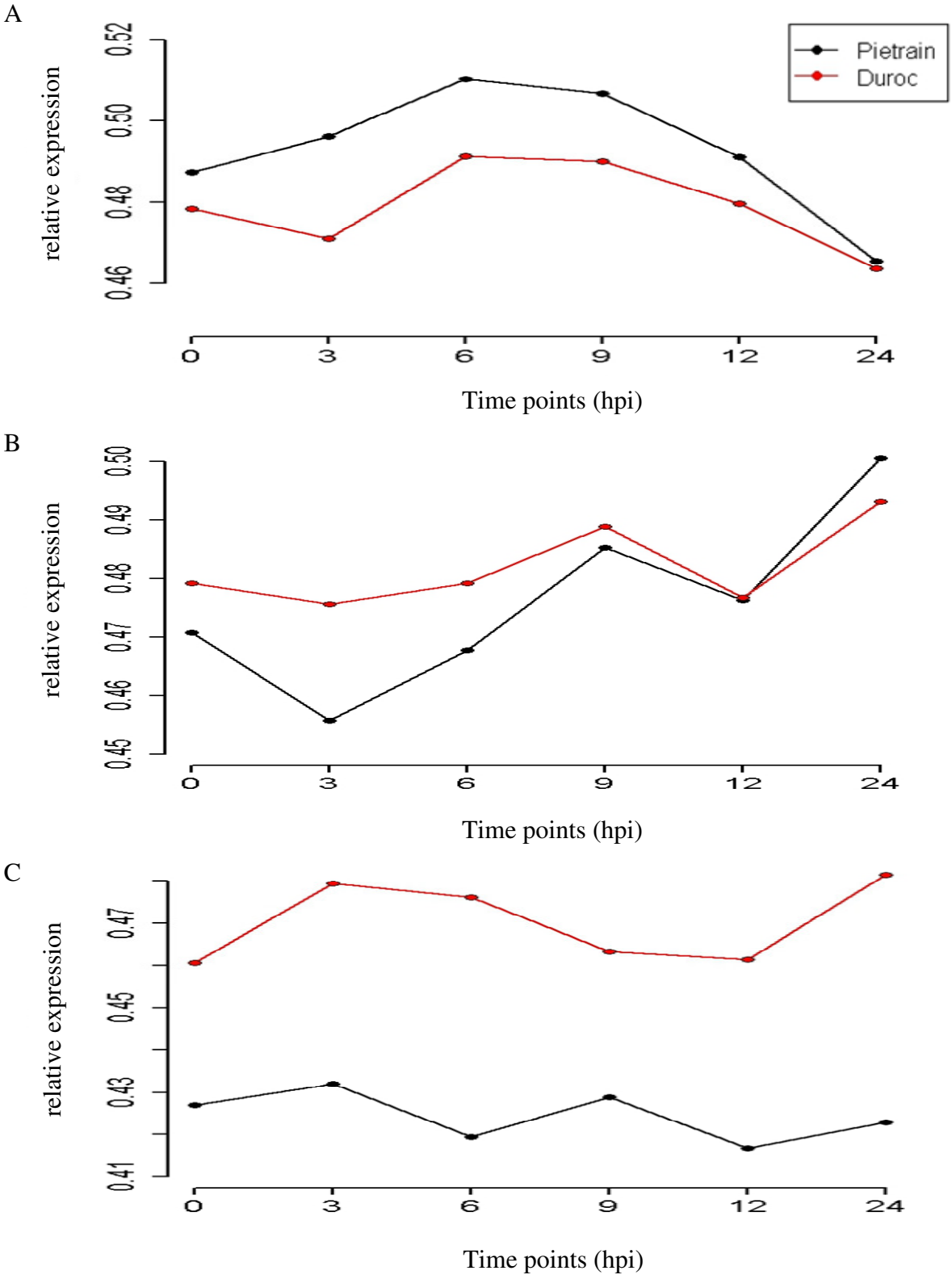

Figure 16: Gene expression levels of IL-8 non-infected (0 h) and infected (3, 6, 9, 12, 24 hpi) lung DCs, PAMs (B) and trachea epithelial cells (C) of Pietrain and Duroc

The gene expression patterns of IL-8, IL-1β, TNF-α and IL-12p40 changed similarly within the same cell types. But the comparison between the different cell types indicated different expression trends. For instance IL-1β in lung DCs showed a declining expression trend after 6 hpi, whereas IL-1β in PAMs represented an increasing expression trend after 3 hpi. Similar observations were made for expression profiles for IL-8 of lung DCs and PAMs. IL-8 in trachea epithelial cells of both breeds represented a rather stable expression pattern. Further figures, containing the graphs of the expression profiles of TNF-α (Figure A4) and IL-12p40 (Figure A5), are arranged in the appendix.

The cytokine secretions and the gene expression profile indicated cell-type differences. Additionally, breed differences were visible with regard to the cytokine secretion results.

4.3 Transcriptome analysis

4.3.1 RNA-Sequencing processing and alignment

In order to investigate the transcriptome profile of PRRSV infected lung DCs, the created RNA libraries of PRRSV infected and non-infected lung DCs were used for deep sequencing with an Illumina HiSeq 2000. The RNA-Seq analysis of infected lung DCs (0 h, 3, 6, 9, 12, 24 hpi) of two different purebred pigs (Pietrain and Duroc) obtained a total number of short reads between 20,9 and 30,2 millions for each library. But one exception existed, concerning the read library at 3 hpi of Pietrain which represented a total number of 13 million reads. The tool FastQC was used for basic statistics, including following parts: per base sequence quality, sequence quality scores, base sequence content, base GC content, sequence GC content, base N content, sequence length distribution, sequence duplication levels as well as overrepresented sequences and Kmer content. Based on these results, the overrepresented sequences and adapter sequences as well as the first 15bp were removed from the raw sequence. The total number of high quality reads after all filtration steps ranged from 12,9 to 29,5 million reads. The values of read counts, mapped to the *Sus scrofa* genome, ranged between 74.8 % to 81.3 % and the unmapped ones between 18.7 % and 25.2 %. The informations, regarding read counts of Pietrain and Duroc before and after the filtration and the read length as well as the mapping statistics, are listed in the appendix (Table A2 and Table A3). The total number of 20,396 porcine predicted gene transcripts was identified and according to these gene transcripts, a gene expression table was listed with read counts between 0 and 762,300.

4.3.2 Virus sequence alignment

Virus sequence alignment was additionally performed in order to detect virus reads in all 12 samples. For the sequence mapping the LV strain was aligned to the whole sequenced reads and to the unmapped reads. At 0 h in non-infected cells no virus read was detected. Just 8 reads of Duroc and 9 reads of Pietrain matched coincidentally somewhere in the virus genome (Figure 17).

But after infection the number of virus specific reads, which mapped, increased with the time points of infection. At 3 hpi the read counts exploded for Pietrain to 9433 and for Duroc to 4924. For Pietrain the read counts continued to increase to 13,941 at 6 hpi, to

25,948 at 9 hpi, to 177,590 at 12 hpi and reduced considerably to 36,435 reads at 24 hpi. In contrast the read counts for Duroc at 3, 6 and 9 hpi were very close to each other and did not present any big variances. But at 12 hpi the counts increased to 49,617 and at 24 hpi, they literally exploded with an increase to 1,119,046 read counts.

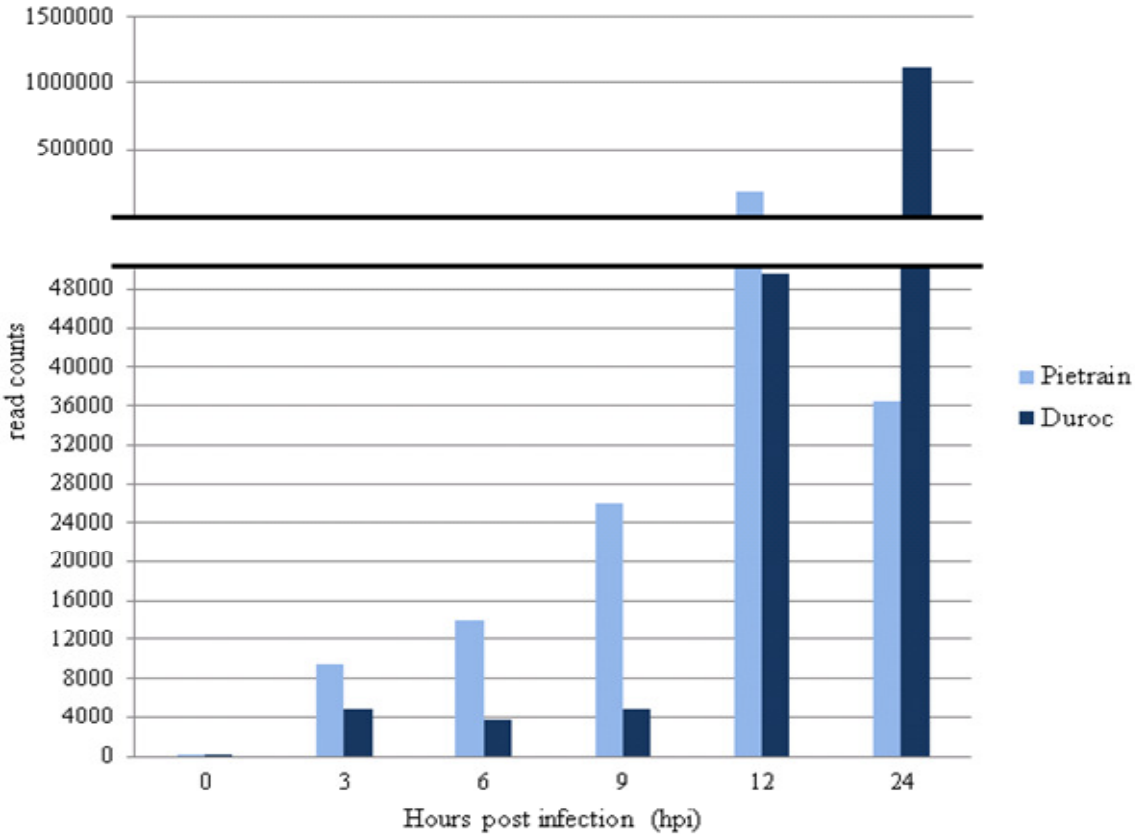

Figure 17: Virus sequence alignment of Pietrain and Duroc lung DCs before and post PRRSV infection

At 3 hpi the virus read counts differed between Pietrain and Duroc at round about 50 %. At 6 hpi and 9 hpi the virus read counts differed between the two breeds more than 50 %. But at 24 hpi a multiple virus growth was visible in Duroc lung DCs, whereas a strong decrease of virus reads in Pietrain lung DCs was detected.

4.4 Clustering gene expression profiles and network analysis

All 20,396 individual gene transcripts (compare chapter 4.3.1) were grouped, according to their similar expression patterns during the time course infection experiment. The D-NetWeaver Software visualized 37 counted clusters for Pietrain (Figure 18, A) and 35 counted clusters for Duroc (Figure 18, B). The assignment to the clusters was based on the transcriptome profile per breed. For example in cluster 26 of Pietrain (Figure 19, A) 450 gene transcripts were identified with a similar expression profile. The red line represents the mean expression curve which was determined by the expression trend of the gene transcripts. Cluster 25 of Duroc (Figure 19, B), another example, included 336 gene transcripts.

The functional analysis of the gene transcripts, organized in these clusters, follows in the next chapters 4.4.1 and 4.4.2.

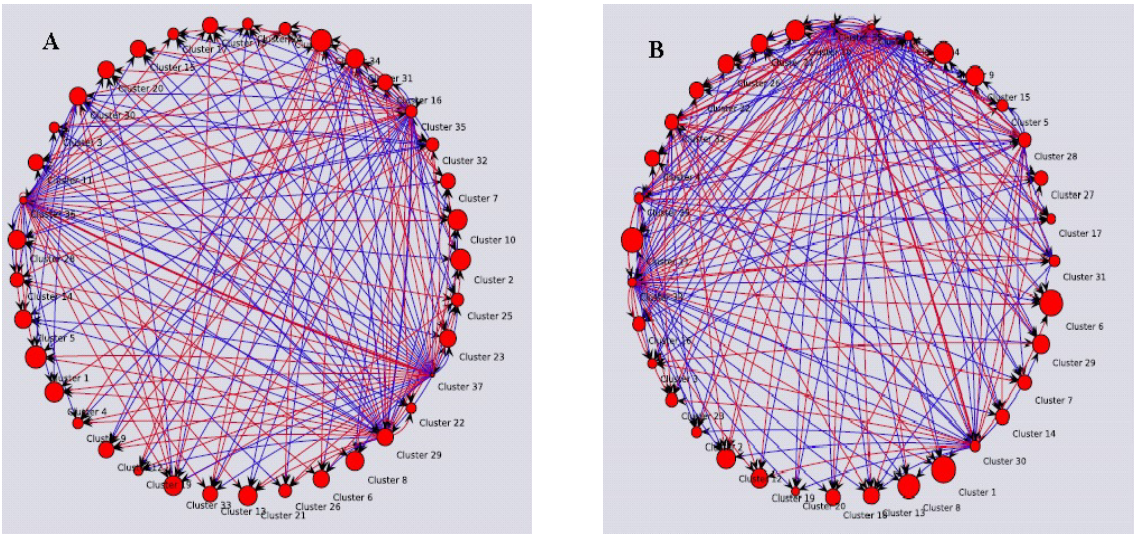

Figure 18: Pietrain network with 37 clusters (A), Duroc network with 35 clusters (B)

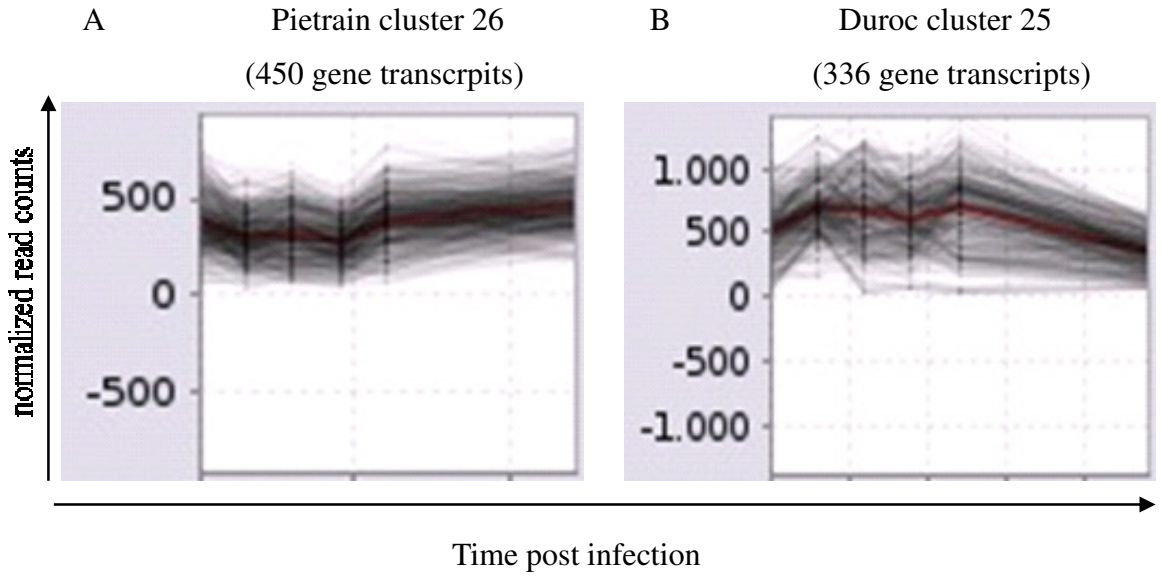

Figure 19: Mean expression curve for cluster 26 of Pietrain (A) and cluster 25 of Duroc (B)

4.4.1 Pathway enrichment analysis after RNA-Sequencing

The pathway enrichment analysis (compare chapter 3.2.13) of RNA-Seq gene transcripts was done with all clusters of Pietrain (37 clusters) and Duroc (35 clusters). For both breeds collectively 171 pathways ($p \leq 0.05$) were identified. Additionally, 47 pathways ($p \leq 0.05$) were investigated only for Duroc. In order to list the top 10 pathways, clusters with read counts lower than 20 were excluded from this analysis. The “Top 10 List” included only clusters with read counts higher than 20 and pathways which occurred with a higher frequency per breed. Table 5 provides the top 10 pathways and the associated clusters.

Table 5: "Top 10 List" of pathways and the associated clusters

Pathways	**Pietrain clusters**	**Duroc clusters**
Phagosome	12, 22, 33, 34, 35, 36, 37	25, 30, 31, 32, 33, 34
Spliceosome	28, 29, 31, 32, 34	22, 23, 29, 32
Protein processing in endoplasmic reticulum	28, 31, 33, 34, 35	28, 29, 31, 32
Focal adhesion	29, 31, 35, 36, 37	26, 33, 34, 35
Endocytosis	28, 32, 34	3, 22, 25, 30, 32
Rheumatoid arthritis	15, 29, 35, 36	25, 30, 32, 34
Homologous recombination	14, 17, 18, 24	1, 6, 18, 19
Cell cycle	16, 18, 21, 25	1, 6, 18, 19
Oxidative phosphorylation	27, 30, 33, 34	27, 28, 31, 32
JAK-STAT signaling pathway	9, 10, 15, 32	7, 20

The Pietrain clusters 28, 29, 31, 32, 33, 35, 36 had a high occurrence in the "Top 10 List" of pathways, the highest occurrence was detected for cluster 34. The same observations were possible for Duroc clusters. Some of the clusters occurred more frequently, for example those of 30, 31, 34. The cluster 32 exhibited a higher occurrence for Duroc. The cluster 34 of Pietrain and the cluster 32 of Duroc demonstrated a homology for 5 pathways. This homology exhibited for the pathways phagosome, spliceosome, and protein processing in endoplasmic reticulum, endocytosis as well as oxidative phosphorylation.

The amount of the gene transcripts, included in the clusters, varied also between the breeds. The graph (Figure 20) represents the total number of gene transcripts, according to the top 10 pathways.

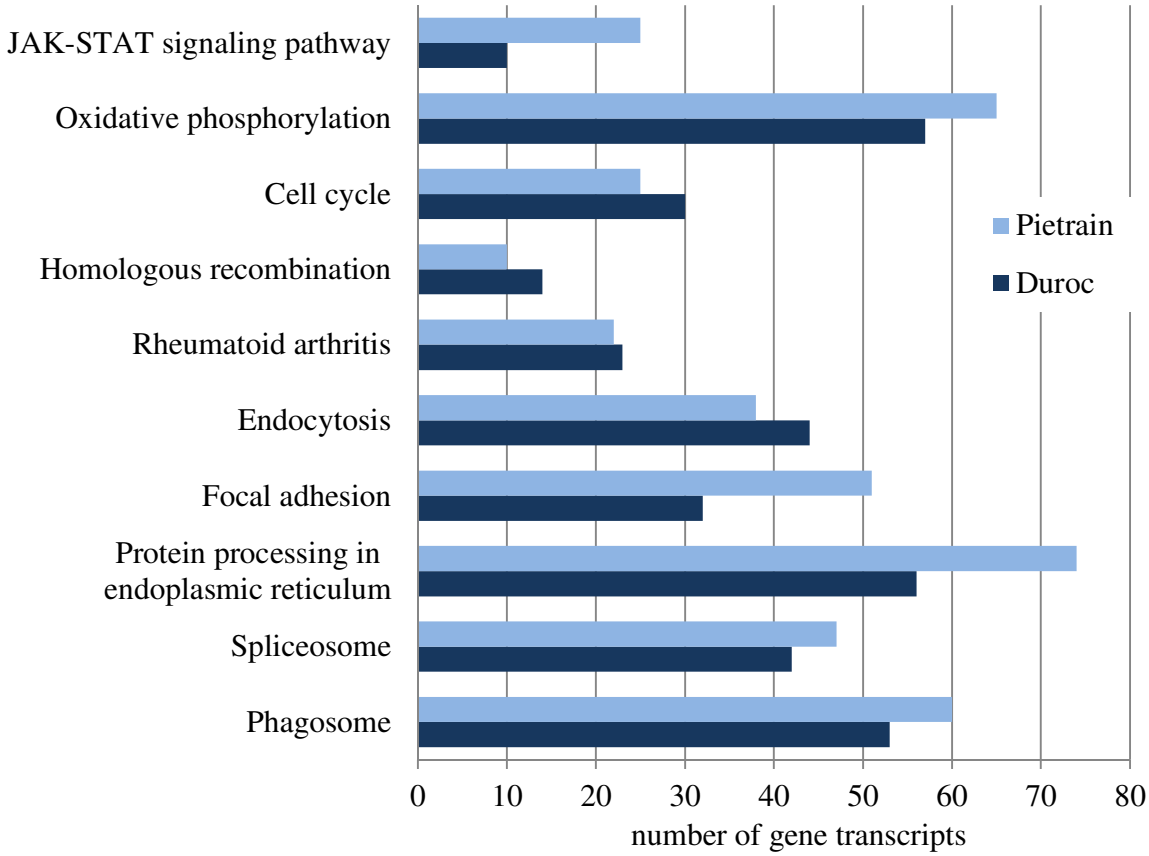

Figure 20: Number of gene transcripts per pathway. Gene transcripts are listed at the y-axis, according to the "Top 10 List" (compare Table 5)

The pathway phagosome was associated with most of the clusters and presented a high level of gene transcripts (53 for Duroc and 60 for Pietrain) (Figure 20). The pathway protein processing in endoplasmic reticulum contained 74 gene transcripts for the breed Pietrain and so it was the pathway with the highest number of gene transcripts. The smallest number of gene transcripts was exposed by the pathway homologous recombination for the breed Pietrain. For the breed Duroc the smallest one was the JAK-STAT signaling pathway. For these both pathways there was only an amount of 10 gene transcripts.

4.4.2 Analysis of gene transcripts frequency

As described above (compare chapter 4.4.1), some clusters showed an increased occurrence like cluster 32 for Duroc and 34 for Pietrain. Additionally, some gene transcripts, originating from one cluster, were working in different pathways. One pathway compromised various clusters and each cluster had its own expression trend.
Through the following frequency analyses possible key pathways, key clusters and specific gene transcripts as well as the connection between different clusters and pathways will be explained. The following subparagraphs illustrate the gene transcripts which had a higher occurrence per breed in different clusters. These gene transcripts were identified by the pathway enrichment analysis of clustered RNA-Seq data.

4.4.2.1 Gene transcripts frequency for Duroc

The pathways phagosome and endocytosis were related to cluster 32. These pathways implied the same gene transcripts like SLA-5, SLA-7, TFRC as well as RAB5C. The pathways phagosome, rheumatoid arthritis and oxidative phosphorylation of cluster 32 included the same genes like ATP6V1B2, ATP6V1F and ATP6V1E1. SLA-DRB1 was presented in the pathways phagosome and rheumatoid arthritis in cluster 32. Cluster 34 revealed pathways like phagosome and focal adhesion, in these both pathways ITGB1 and ITGA5 were involved. The gene transcript VEGFA was found in cluster 34 in the pathways rheumatoid arthritis and focal adhesion. Cluster 33 included the gene transcript LOC100153940 which was involved in the pathways phagosome as well as in focal adhesion. The gene transcripts ITGB2, SLA-DQB1, SLA-DRA and SLA-DQA1 were found in the pathways phagosome and rheumatoid arthritis in cluster 30. The cluster 25 comprised the pathways rheumatoid arthritis and endocytosis and the gene transcript FLT1 had a function for both. For the pathways rheumatoid arthritis and phagosome in cluster 25 three gene transcripts TLR2, TLR4 and SLA-DMB were identified. SEC61A1 and SEC61B were involved in the protein processing in endoplasmic reticulum and in the phagosome pathways in cluster 32 and 31. LOC733646, ATP6V1G1, ATP6V1C1, ATP6V0D1 and TCIRG1 were present in the phagosome and oxidative phosphorylation pathways in cluster 31.

4.4.2.2 Gene transcripts frequency for Pietrain

In cluster 33 for the pathways phagosome and oxidative phosphorylation the gene transcripts LOC733646, ATP6V1G1, ATP6V1C1, ATP6V1F and TCIRG1 were found. For the same cluster the genes SEC61B and SEC61G were identified in the pathways phagosome and protein processing in endoplasmic reticulum. The pathways phagosome and endocytosis included following five common gene transcripts: SLA-2, SLA-6, SLA-7 and EEA1, RAB5C in cluster 34. In the same cluster the gene transcript SEC61A1 was identified in the pathways phagosome and protein processing in endoplasmic reticulum. The gene transcripts ATP6V1E1, ATP6V1B2 and ATP6V0D1 existed in the pathways phagosome and oxidative phosphorylation in cluster 34. For cluster 35 phagosome and rheumatoid arthritis pathways the frequency analysis showed two gene transcripts: CTSL and ATP6V0C. The pathways phagosome and protein processing in endoplasmic reticulum pathways compromised the gene transcript CANX. Focal adhesion and rheumatoid arthritis had one common gene transcript per cluster: in cluster 29 VEGFB, in cluster 35 C-JUN and in cluster 36 VEGFA. The pathways focal adhesion and phagosome in cluster 36 included the gene transcripts ITGB1, ITGA5 and LOC100153940. ACTB and THBS1 were involved in both pathways in cluster 37.

4.4.2.3 Comparison of Duroc and Pietrain gene transcript frequency analysis

The comparison of the gene transcripts analysis between the two breeds showed that for Duroc and Pietrain the following common elements existed with a high pathway frequency: LOC733646, ATP6V1G1, ATP6V1C1, ATP6V1F and TCIRG1, SEC61B, SEC61A1, ITGB1, ITGA5 as well as VEGFA. The gene transcripts SLA-7 and RAB5C were found in the same pathways endocytosis and phagosome for both breeds. The gene transcripts ATP6V1B2, ATP6V1F and ATP6V1E1 were detected for Duroc and Pietrain in the same pathways phagosome and oxidative phosphorylation. Furthermore LOC100153940 was also found for Duroc and Piertain in same pathways focal adhesion and phagosome.

There was no uniform regulation of the gene transcripts, due to the fact that the gene transcripts of one pathway had their origin in different clusters. So each pathway consisted of different gene transcripts which had various expression trends after PRRSV infection.

The following three pathways: phagosome, oxidative phosphorylation and endocytosis stood out because of their high common gene transcript frequency and can be declared as key pathways. In combination with the above mentioned key clusters of Pietrain (cluster 34) and of Duroc (cluster 32) and the detected accordance to specific gene transcripts let to identify a kind of parallelism and homology in the response to PRRSV for both breeds.

4.5 Differentially expressed gene transcripts after RNA-Sequencing

In order to determine the effect of PRRSV infection on the porcine lung DCs transcriptome, pairwise comparisons were performed between non-infected cells (0 h) and PRRSV infected cells (3, 6, 9, 12, 24 hpi) per breed. Based on the RNA-Seq analyses, the temporal expression profile of Pietrain and Duroc lung DCs (compare experimental design II, Figure 7) was presented in two categories: the first category contained differentially expressed genes with a $p \leq 0.05$ and FDR of 10 %, the second category presented gene transcripts with a $p \leq 0.05$ and FDR over 10 %. The expression of 4472 gene transcripts varied ($p \leq 0.05$) in PRRSV infected lung DCs. The gene expression of 170 genes in total varied ($p \leq 0.05$, FDR 10 %) in Pietrain PRRSV infected lung DCs. Among them 133 exhibited a down-orientated (Figure 21) and 37 genes an up-orientated (Figure 22) gene expression. For PRRSV infected Duroc lung DCs, 228 differently expressed ($p \leq 0.05$, FDR 10 %) gene transcripts were identified. 41 gene transcripts showed a down-regulated (Figure 21) and 187 an up-regulated (Figure 22) expression trend.

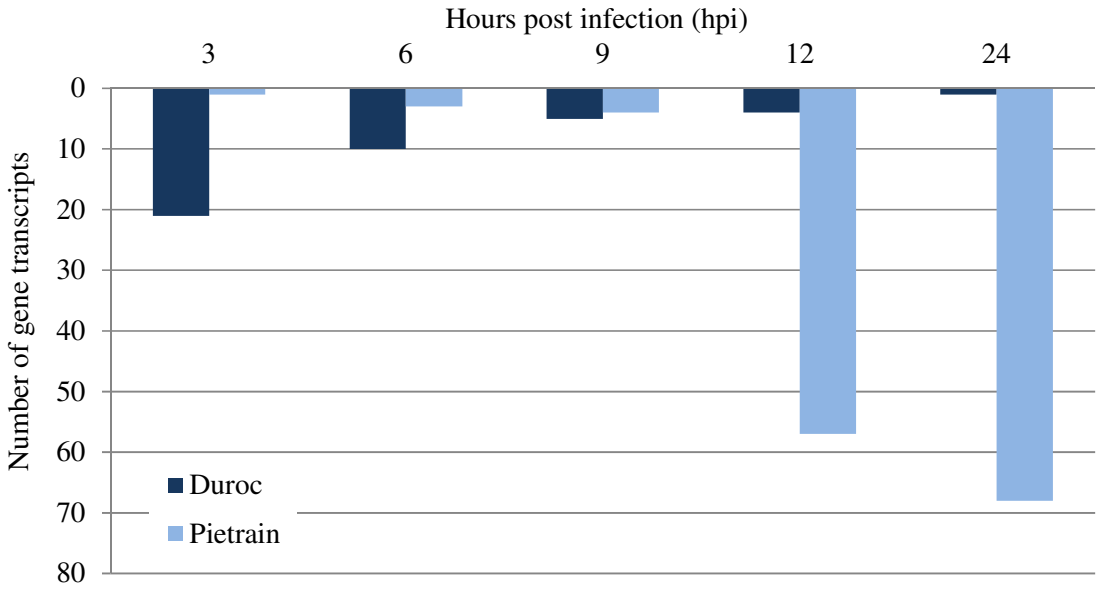

Figure 21: Number of down-regulated Duroc and Pietrain lung DCs gene transcripts during the course of infection with PRRSV (3, 6, 9, 12, 24 hpi)

At the early stage of infection (3 hpi) Pietrain lung DCs showed a smaller number of down-regulated gene transcripts, followed by an extreme increase till 24 hpi. Duroc infected lung DCs showed a contrary development.

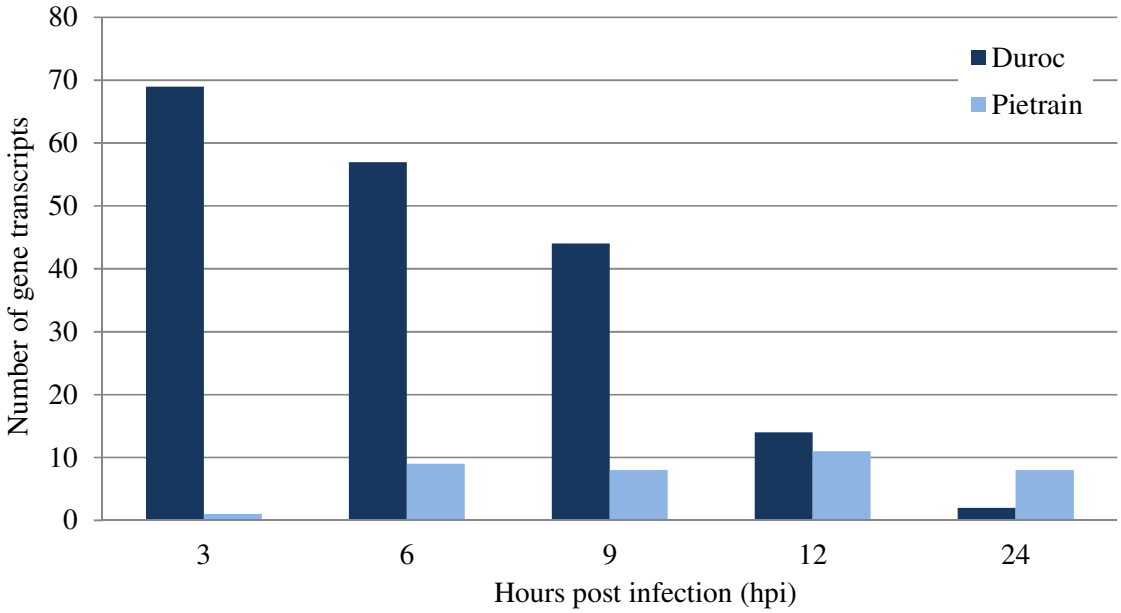

Figure 22: Number of up-regulated Duroc and Pietrain lung DCs gene transcripts during the course of infection with PRRSV (3, 6, 9, 12, 24 hpi)

At the early stage of infection (3 hpi) Duroc lung DCs showed a high up-regulation, followed by an extreme reduction of the gene expression till 24 hpi. Pietrain infected lung DCs varied slightly in their up-regulated expression.

There was a remarkable increase of down-regulated immune gene transcripts (CXCL2, IL-6, IL-1β, TNF, CCL4, IL-1α, SLA-DRA, CCL3L1, CCL23, CCL20) visible of Pietrain infected lung DCs at 9 hpi to 24 hpi (Figure 21). Once more, differences between the two breeds Pietrain and Duroc could be observed. For infected Duroc lung DCs a notable decrease of up-regulated immune gene transcripts (CCL4, CXCL2, IL-1β, CXCL10, and CCL8) at 3 hpi to 24 hpi was detected (Figure 22).
There were remarkable different reactions to PRRSV infection for the two breeds. The time point 9 hpi could be considered as a turning point of the expression trends of both breeds.

4.6 Validation of RNA-Sequencing data

Ten gene transcripts (compare chapter 3.2.11, Table 3) were selected to validate the results of RNA-Seq and to confirm the importance of key pathways, involved in the immune response to PRRSV infection. The genes were carefully selected from the results of RNA-Seq data set. Eight out of ten gene transcripts are presented in this chapter. Additional graphs can be found in the appendix (Figure A6, A7, A8).
The measurements were done with non-pooled lung DCs, non-pooled trachea epithelial cells and pooled PAMs (compare experimental design II, Figure 7) for all time points. The analyses were performed on the basis of a pairwise expression comparison between non-infected (0 h) and PRRSV infected (3, 6, 9, 12, 24 hpi) cells. For a better understanding these analyses comprised the temporal expression course of pooled lung DCs, done by RNA-Seq, and the expression profile of different respiratory cells as described above, measured by real-time PCR. The time point 24 hpi of Duroc lung DCs could not be analyzed.

4.6.1 Interleukin-6

The inflammatory cytokine interleukin-6 (IL-6) displayed in the RNA-Seq analysis an altered ($p \leq 0.05$, FDR 10 %) expression profile at 12 hpi in Pietrain lung DCs. Even at 3, 6, 9 and 24 hpi for Pietrain and at 12 hpi for Duroc IL-6 represented reduced expression trends ($p \leq 0.05$) in comparison to non-infected lung DCs at 0 h (Figure 23, A). The expression results of the real-time PCR analysis of lung DCs were characterized by a down-regulation of the gene expression in infected Duroc cells at 12 hpi in comparison to 0 h ($p \leq 0.05$) and to 6 hpi ($p \leq 0.01$). The same trend was visible for Pietrain lung DCs by comparing 0 h with 24 hpi ($p \leq 0.001$) as well as 9 hpi with 24 hpi ($p \leq 0.05$) (Figure 23, B). The expression profile of PAMs presented another expression course in contrast to infected lung DCs and trachea epithelial cells (Figure 23). The expression profile of lung DCs ($p \leq 0.1$) and trachea epithelial cells ($p < 0.001$) showed a global breed difference across all time points which was measured by real-time PCR (Figure 23, D).

A

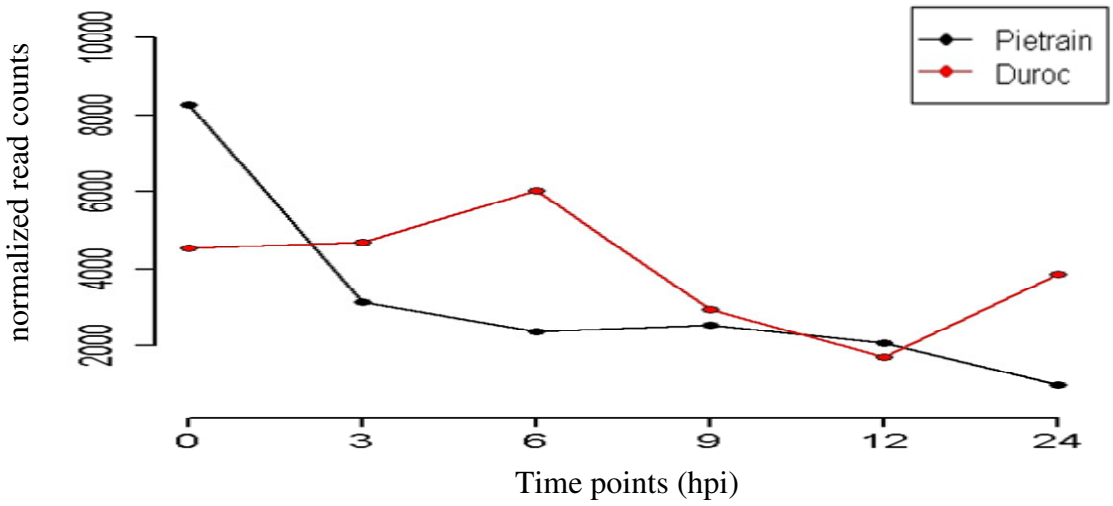
normalized read counts
2000
4000
6000
8000
10000
Pietrain
Duroc
0
3
6
9
12
24
Time points (hpi)

B

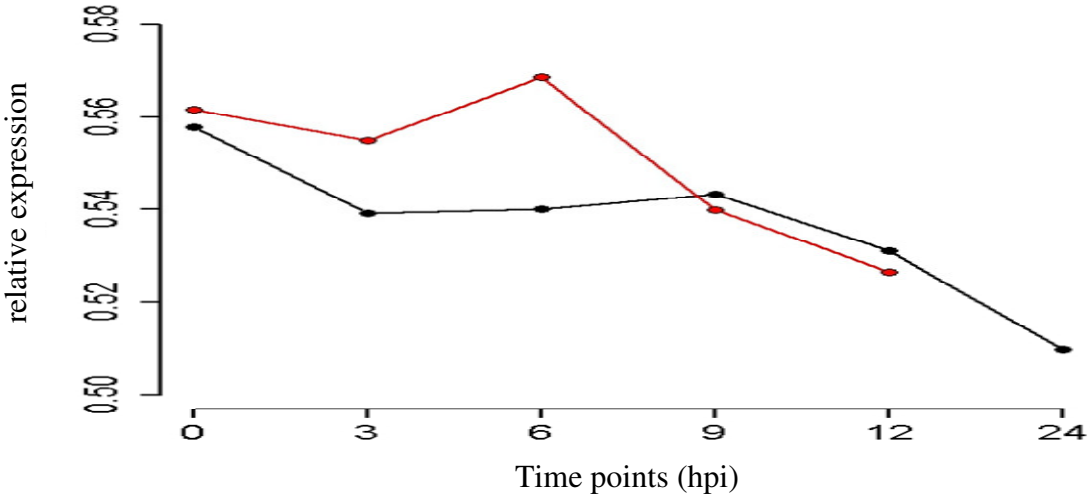
relative expression
0.50
0.52
0.54
0.56
0.58
0
3
6
9
12
24
Time points (hpi)

C

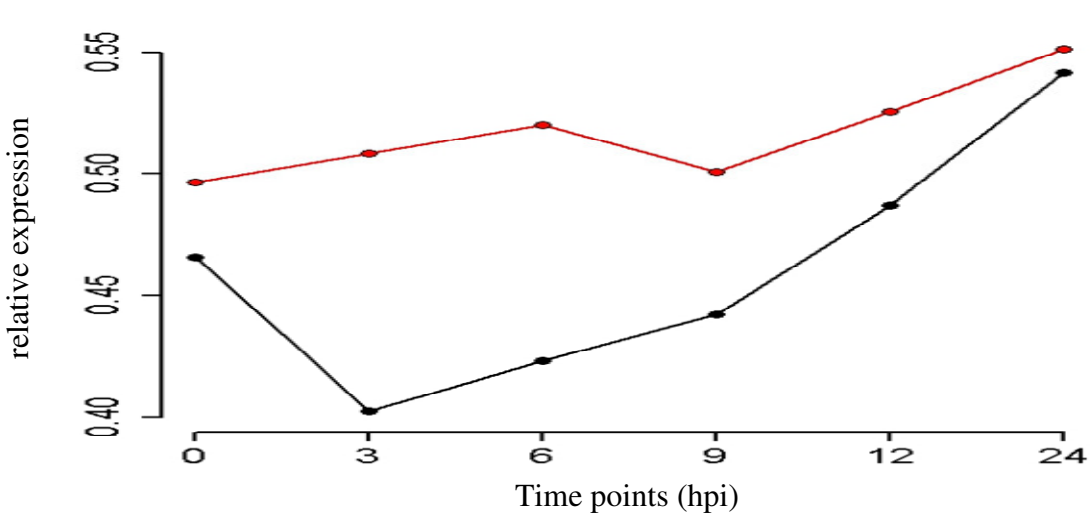
relative expression
0.40
0.45
0.50
0.55
0
3
6
9
12
24
Time points (hpi)

D

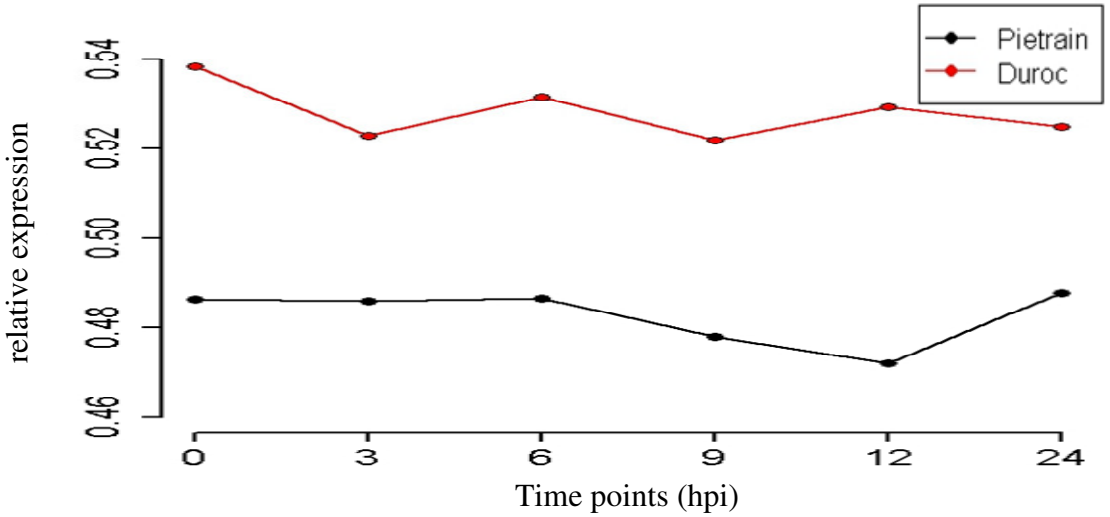

Figure 23: Gene expression profile of IL-6 in infected and non-infected lung DCs, detected by RNA-Seq (A) and by real-time PCR (B), gene expression profile of IL-6 in infected and non-infected PAMs, detected by real-time PCR (C) and gene expression profile of IL-6 in infected and non-infected trachea epithelial cells, detected by real-time PCR (D) of Pietrain (black line) and of Duroc (red line). All measurements were done at 0 h and at 3, 6, 9, 12, 24 hpi

4.6.2 Chemokine (C-C motif) ligand 4

The chemokine (C-C motif) ligand 4 (CCL4) was differently expressed with a higher expression trend in Duroc lung DCs at 3 and 6 hpi ($p \leq 0.05$, FDR 10 %) and a reduced expression level at 9 and 24 hpi ($p \leq 0.05$). In contrast, CCL4 represented a lower expression level between non-infected Pietrain lung DCs in comparison to the expression measured at 6, 9 and 12 hpi ($p \leq 0.05$) as well as at 24 hpi ($p \leq 0.05$, FDR 10 %) (Figure 24, A). The results, recorded through the real-time PCR, showed no statistical differences. Once more the expression profile of infected PAMs exhibited a different expression trend in comparison to infected lung DCs and trachea epithelial cells (Figure 24).

A

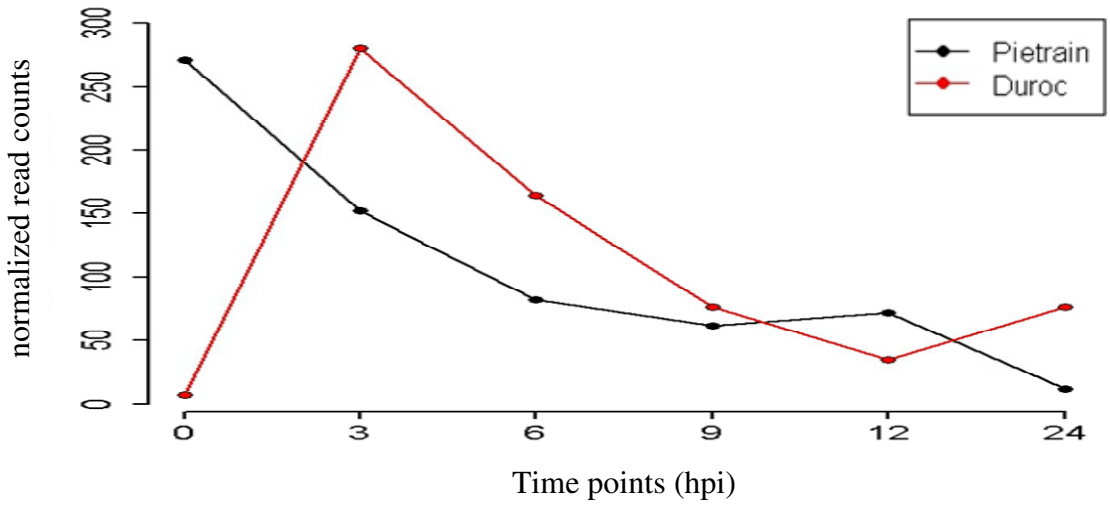
normalized read counts
0
50
100
150
200
250
300
Pietrain
Duroc
0
3
6
9
12
24
Time points (hpi)

B

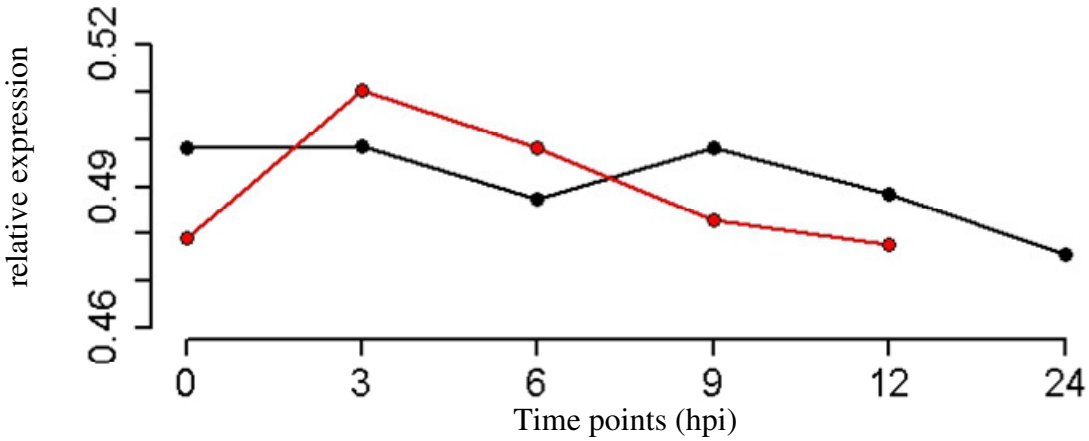
relative expression
0.46
0.49
0.52
0
3
6
9
12
24
Time points (hpi)

C

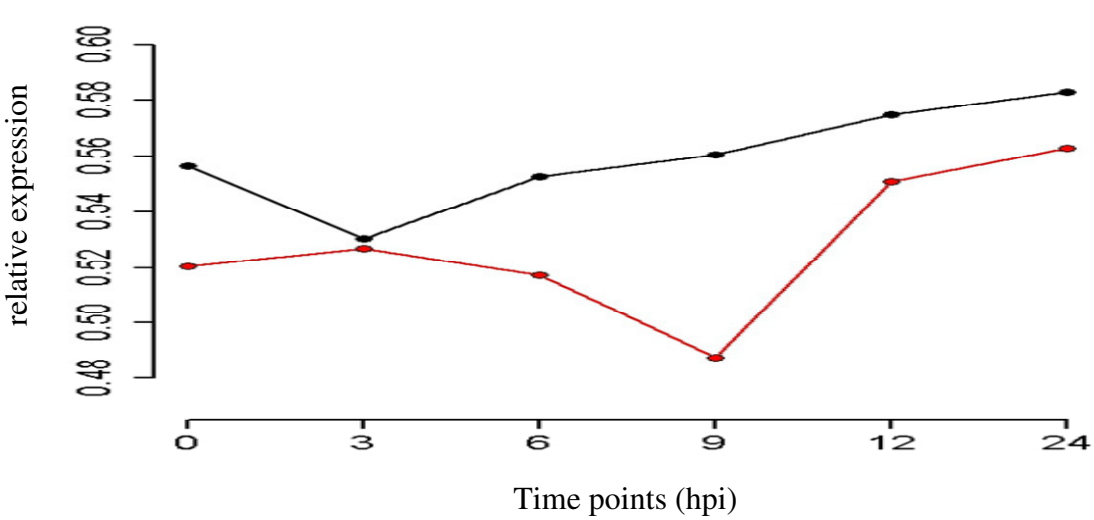
relative expression
0.48
0.50
0.52
0.54
0.56
0.58
0.60
0
3
6
9
12
24
Time points (hpi)

D

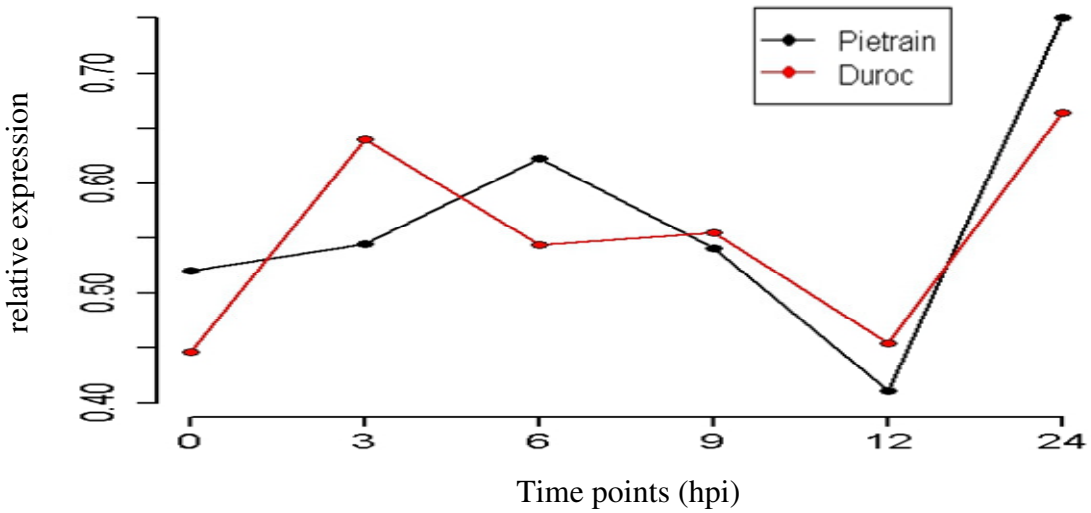

Figure 24: Gene expression profile of CCL4 in infected and non-infected lung DCs, detected by RNA-Seq (A) and by real-time PCR (B), gene expression profile of CCL4 in infected and non-infected PAMs, detected by real-time PCR (C) and gene expression profile of CCL4 in infected and non-infected trachea epithelial cells, detected by real-time PCR (D) of Pietrain (black line) and of Duroc (red line). All measurements were done at 0 h and at 3, 6, 9, 12, 24 hpi

4.6.3 Chemokine (C-X-C motif) ligand 2

In the results of RNA-Seq the chemokine (C-X-C motif) ligand 2 (CXCL2) represented an altered ($p \leq 0.05$, FDR 10 %) expression profile at 12 and 24 hpi in Pietrain lung DCs. Changes of the expression trend were also visible ($p \leq 0.05$) at 3, 6, and 9 hpi with a continuously reduced expression level. During this period (3, 6, 9 hpi) in Duroc samples the expression trend of CXCL2 increased in comparison to time point 0 h ($p \leq 0.05$) (Figure 25, A). The expression profile of lung DCs showed a global breed difference across all time points ($p \leq 0.01$) which was measured by real-time PCR (Figure 25, B). No further statistical differences were observed for CXCL2 in real-time PCR lung DCs, trachea epithelial cells and PAMs (Figure 25).

A

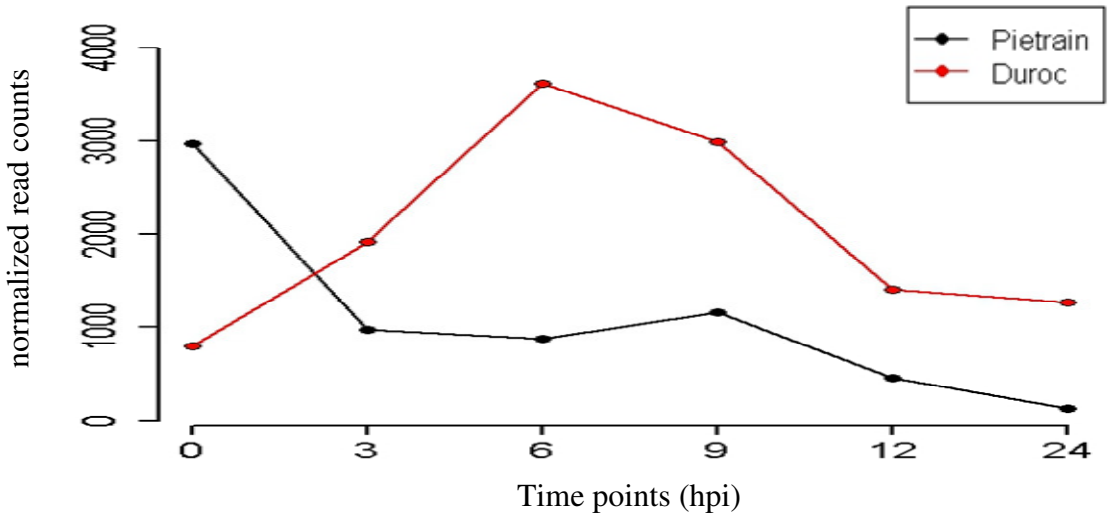
normalized read counts
0
1000
2000
3000
4000
Pietrain
Duroc
0
3
6
9
12
24
Time points (hpi)

B

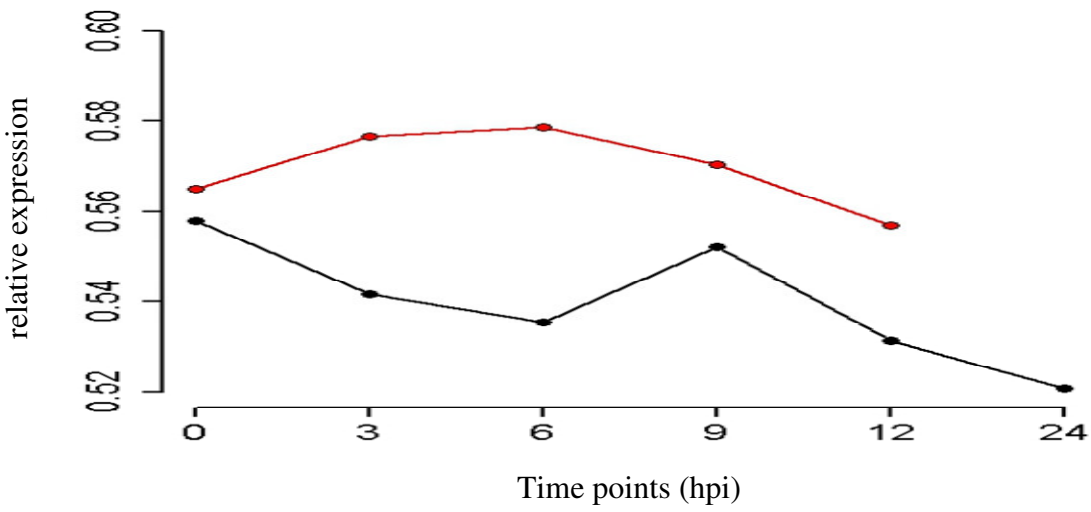
relative expression
0.52
0.54
0.56
0.58
0.60
0
3
6
9
12
24
Time points (hpi)

C

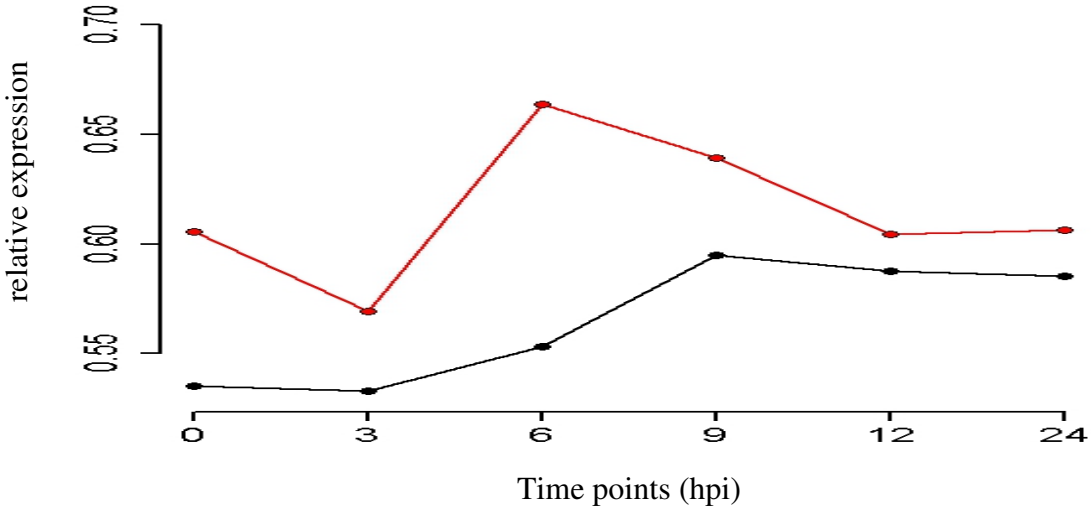
relative expression
0.55
0.60
0.65
0.70
0
3
6
9
12
24
Time points (hpi)

D

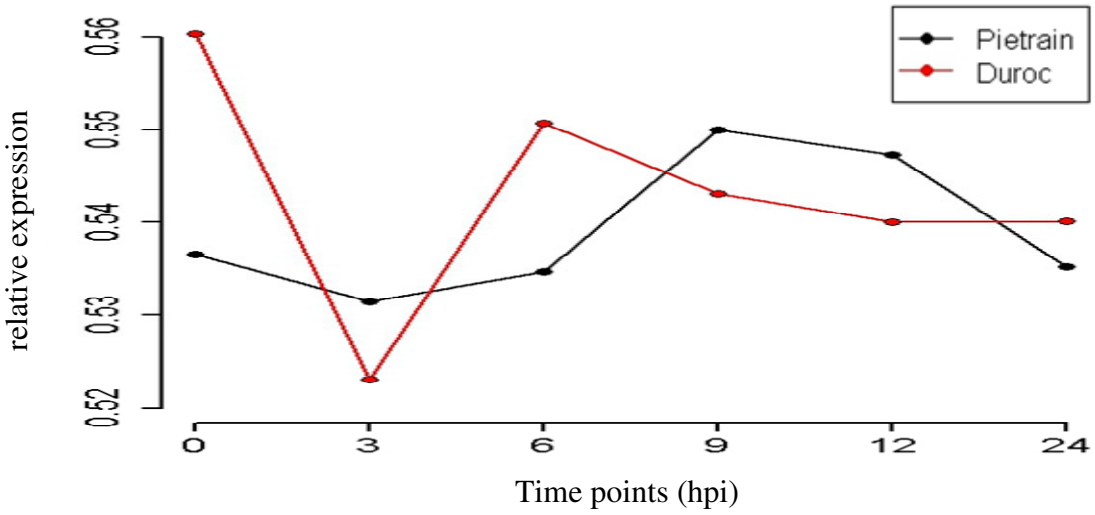

Figure 25: Gene expression profile of CXCL2 in infected and non-infected lung DCs, detected by RNA-Seq (A) and by real-time PCR (B), gene expression profile of CXCL2 in infected and non-infected PAMs, detected by real-time PCR (C) and gene expression profile of CXCL2 in infected and non-infected trachea epithelial cells, detected by real-time PCR (D) of Pietrain (black line) and of Duroc (red line). All measurements were done at 0 h and at 3, 6, 9, 12, 24 hpi

4.6.4 SLA-DRA MHC class II DR-alpha

The expression profile of SLA-DRA MHC class II DR-alpha (SLA-DRA) was down-regulated in Pietrain lung DCs at 24 hpi ($p \leq 0.05$, FDR 10 %). For time point 6 and 12 hpi it represented also a reduced expression level ($p \leq 0.05$) in contrast to non-infected cells (Figure 26, A). The results of infected trachea epithelial cells showed expression differences between 3 and 9 hpi ($p \leq 0.05$) as well as between 3 and 12 hpi ($p \leq 0.05$) for the breed Duroc (Figure 26, D). The expression profile of trachea epithelial cells showed a global breed difference across all time points ($p \leq 0.1$) which was measured by real-time PCR (Figure 26, D).

A

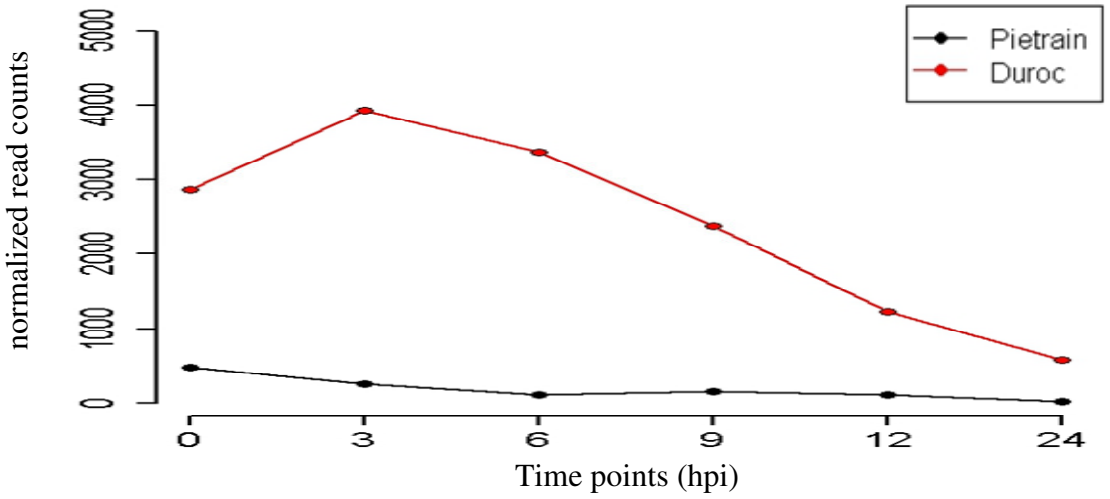
normalized read counts
0
1000
2000
3000
4000
5000
Pietrain
Duroc
0
3
6
9
12
24
Time points (hpi)

B

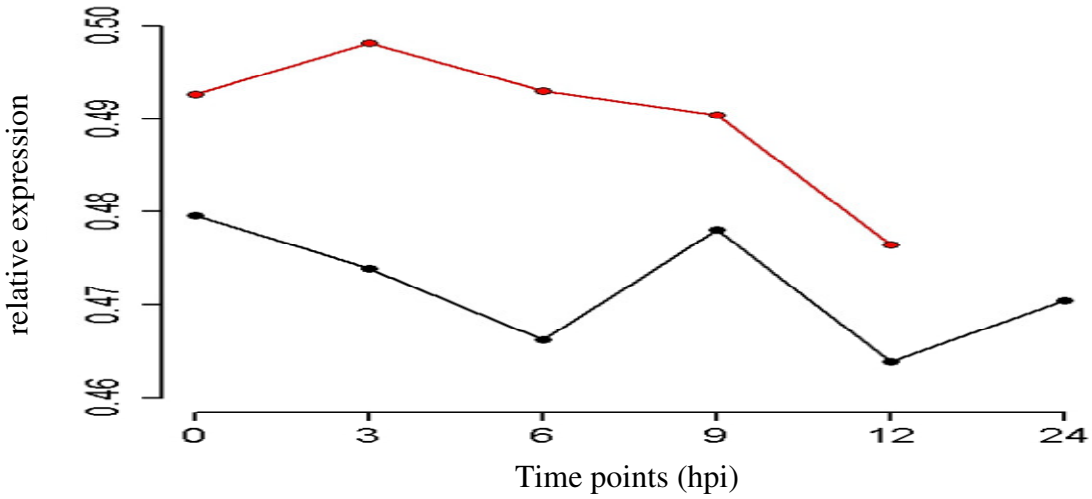
relative expression
0.46
0.47
0.48
0.49
0.50
0
3
6
9
12
24
Time points (hpi)

C

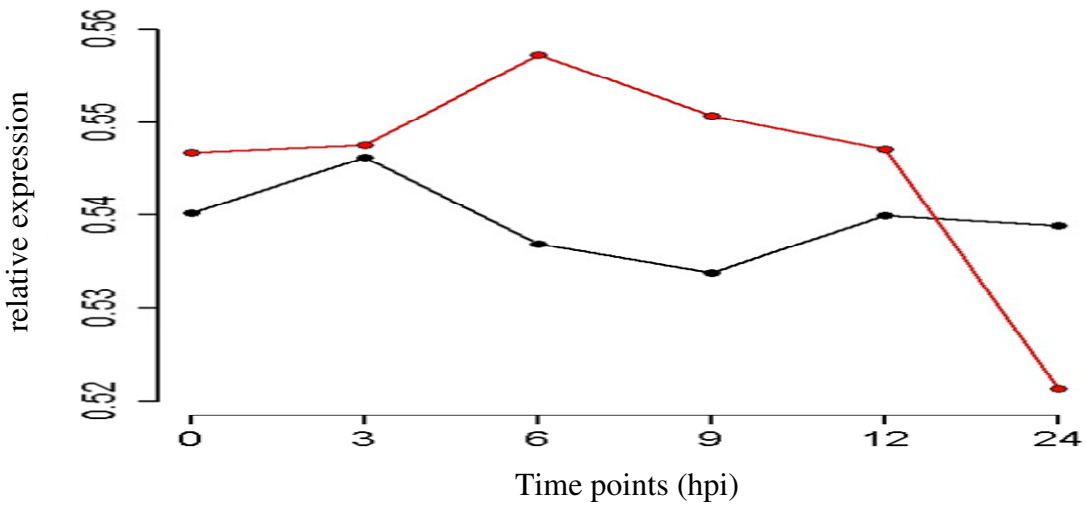
relative expression
0.52
0.53
0.54
0.55
0.56
0
3
6
9
12
24
Time points (hpi)

D

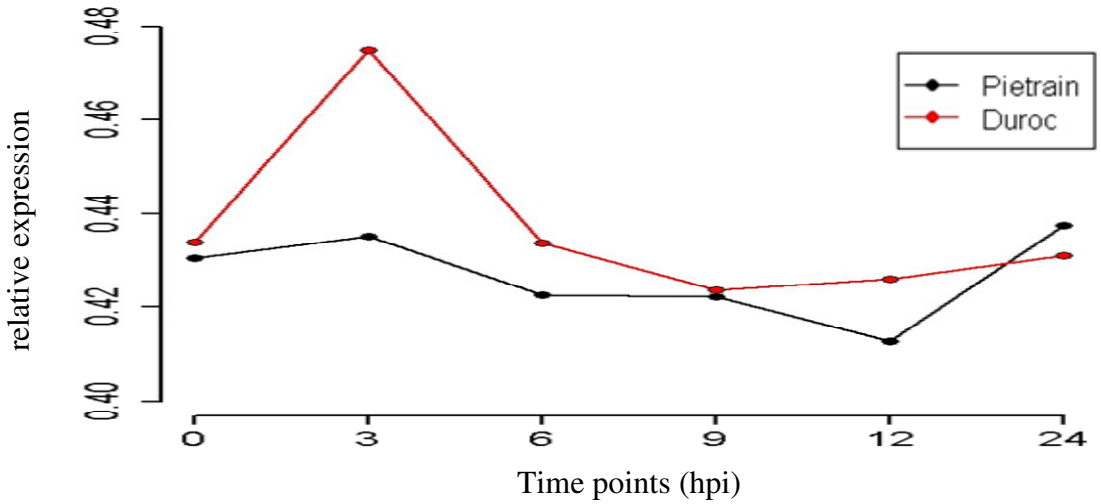

Figure 26: Gene expression profile of SLA-DRA in infected and non-infected lung DCs, detected by RNA-Seq (A) and by real-time PCR (B), gene expression profile of SLA-DRA in infected and non-infected PAMs, detected by real-time PCR (C) and gene expression profile of SLA-DRA in infected and non-infected trachea epithelial cells, detected by real-time PCR (D) of Pietrain (black line) and of Duroc (red line). All measurements were done at 0 h and at 3, 6, 9, 12, 24 hpi

4.6.5 Janus kinase 2

The expression of Janus kinase 2 (JAK2) was down-regulated in Pietrain lung DCs at 12 and 24 hpi ($p \leq 0.05$), represented in the RNA-Seq data (Figure 27, A). The expression profile of lung DCs showed a global breed difference across all time points ($p \leq 0.1$) which was measured by real-time PCR (Figure 27, B). Once more the expression profile of infected PAMs exhibited a different expression trend in comparison to infected Pietrain lung DCs and trachea epithelial cells. But Duroc PAMs showed between 12 to 24 hpi a similar expression course in comparison to lung DCs, measured by RNA-Seq (Figure 27).

A

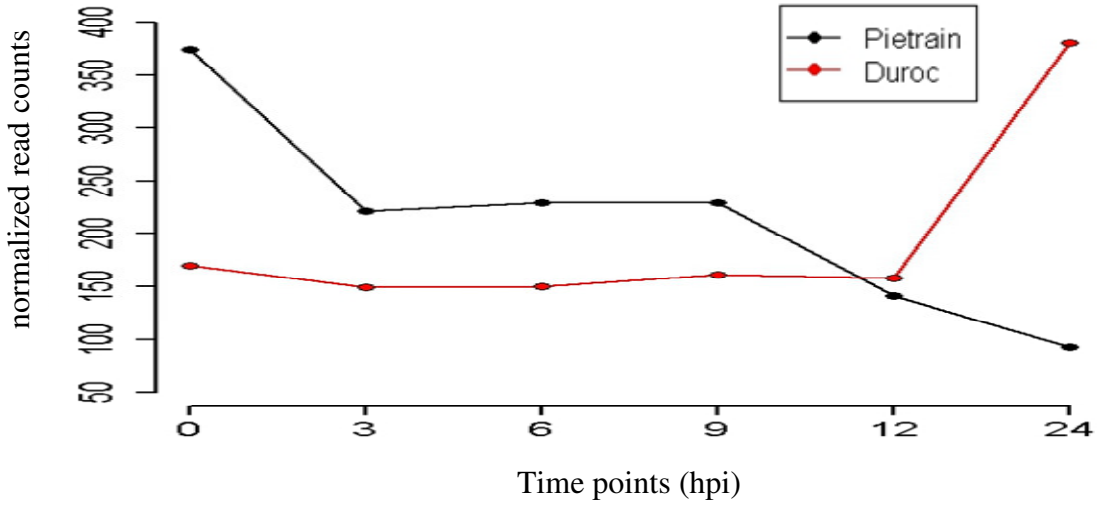
normalized read counts
50
100
150
200
250
300
350
400
Pietrain
Duroc
0
3
6
9
12
24
Time points (hpi)

B

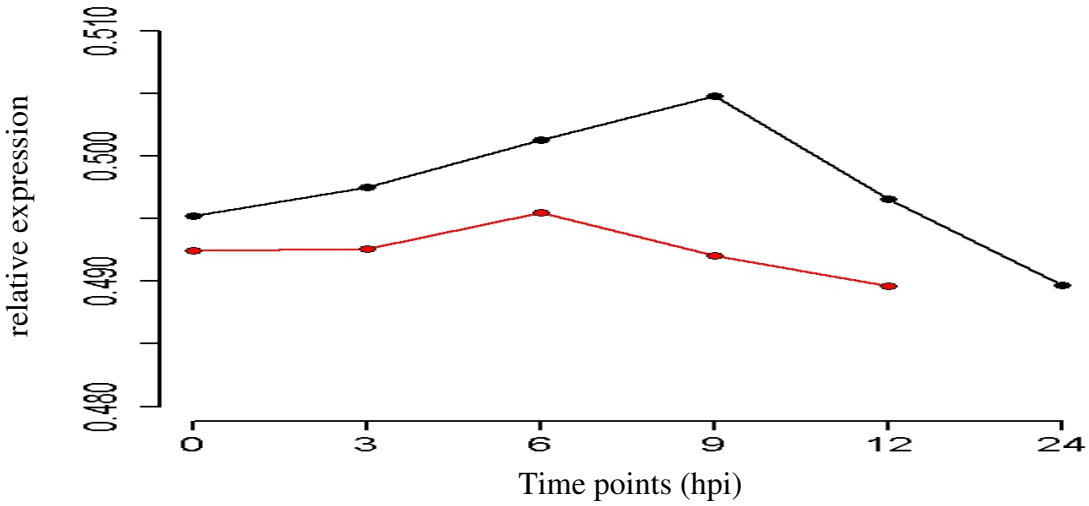
relative expression
0.480
0.490
0.500
0.510
0
3
6
9
12
24
Time points (hpi)

C

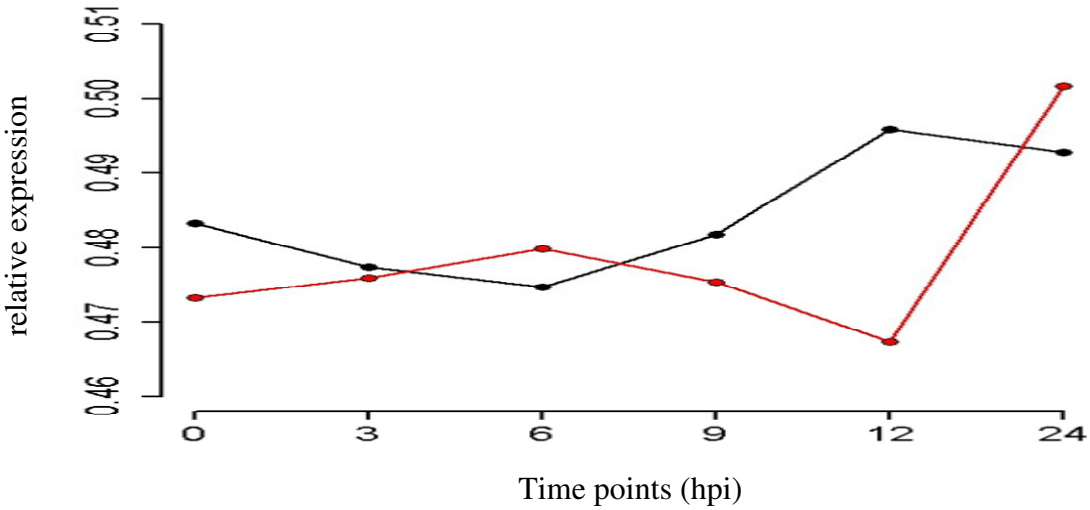
relative expression
0.46
0.47
0.48
0.49
0.50
0.51
0
3
6
9
12
24
Time points (hpi)

D

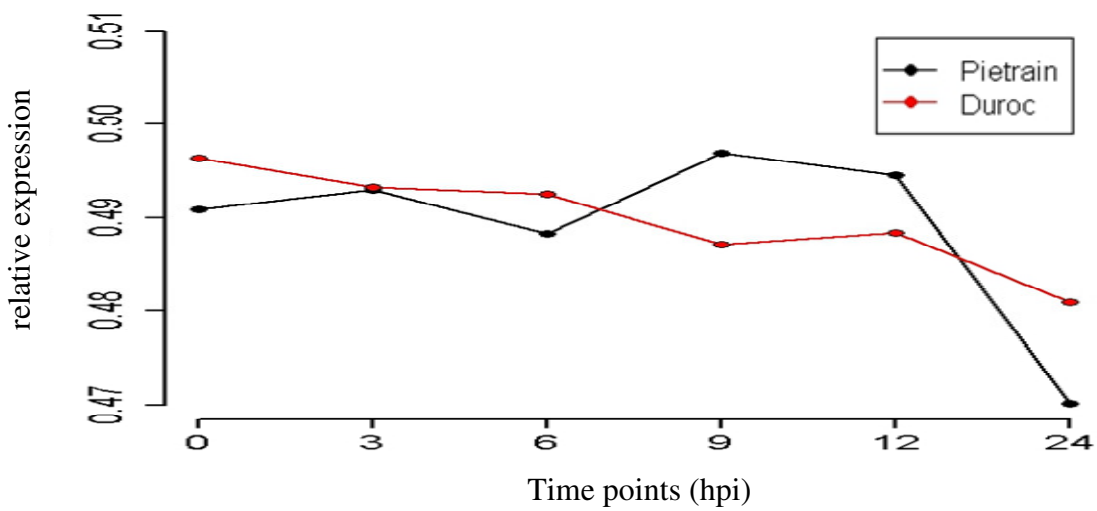

Figure 27: Gene expression profile of JAK2 in infected and non-infected lung DCs, detected by RNA-Seq (A) and by real-time PCR (B), gene expression profile of JAK2 in infected and non-infected PAMs, detected by real-time PCR (C) and gene expression profile of JAK2 in infected and non-infected trachea epithelial cells, detected by real-time PCR (D) of Pietrain (black line) and of Duroc (red line). All measurements were done at 0 h and at 3, 6, 9, 12, 24 hpi

4.6.6 MHC class I antigen 1, CD86 and IFNβ1

The gene expression profiles of MHC class I antigen 1 (SLA-1) (compare chapter 8, Figure A6) represented a global expression difference between the two breeds Pietrain and Duroc in lung DCs ($p < 0.001$) and in trachea epithelial cells ($p < 0.001$).

The expression profile of CD86 of lung DCs showed a global breed difference across all time points ($p \leq 0.01$) which was measured by real-time PCR (compare chapter 8, Figure A7).

The IFNβ1 (compare chapter 8, Figure A8) expression profile of infected lung DCs exhibited a different expression trend in comparison to infected PAMs and trachea epithelial cells. The graphs per gene transcript and respiratory cell line are arranged in the appendix (Figure A6, A7, A8).

4.6.7 Cell-type dependent expression trends

For most of the gene transcripts the expression courses of infected PAMs increased in comparison to the expression trends of lung DCs. The following gene transcripts showed these trends: IL-6, CCL4, JAK2, CD86 and IFNβ1. It was also possible to observe increased gene expression characteristics for IL-6, JAK2, CD86 and IFNβ1 in comparison to PAMs and trachea epithelial cells. The genes SLA-DRA and CXCL2 represented breed differences in the expression trends of PAMs. CXCL2 showed for Pietrain PAMs an increased but for Duroc PAMs a decreased expression trend. These results exhibited once more for Pietrain PAMs a different expression trend of SLA-DRA and CXCL2 in comparison to Pietrain lung DCs.
Trachea epithelial cells also varied in their expression trends. CXCL2 Duroc trachea epithelial cells showed a reduced expression tendency. For Pietrain the expression trend of CXCL2, CCL4 and IFNβ1 switched between a decreased and an increased expression course. At 24 hpi CXCL2 showed for Pietrain a reduced expression tendency and for the gene CCL4 as well as for IFNβ1 an increasing expression trend. At an early infection time point (3 hpi) CCL4 represented an increasing expression trend for Duroc. An immense decrease followed from 3 hpi to 6 hpi but from 12 hpi to 24 hpi an increasing expression tendency was visible. For trachea epithelial cells IL-6 and SLA-1 showed an uniform expression course for both breeds. In different gene expression scenarios the expression trends of trachea epithelial cells differed to the expression trends of PAMs.
It is a notable fact that changes of the gene expression arose at certain time points which could be declared as turning points of the expression trend. In general these turning points appeared 3 h earlier for Duroc than for Pietrain, often at 3 hpi and 6 hpi for Duroc and at 9 hpi for Pietrain. These scenarios could be detected for lung DCs, PAMs and trachea epithelial cells.

In summary, there were cell-type dependent variations in the expression profiles of IL-6, CCL4, JAK2, CD86 and IFNβ1 visible. For these genes PAMs showed remarkable differences in the expression profiles in comparison to lung DCs and trachea epithelial cells.

5 Discussion

The immune responses of pigs to a PRRSV infection are characterized by weak immune reactions. The virus itself has multiple strategies to evade and modulate the host immune response (Beura et al. 2010, Chen et al. 2010, Genini et al. 2008, Li et al. 2010, Wang et al. 2013). The ineffective immune reaction results in persistently infected pigs and induces high economical costs for the pig industry worldwide (reviewed by Murtaugh et al. 2002, reviewed by Zimmerman et al. 2012). Until now, the protective immunity to PRRSV is still not clear, so the question arises what are the causes and implications of an ineffective immune response in pigs?

The research group of Miller et al. (2010) gave an important hint: "The character of the innate immune response to a virus thought to dictate the quality of the adaptive immune response that ensues." In the body defence DCs play the role of "gatekeepers" of the adaptive immune system (reviewed by Stumbles et al. 2003). Their antigen processing and presentation, their vital aspects in the secretion of inflammatory cytokines ultimately induct the innate and adaptive immune responses (Schmid et al. 2011). In the antiviral responses to common respiratory viruses, like influenza and respiratory syncytial virus, lung DCs play a major role as mentioned in the review of Grayson and Holtzman (2007).

In a review the authors Rodriguez-Gomez et al. (2013) mentioned an interaction between PRRSV infection and APCs which results in a decreased expression of MHC II, of CD80/CD86 or even both of them. The consequence is an inaccurate or a non-effective immune response. Rodriguez-Gomez et al. (2013) concluded that all their reviewed studies "[…] lack of the co-localization of PRRSV and the molecule involved in.".

The above mentioned investigations show a selected part of the scientific genesis to the aims of this thesis and underline the actuality and necessity of the study, performed here.

The structure of the discussion follows the outline of the result section (compare chapter 4), within each paragraph a comparison between current publications (researches and reviews) and own findings will be presented and discussed critically.

5.1 Respiratory cells and their phenotypic characterization

In order to obtain an accurate mirroring of the processes which are going on in pigs post PRRSV infection in vivo, primary cell lines were infected for in vitro studies (reviewed by Mercer and Greber 2013). Loving et al. (2007) observed a low expression of the co-stimulatory molecules, CD80 and CD86, this low expression is characteristic for immature DCs (Murphy et al. 2008).

For the present study, relating to the virus cell tropism, lung DCs and PAMs as well as trachea epithelial cells were selected. Flow cytometric analysis helped to characterize lung DCs and PAMs, based on their surface receptor nature. The lung DCs phenotypes were characterized by $CD11c^{+}$, $CD80^{low}$, $CD86^{low}$ and $CD40^{+}$ occurrences. The results, concerning the low expression of CD80 and CD86, showed an accordance with the findings of Loving et al. (2007).

Soudi et al. (2013) mentioned that the phagocytosis assay provides a possibility to detect different genetic background effects on phagocytosis. These authors analyzed the phagocytosis activity of macrophages of two different mice populations, BALB/c and C57BL/6. Their results showed that C57BL/6 mice had a greater phagocytic capacity than BALB/c ones, stimulated with the same LPS treatment. Soudi et al. (2013) indicated that macrophages with different genetic backgrounds respond with different kinetics and with different capacities.

In the present study the different genetic background had an effect on the phagocytosis activity of two pig breeds (compare chapter 4.1.3). The respiratory cells were stimulated with LPS treatment. The breed dependent differences appeared between Pietrain and Duroc PAMs and lung DCs. Pietrain stimulated lung DCs and PAMs had a relative higher phagocytic capacity than stimulated lung DCs and PAMs of Duroc. These results indicated that PAMs and lung DCs with different genetic backgrounds respond to the same stimuli with different phagocytic capacities. Regarding these phagocytosis capacities and considering the results of Soudi et al. (2013), genetic effects on the phagocytosis capacity could not only be found for two mice populations but also here for two pig breeds.

PRRSV and some other viruses are able to repress host cell apoptosis and to facilitate mass viral replication (Sieg et al. 1996, Xiao et al. 2010b, reviewed by Zhou and Zhang 2012). The results, concerning the host cell apoptosis, are described in different studies. Costers et al. (2008) reported about an early stimulation of anti-apoptotic pathways in macrophages post PRRSV infection. Xiao et al. (2010b) detected an up-regulated expression of anti-

apoptotic genes and a down-regulated expression of some pro-apoptotic genes. Jiang et al. (2013) found and described one of the major reactomes of PAMs post PRRSV infection as cell growth and cell death. Additionally, there was a particularly minimized pathway function of anti-apoptosis. Similar results were presented in the study of Badaoui et al. (2014) with a strong activated death/survival biological function.

In the present study the cell viability of respiratory cells was tested post PRRSV infection. The cell viability of infected PAMs showed no fluctuations over all infection time points. PRRSV infected lung DCs and trachea epithelial cells had a lower cell viability at 12 hpi than at 6 hpi.

These aspects let estimate that PRRSV has a temporal effect on the cell viability of lung DCs and trachea epithelial cells at 12 hpi.

5.2 Cytokine profiling

Infection of DCs induces the production of cytokines, intercellular messengers. They are important for the regulation of intracellular signaling events and for the activation of the innate and the adaptive immune response (Tizard 2013). But PRRSV has developed various strategies to modulate the host immune response (Beura et al. 2010, Chen et al. 2010, Genini et al. 2008, Li et al. 2010, Wang et al. 2013).

Some authors discussed that PRRSV may modulate the innate immune response by altering cytokine patterns of macrophages and DCs (Genini et al. 2008, Loving et al. 2007, Miller et al. 2010, Xiao et al. 2010b). Park et al. (2008) detected increasing cytokine concentrations of TNF-α and IL-12 between 24 hpi and 48 hpi. The cytokine concentrations of PRRSV infected DCs were higher at all time points than the cytokine secretion of UV-inactivated PRRSV infected DCs. In the literature the expression of TNF-α in PRRSV infection is described contrarily. On the one hand TNF-α was activated in PAMs (Genini et al. 2008, Thanawongnuwech et al. 2004) and in lung tissue samples (Xiao et al. 2010b), on the other hand a significant reduction of TNF-α had been detected in infected T cell subsets of monocyte cultures (Charerntantanakul et al. 2006). They also found a significant reduction of IFN-γ after PRRSV infection. Furthermore they described a different cell susceptibility to PRRSV where monocyte-derived macrophages were significantly more susceptible to PRRSV, more than monocytes and more than immature MDDCs. Post PRRSV infection cell-type dependent differences in cytokine levels were also detected by Gimeno et al. (2011).

Pro-inflammatory and pro-immune cytokines which were investigated in the present study have different functions.

IL-8 (CXCL8) activates lymphocytes and basophiles. It is involved in neutrophil chemotaxis, these phagocytic cells play a major role in the defence of a host against infections (Badaoui et al. 2014, Petry et al. 2007, Tizard 2013).

IL-1β is one of the most critical mediators of inflammation and of the host response to infections (Abbas et al. 2012).

TNF-α is a mediator of the acute inflammation response with similar biological activities as IL-1 (Abbas et al. 2012, Murphy et al. 2008). It has a stimulating effect on cells to produce acute-phase proteins, on the recruitment of neutrophils (Murphy et al. 2008).

IFN-γ is important in early host defence against infections and it controls many distinct cellular programs over the signaling with a large number of genes. It acts locally in the cell self-activation and in the activation of nearby cells. IFN-γ increases MHC class I and MHC class II molecules and the antigen presentation (Kindt et al. 2007). Additionally, it has the ability to synergize or to antagonize effects of cytokines. Its production is controlled e.g. by cytokines which were secreted by APCs, most notably by IL-12 and IL-18, mentioned in the review of Schroder et al. (2004).

IL-12p40 synthesis is stimulated by PRRs and by IFN-γ. IL-12 is secreted by DCs during the antigen presentation to naïve T cells which will differentiate into T_H1 subset of helper T cells (Abbas et al. 2012).

In the present study the secretion levels of TNF-α and IFN-γ were lower in comparison to the levels of IL-8 and IL-1β. Furthermore, the cytokine concentrations varied between Pietrain and Duroc and there were concentration differences between the three respiratory cell lines. The cytokine concentrations of IFN-γ, IL-1β and IL-8 were higher for Pietrain lung DCs than the concentrations for Duroc lung DCs, PAMs and trachea epithelial cells (compare chapter 4.2).

The understanding of the modified cytokine secretions, of the above mentioned gene functions and of the previously described relations between PRRSV infection and cytokines (Genini et al. 2008, Loving et al. 2007, Miller et al. 2010, Xiao et al. 2010b) helped to interpret the results of the present study. Weak activated cytokines do not have enough power to stimulate or to activate the following gene signaling cascade in a markedly effective way. In the present study weak TNF-α and IFN-γ cytokine secretions were observed, this led to a reduced cell self-activation and to a reduced activation of nearby cells. Ineffective cytokine activation provides a lack of increased transcription of

cytokine and chemokine genes which are needed to develop a protective immune response to PRRSV infection.

In the present study the cytokine mRNA expression was performed over all infection time points (compare chapter 4.2). The expression profiles of IL-8 and IL-1β varied within each respiratory cell line and between lung DCs, PAMs and trachea epithelial cells. As mentioned above, IL-1β and IL-8 had a high secretion at 9 hpi. This was the time point where the cytokine expression trend changed, a decurrent expression trend for lung DCs followed. Different results were identified for IL-1β and IL-8 mRNA expression profiles of infected PAMs. There were upward trends visible in both expression courses. It can be estimated that there might be higher cytokine concentrations of PAMs after 9 hpi. For PAMs the turning point of the gene expression was at 3 hpi, for lung DCs at 6 hpi. The PRRSV infection resulted in a down-orientated expression trend for lung DCs and in an up-regulated one for PAMs.

In the present study the previous observed cell-type dependent differences of the cytokine secretion were confirmed by the cytokine mRNA expression. The cell-type responses to PRRSV showed that there were different cell-type susceptibilities to PRRSV in the investigated time frame.

5.3 Transcriptome profiling post virus infection

The latest technology was used to characterize transcriptional changes after PRRSV infection in lung DCs of two different pig breeds.

The sequencing technology is based on the detection of counts of transcripts and measures the overall gene expression profile, so this measurement exceeds the measurement of probes on an array (Marioni et al. 2008). This new technology makes it possible to identify large amounts of gene transcripts and different signaling cascades that are affected by PRRSV infection. In Table 6 different studies were listed which were done with microarray approaches and with next generation sequencing (NGS) post PRRSV infection.

Table 6: Microarray and sequencing approaches post PRRSV infection

Technology	Tissue/cell-type	Breed and animal no	References
Microarray	PAMs	Rattlerow-Seghers genetic line (n=6)	Genini et al. (2008)
Microarray	PAMs	Tongcheng boars (a Chinese indigenous breed) (n=3 uninfected and n=3 infected)	Zhou et al. (2011a)
Microarray	PAMs	Landrace (n=3), Pietrain (n=3)	Ait-Ali et al. (2011)
NGS	Lung tissues	Landrace×Yorkshire (n=9)	Xiao et al. (2010b)
SAGE*	PAMs	Breed unpublished (n=3)	Miller et al. (2010)
SAGE*	PAMs	Breed unpublished (n=3)	Jiang et al. (2013)
NGS	PAMs	Piglets (n=3) from JSR Genepacker 90 English: Landrace×Large White and Pietrain boars	Badaoui et al. (2014)

SAGE*= Serial Analysis of Gene Expression

In previous studies (Table 6) the new technology was used for the investigation of PAMs and lung tissues, in the present study it was utilized to get the temporal (0 h, 3, 6, 9, 12, 24 hpi) transcriptome profile of PRRSV infected lung DCs of two different breeds. With RNA-Seq it was possible to extract an amount of 20,396 porcine predicted gene transcripts which were further analyzed on different ways, using various biotechnological tools and software packages (compare chapter 3.2.13).

The costs for the transcriptome profiling are high but the output is extremely efficient (reviewed by Khatoon et al. 2014). Beside the transcriptome profiling new statistical methods were developed to analyze the RNA-Seq data of no replicated samples (Jungsoo and Taesung 2012, Wu and Wu 2013). These methods support the investigations of transcriptome profiles of exceptional, infrequent and rare samples (Tang et al. 2009).

5.3.1 Virus replication

Loving et al. (2007) described that PRRSV did not show any replication in lung DCs. These authors concluded that PRRSV is able to utilize lung DCs without a viral replication.

In the present study the alignment analyses after NGS were done with the LV strain complete genome (compare chapter 3.2.13), to detect the virus replication in lung DCs. The investigations showed that LV was able to infect lung DCs and to replicate there (compare chapter 4.3). These results are in contrast to those of Loving et al. (2007). A possible cause for these different results may be the application of various virus strains in both studies.

The results showed breed differences, related to the measured viral read amounts. First the PRRSV replication was extremely increased in Pietrain lung DCs until 12 hpi. But for the same time period the virus replication in Duroc lung DCs was very low. The viral amount decreased for Pietrain lung DCs until 24 hpi. But with a big difference, the replication of PRRSV significantly rose for Duroc until 24 hpi. Once more the differences between the two pig breeds were visible (compare chapter 5.2), the detected amounts of viral read counts in lung DCs varied between Duroc and Pietrain. For both breeds two time points were important, for Pietrain 12 hpi and for Duroc 9 hpi. It can be supposed that at these two different time points, important molecular changes in the cells appeared so that the virus replication for Pietrain decreased until 24 hpi and extremely increased for Duroc till 24 hpi.

Estimations for these different reactions could be that PRRSV modulates an early apoptosis reaction of lung DCs of Pietrain and that for Duroc modulations of the immune response happen later. Concerning the virus replication at the fist time points, Duroc lung DCs reacted more effectively than Pietrain lung DCs during this period of infection.

5.4 Cluster analyses of RNA-Sequencing data

Cluster analyses were performed, to separate the data clearly, according to their similar expression patterns. These results allowed to identify different attributes on the detected transcriptome profiles. Clustering approaches are effective and helpful tools to explain the temporal expression profiles of thousands of gene transcripts and allow furthermore to characterize the genes' role during the observed process (Ma and Zhong 2008). With a transcriptional dataset of pre- and peri-implantation-stage of bovine conceputses, Mamo et al. (2011) performed nine gene clusters which were different in their expression patterns. These nine clusters reflected clearly the transcriptional changes during the development stages.

In the present study 37 clusters for Pietrain and 35 clusters for Duroc were identified from 20,396 porcine predicted gene transcripts (compare chapter 4.4). Each cluster arose, due to the fusion of different transcriptome profiles which had developed during the infection period. Derived from the same number of genes and analyzed, using the same statistical method, it is remarkable that the number of clusters for both breeds was nearly the same (Pietrain 37/ Duroc 35).

The following functional analyses were necessary in order to understand the possible viral influences on the gene expression and to understand the interplay of the virus with the host immune response.

5.4.1 Functional analyses of clustered gene transcripts

The analyses of this transcriptome data, regarding the pathway enrichment, allow the description of biological functions of the clustered gene transcripts.

Jiang et al. (2013) found differentially expressed genes in PRRSV infected PAMs. They presented an overview of functional pathways and the reactomes of PAMs. Their results consisted of a composite dataset of three different databases. The authors classified their data in six functional systems, including cellular processes, genetic information processing, environmental information processing, metabolism, organismal systems and human diseases.

Badaoui et al. (2014) investigated the response of PAMs after infection with two different strains of PRRSV. For their investigations they used canonical pathways, biological functions and individual genes. The authors identified the cell death/survival as a very

strongly activated biological function post infection with the strain LV in comparison to the Lena strain.

The present study is the first comprehensive one that showed the involved pathways post PRRSV infection in lung DCs and characterized the functional background. The main biological functions of Pietrain and Duroc were performed in a “Top 10 list” (compare chapter 4.4.1 and 4.4.2). Four of these pathways dominated the frequency analyses, phagosome, rheumatoid arthritis, focal adhesion and protein processing in endoplasmic reticulum. Additionally, three pathways: phagosome, oxidative phosphorylation and endocytosis stood out because of their high common gene transcript frequency for both breeds. They can be designated as key pathways. Beside these key pathways, the functional analyses made it possible to detect a key cluster for each breed, cluster 34 for Pietrain and cluster 32 for Duroc.

During the virus entry the endocytic pathway is used, the receptor mediated endocytosis might be a common entry route for arteriviruses (Nauwynck et al. 1999).

The importance of the phagocytosis pathway for the virus-host interplay was also mentioned by De Baere et al. (2012). They detected that the European genotype PRRSV inhibited the phagocytosis of PAMs at an early stage of the virus entry.

Chen et al. (2010) indicated that the viral NSP1β inhibits the phosphorylation and the activation of the STAT1 in JAK–STAT signaling pathway. Through their findings they highlighted the importance of the JAK–STAT signaling pathway for the virus-host interplay.

The key pathways of the present study are different to those of earlier studies, mentioned above. The key pathways here are related to functional tasks of DCs and play important roles in the virus-host interplay, like phagocytosis, endocytosis and rheumatoid arthritis as well as JAK–STAT signaling pathway. Lung DCs, PAMs and trachea epithelia cells presented a good phagocytosis effect after LPS stimulation (compare chapter 4.1.3).

In order to get a better understanding of the virus-host interaction, it could be helpful to investigate the interplay of the genes of the key clusters with the key pathways. A selection of genes of the above mentioned pathways are discussed next.

Genes of the v-ATPase complex facilitate the entry of enveloped viruses and bacterial toxins, they play roles in the proton transport and are involved in the acidification of endosomes and in the intracellular transport (Hinton et al. 2009). Zhou et al. (2011a) detected the gene ATP6V1B2 in their study with Tongcheng piglets. ATP6V1B2 was up-regulated in PAMs after infection with the HP-PRRSV WUH3 strain.

In the present study for both breeds several genes of the v-ATPase complex stood out (ATP6V1G1, ATP6V1C1, ATP6V1B2, ATP6V1F and ATP6V1E1).

The gene transcripts SEC61B and SEC61A1 were also detected in the present study. This gene group belongs to the ER-resident multimeric protein complex (Abada et al. 2012). They concluded that the gene SEC61β modulates the cytotoxicity of many chemotherapeutic agents and is sensitive to the cytotoxic effects of platinum-containing drugs.

SLA-7 was found in the present study, too. This gene is related to the swine major histocompatibility complex, especially to the non classical MHC class Ib genes. These genes seem to be good candidates for investigations of species-specific immunity-related roles. Further studies are necessary to explain the functional skills of SLA-7 (Hu et al. 2011).

All the just mentioned genes of the present study play, according to their functions – virus entry, drug performance and species-specific immunity – important roles for the health care. This way of transcriptome analyses post PRRSV infection identified a kind of parallelism and homology of both breeds with regard to the detected key pathways, key clusters and the above mentioned genes.

5.5 Differentially expressed gene transcripts post infection

Genini et al. (2008) and Ait-Ali et al. (2011) reported that already in a short period of time (within 24 h) post virus infection, remarkable reactions can be observed in pigs' cells. Both described that the first 8 - 10 hpi built the critical time frame. Ait-Ali et al. (2011) interpreted this time as critical when PRRSV evades the host responses and enhances its own chances for virus growth. Genini et al. (2008) mentioned the effect of PRRSV infection after 3 and 6 hpi with a consistent down-regulation of genes, followed by the start of innate immune responses at 9 hpi.

The present study is one of the first investigations to generate comprehensive analyses of PRRSV infected lung DCs of two different breeds at various time points. The results delivered transcriptions of genes which altered through PRRSV infection. An early host transcriptional variation was measured during the PRRSV infection (3 - 24 hpi). At the beginning of the infection of Duroc (3 hpi), there was a high up-regulation and next an extreme reduction of the gene expression till 24 hpi. Pietrain infected lung DCs varied slightly in their up-regulated expression, but the number of down-regulated genes increased extremely till 24 hpi. Duroc infected lung DCs showed a contrary course with their down-regulated gene expression in comparison to Pietrain. The increasing down-regulated gene transcripts of Pietrain infected lung DCs from 9 hpi to 24 hpi included important immune genes like CCL4, CXCL2, IL-1β, IL-6, TNF, IL-1α, SLA-DRA, CCL3L1, CCL23 and CCL20. The decreasing up-regulated gene transcripts of Duroc lung DCs between 3 hpi and 24 hpi also contained important immune genes like CCL4, CXCL2, IL-1β, CXCL10 and CCL8 (compare chapter 4.5). It is remarkable that CCL4, CXCL2 and IL-1ß were differently regulated for Pietrain and Duroc. At 9 hpi for the response to PRRSV, it seems that essential processes happened with drastic changes in the host expression trends of both breeds.

In the first hpi of PRRSV Genini et al. (2008) observed a down-regulation of genes, followed by the start of innate immune responses at 9 hpi. Ait-Ali et al. (2011) also described an early host response to PRRSV. They detected a large number of differently expressed transcripts for infected PAMs between 0 h and 8 hpi. These observations were followed by a reduction of up- and down-regulated gene transcripts between 12 to 30 hpi for the breeds Landrace and Pietrain. They responded identically to PRRSV but the amounts of regulated genes were higher for Landrace than for Pietrain at all time points.

In contrast to the above mentioned gene regulations of Landrace and Pietrain, in the present study Duroc and Pietrain responded differently to PRRSV infection in their up- and down-regulation of gene transcripts, breed differences were visible. Concerning the up- and down-regulated expression courses of the above investigated genes, it seems that Duroc lung DCs reacted better than Pietrain lung DCs during the first 24 hpi, regarding the immune response.

5.5.1 Virus-host interaction

The following Figure 28 shows a scheme of the virus-host interaction.

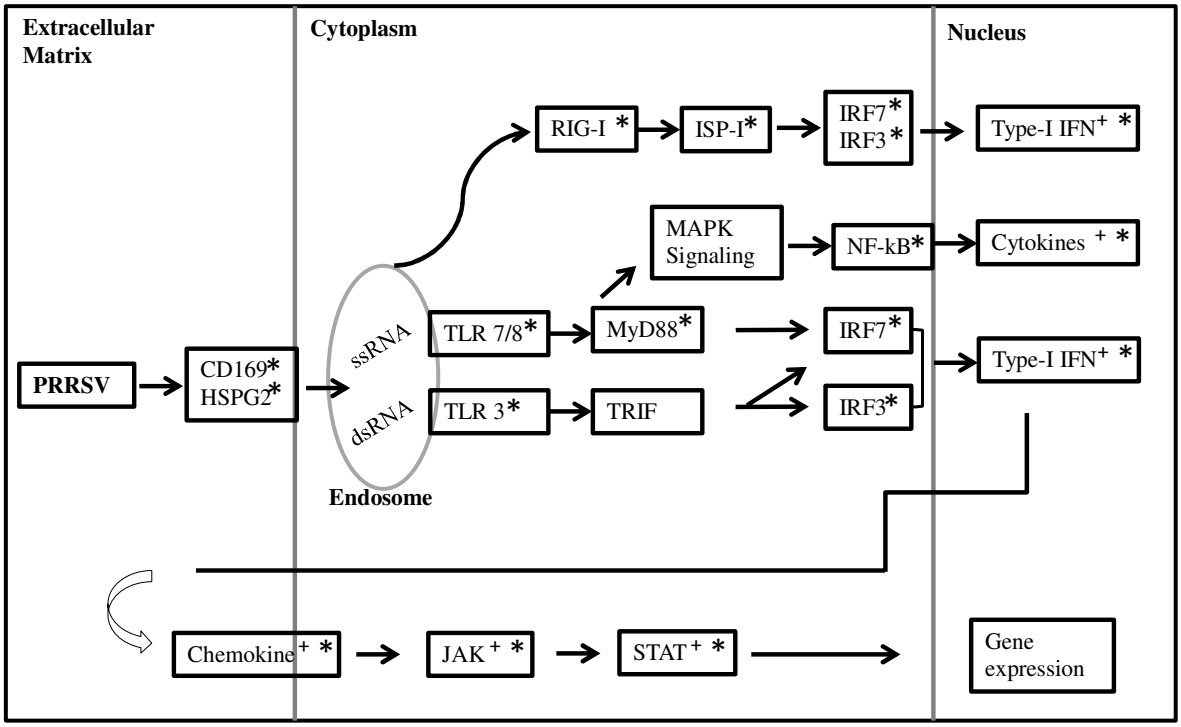

Figure 28: Virus-host interaction. Schema modified, compare Zhou et al. (2011a), * genes and gene families which were identified by RNA-Seq, + genes which were validated through real-time PCR

The scheme (Figure 28) and the next sections depict and explain the involved genes of virus infection and the following gene cascade through the host cells.

Specific cell surface markers are important for the virus entry into the cells. For example SIGLEC-1/CD169 and HSPG2 are such receptors, as mentioned in chapter 2.1.3 (Delputte et al. 2002, Duan et al. 1998, Nauwynck et al. 1999). In the present study these two genes were identified across all investigated time points in both breeds.

Next the virus is transported to the endosomes (Nauwynck et al. 1999) where it starts its replication process and is recognized by PRRs, like TLR3 (Liu et al. 2009a) or TLR7/8 (Diebold et al. 2004, Lund et al. 2004) which activate a cascade of gene signaling.
In the present study TLR1 to TLR10 were identified. The amounts of the read counts of TLR7/8 were extremely low (Figure 28). Further gene transcripts were identified which play important roles in the gene signaling cascade in the response to PRRSV like MyD88, IRF3, IRF7, IRAK4, DDX58/RIG-I, MAVS/IPS-1 and RELA/NF-$_K$B (Figure 28) (Zhou et al. 2011a). They are responsible for the activation of genes like members of the Type I IFN family (e.g. IFNα, IFNβ) as well as different cytokines and chemokines (e.g. IL-1β, IL-6, IL-8, IL-12, TNF-α). Different cytokines and chemokines (e.g. IL-12, IL-6) stimulate the JAK-STAT-signaling pathway by receptor binding. This pathway activates among others the expression of IFN-stimulated genes (ISGs) (Figure 28) (Alberts et al. 2008, Kindt et al. 2007, Zhou et al. 2011a).
Some of these genes were analyzed in the present study (compare chapter 4.2 and 4.6) and discussed in the chapters 5.2 and 5.5.2.
During the viral entry, viral detection and viral replication modulations of DCs surface molecules appear. Weesendorp et al. (2013) described large modification effects on the cell surface molecules like CD80, CD86 and MHC class antigens (MHC I and MHC II). These changes can extremely influence the antigen presentation features of lung DCs which has an additional impact on the following immune response. In a review Rodriguez-Gomez et al. (2013) emphasized the impact of PRRSV on APCs. They described the modulation of DCs' essential surface molecules. Wang et al. (2007) suggested that PRRSV infected DCs present antigens less efficiently. The authors Park et al. (2008) concluded that PRRSV infected DCs may be the causes for a weak immune response.
In the present study a down-regulated gene expression profile of the surface molecule SLA-DRA (MHC class II) was visible in infected Duroc lung DCs. Differences in the expression trend of infected Duroc trachea epithelial cells were detected. Additionally, gene expression variations of DCs surface markers CD80 and CD86 implied changes for the further signaling way.
In the present study CD80 represented lower read counts in comparison to CD86 across all infection time points for lung DCs for both breeds, whereas no breed differences were detected for CD80. However, the read counts of CD86 made it possible to suppose a different expression trend between the two breeds. For Pietrain the read counts of CD86 were remarkable lower than those of Duroc. The breed differences were confirmed through

the results of the real-time PCR. They also showed a massive expression difference between the lung DCs of the two breeds Pietrain and Duroc for CD86. These results support the above mentioned assumption that Duroc performed better in the response to PRRSV infection during the first 24 hpi.
The expression trend of SLA-DRA (MHC class II) also showed breed differences. For Duroc different expression courses (compare chapter 4.6.4) were observed in trachea epithelial cells and lung DCs as well as in trachea epithelial cells and PAMs. In contrast all respiratory cell types of Pietrain followed a similar expression course.

5.5.2 Gene signaling post infection

PRRSV has the ability to escape or to modulate the host immune system by inhibiting key cytokines and by inducing regulatory cytokines (Genini et al. 2008, Miller et al. 2010, Xiao et al. 2010a, Xiao et al. 2010b). Cytokines and chemokines play a crucial role in the immune system. They are able to interact with other immune cells and to induce the inflammatory and adaptive immune response. Cytokines and chemokines are working as mediators (Abbas et al. 2012, Alberts et al. 2008).
In the present study modulations of cytokine expressions were visible for the gene transcripts IL-6, CCL4, CXCL2, IFNβ1 as well as for JAK2 (Figure 28). Differences of the expression profile of the following cytokines and chemokines were observed.
IL-6, an acute inflammatory cytokine, primes B and T cell response against infections. The IL-6 signaling activates the transcription factor STAT3 and plays an anti-inflammatory role (Abbas et al. 2012, Kindt et al. 2007, Tizard 2013).
In the present study for both breeds IL-6 represented a down-regulated expression course in lung DCs but an increased expression trend for PAMs (compare chapter 4.6.1). A global breed difference was detected for trachea epithelial cells of Pietrain and Duroc, concerning IL-6 across all time points.
Chemokines constitute a family of at least 50 chemoattractants. They coordinate the migration of cells and play an important role in selective recruiting of monocytes, neutrophils and lymphocytes. Chemokines are involved in the course of many inflammatory and immune responses (Kindt et al. 2007, Tizard 2013).
CCL4 is an important chemoattractant and plays a role in virus-induced diseases (Chen et al. 2014, Murphy et al. 2008, Zhao et al. 2007). CXCL2 is a pro-inflammatory chemokine

and attracts neutrophils as well as T cells (reviewed by Mantovani et al. 2011, Murphy et al. 2008).

In the present study CCL4 showed a down-regulated expression trend for Duroc and Pietrain lung DCs but an up-regulated one for PAMs of both breeds. An up-orientated expression course of Duroc lung DCs and a down-orientated expression trend for Pietrain lung DCs post PRRSV infection was visible for CXCL2. An opposite trend for CXCL2 was detected for Pietrain PAMs (compare chapter 4.6.2 and chapter 4.6.3). The expression profile of CXCL2 of lung DCs showed a global breed difference across all investigated time points.

IFN-α and IFN-β are two major type I interferons. These cytokines play crucial roles in the response to virus infection or in the immune stimulation (Kindt et al. 2007). They interfere with viral RNA and with protein synthesis. They are produced by virus infected cells within few hours post virus invasion. After IFN-α and IFN-β secretion, they bind to IFNAR and trigger the JAK-STAT signaling pathway (Dimmock et al. 2007, Tizard 2013).

In the present study IFNß1 showed an up-orientated expression course during the first hpi and a down-orientated expression trend for Pietrain lung DCs at 24 hpi. An extreme increasing expression trend for IFNß1 was detected for PAMs of both breeds.

The JAK-STAT signaling pathway plays an important role in the immune response. It works with four known Janus kinases (JAK1-3, TYK2) and with seven transcription factors, called signal transducers and activators of transcription (STAT1-4, 5a, 5b and 6) and depends on a cytokine-mediated activation process (Abbas et al. 2012, Alberts et al. 2008, Kindt et al. 2007). A rapid JAK-mediated phosphorylation of STATs can be induced by the binding of IFNs to cell receptors. The gene regulatory protein STATs migrate to the nucleus and activate the transcription of various genes. The following cytokines and different hormones can activate JAK-STAT signaling pathways as IFN-γ, IFN-α, IL-3 and the growth hormone (Alberts et al. 2008, reviewed by Shuai and Liu 2003).

In the present study a down-regulation in the expression trend of Pietrain lung DCs was detected for JAK2 (compare chapter 4.6.5). Especially the down-regulated expression trend for Pietrain lung DCs from 12 hpi to 24 hpi stood out, the change started already at 9 hpi. The gene expression of Duroc lung DCs passed in a similar way as for Pietrain but the expression change started already at 6 hpi. An opposite trend for JAK2 was detected for PAMs (compare chapter 4.6.5).

In the present study a common reduced gene expression trend of the cytokines and chemokines for lung DCs was visible particularly with regard to 24 hpi. Other expression

trends could be detected for PAMs as well as for trachea epithelial cells. The orientation of the expression trends with regard to 24 hpi seemed to be cell-type dependent. There were more up-orientated gene expression trends of the cytokines and chemokines for PAMs in comparison to the common down-orientated gene expression trends for lung DCs. For trachea epithelial cells there was no uniform expression trend visible. Additionally, turning points of the expression courses appeared 3 h earlier for Duroc than for Pietrain.

Concerning the gene expressions, the investigated Duroc cells responded in general 3 h earlier than the Pietrain cells. This supports the estimation, already mentioned under paragraph 5.3.1 that Duroc cells reacted more efficiently than Pietrain cells in the first time points post PRRSV infection.

The results also showed that the virus-host interaction was different for the various respiratory cell-types. With regard to time point 24 hpi and the down-orientated cytokine and chemokine expression trends of lung DCs, it can be estimated that these cells did not have enough power to activate following gene cascades and/or to stimulate other immune reactions. In contrast, regarding the same time point and the up-orientated expression course of PAMs, it can be estimated that these cells have enough capacity to give signals to the immune system. Regarding the expression trend of trachea epithelial cells at time point 24 hpi, no clear estimation, concerning the influence of these cells on the following immune reaction, can be mentioned.

5.6 Conclusion

The above discussed results (compare chapter 5.2, 5.3, 5.4 and 5.5) which were achieved in this thesis, verified the following hypotheses:

1. After a short period (within 24 h) of infection with PRRSV remarkable transcriptional reactions can be observed in DCs of pigs.

2. These reactions have an essential influence on the following pigs' immune responses to PRRSV, especially on immune related genes and proteins.

3. Based on the different genetic background of Pietrain and Duroc pigs, their cellular immune reactions are different during PRRSV infection.

The results will also be used to clarify if, how and to what extend the aims of the present study (compare chapter 2.4) were achieved.
For this thesis the RNA-Seq was a very supporting technology which identified large amounts of gene transcripts. The technology made it possible to determine the viral replication per breed. This result showed that LV was able to infect and to replicate in lung DCs. The detected virus replications were breed-dependent differently. Duroc lung DCs reacted more effectively at the fist time points of the virus replication. It can be estimated that the genetic background of Pietrain and Duroc had an influence on the immune response to PRRSV.

After a short infection period and within 24 hpi remarkable reactions in lung DCs were observed (hypothese 1). Investigations of the differently expressed genes, especially the up-regulation of immune genes at 3 hpi for Duroc and the increasing amounts of down-regulated immune genes between 9 hpi and 24 hpi for Pietrain determined the short time period after infection as important and relevant (hypotheses 1 and 3). Not only the fast immune response to PRRSV but also the detected various and contrary responses to PRRSV of both breeds are important results of this thesis.
Duroc cells responded 3 h earlier with an up-regulation of immune gene transcripts in contrast to Pietrain cells which reacted with an increased amount of down-regulated immune gene transcripts. These notable findings could be an indication that the

investigated Duroc cells responded better in the first 24 hpi than Pietrain cells (hypotheses 1 and 3). Contrary to the assumption that Duroc cells reacted more efficiently, the high amount of virus growth in Duroc lung DCs until 24 hpi has to be considered. An explanation might be the reduction of the amounts of gene transcripts – down- as well as up-regulated ones – until 24 hpi in Duroc cells.

Not only differences in the response to PRRSV between the breeds were detected but also cell-type dependent differences in the response to PRRSV. These findings allow to indicate that different cell-type susceptibilities to PRRSV exist. The PRRSV infection resulted in a vigorous different cell-type response, indicated through aberrant expression trends between lung DCs and PAMs as well as between trachea epithelial cells and PAMs. The developed trend of lung DCs post PRRSV infection let to estimate that the bridging effect between the innate and the adaptive immunity of lung DCs is too weak or too ineffective to initiate a protective immune response against PRRSV. These observations were made for lung DCs of both breeds with regard to the expression profile at 24 hpi. This situation was different for PRRSV infected PAMs. At 24 hpi it seemed that PAMs were “activated” and might be more effective for further immune responses.
Beside the already named differences also accordances in the response to PRRSV were identified. A kind of parallelism and homology of both breeds in the response to PRRSV through the functional analyses were detected. According to their functions – virus entry, drug performance and species-specific immunity – the gene transcripts which derived from the functional analyses of the present study play important roles for the health care.

This is the first comprehensive study that described the transcriptome profiles of two different breeds post PRRSV infection, especially of infected lung DCs. The results of this thesis revealed breed differences and cell-type differences in response to PRRSV infection. Additionally, it was possible to identify key clusters, key pathways and specific gene transcripts. The way of investigations, the new technology of RNA-Seq and the results helped to achieve all aims. The two main observations were the clearly different reactions of Duroc and Pietrain in the first hours post infection as well as the capacity of PRRSV to infect lung DCs and to replicate extremely there.

5.7 Perspective

The investigations and the results improved the knowledge about breed-dependent differences in response to PRRSV infection. Duroc respiratory cells responded more effectively in the first hours of infection than Pietrain respiratory cells. In this context the question arises if this result could be used for the improvement of breeding strategies. If breeding strategies help to develop disease resistant pigs and so to improve the pigs' health, the medical costs, the medical treatments and the economic losses in the pig industry will be reduced in the long run.

In Germany the new pharmaceutical drug law has the aim to minimize antibiotic applications and in a long-term to prevent antibiotic resistance, it entered into force on April 1st, 2014 (BMEL 2014). As the application of antibiotics must be reduced, the question gets more important how the secondary bacterial infections, promoted by PRRSV, can be treated adequately. The outbreak and the spreading of PRRSV infection must be prevented or at least limited. The pigs' close environment, an already mentioned essential factor for the transmission of airborne pathogens, like PRRSV, still has a big influence on the pigs' health, on the antibiotics applications and on the followed antibiotics resistance.

In addition to the enhancement of the pigs' environment, higher prevention must be achieved with the development of more effective and more efficient vaccines. Regarding the prevention aspects through vaccines, the here identified cell-type dependent variations can give hints for the development of adjuvants. For the performance of applications, DCs might be used as adjuvants to enhance the host immunity post PRRSV infection. Therapeutic strategies with DCs to enhance host immunity have already been described for diverse human diseases like asthma, allergic lung inflammation, lung cancer and other lung diseases.

In the pathway analyses of the present study genes were identified which played, according to their tasks – virus entry, drug performance and species-specific immunity – important roles for the health care. These genes which stood out through the functional analyses should be investigated in further studies because they might be candidate genes before and after PRRSV infection. Additionally, further knowledge is needed of immune-related QTL regions and SNP which have an impact on pig's health. Comparative studies should be performed on different levels of the global transcriptome and the global genome in order to improve pigs' immune response post PRRSV infection and in order to identify potential genetic markers.

6 Summary

The porcine reproductive and respiratory syndrome (PRRS) is infectious and one of the most important viral diseases of the swine industry worldwide. Its aetiological agent is the PRRS virus (PRRSV), a single-stranded (ss) 15 kb positive-sense RNA virus. This disease costs the global swine industry significant production losses, leads to critical financial circumstances annually and can become endemic in the major swine-producing nations of Europe, Asia, North and South America.

PRRS causes high mortality of nursery piglets, massive reproductive failures, including abortions, stillbirth and premature farrowings as well as weak or mummified piglets. In pigs of all ages, PRRS is associated with respiratory distress, interstitial pneumonia in growing and finishing swines and it can cause decreased growth performance. The development of these diseases is based on a multifactorial complex, including infectious agents, the host, environmental and management conditions as well as genetic factors. Generally the control remains problematic as the efficacy and universality of PRRS vaccination has not been established. Nearby the development of better vaccines, another possibility to control and to combat PRRS, could be the development of breeding programs, including host genetic improvement for disease resistance and tolerance. The understanding of the genetic elements and functions, involved in the response to PRRSV, remains still unclear.

Therefore the aims of this thesis were to characterize - by using the high-throughput sequencing technology - the transcriptome profile post PRRSV infection of Pietrain and Duroc respiratory cells, to improve the understanding of genetic components and functions in the response to PRRSV as well as to determine the changes in the global transcriptome profile after PRRSV infection.

For these investigations six female 30 days old piglets of two different porcine breeds (Pietrain and Duroc) were selected, PAMs, lung DCs and trachea epithelial cells were isolated and infected with the European prototype PRRSV strain LV. Non-infected (0 h) and infected (3, 6, 9, 12, 24 hpi) lung DCs, PAMs and trachea epithelial cells as well as the cell culture supernatants were collected. Non-infected and infected lung DCs of both breeds were used for RNA-Seq. The sequence alignment was done with the reference genome build Suscrofa 10.2 and with the complete genome of LV strain. Ten gene transcripts were selected to validate the results of RNA-Seq in PRRSV infected lung DCs, PAMs and trachea epithelial cells of both breeds. Additionally, in order to investigate the

cytokine profile of PRRSV infected lung DCs, PAMs and trachea epithelial cells, the cytokine concentrations were investigated by ELISA and the mRNA expression by real-time PCR.

The transcriptome analyses of PRRSV infected lung DCs of Pietrain and Duroc resulted in an amount of 20,396 porcine predicted gene transcripts. The virus sequence alignment exhibited that the LV strain was able to infect lung DCs and to replicate there. Not only breed-differences post PRRSV infection in the virus growth but also breed-differences were identified in the cytokine concentrations as well as in the detected differently expressed genes and in the mRNA expression profiles. Beside these breed-dependent differences, cell-type dependent differences in the response to PRRSV were characterized. By using the cluster analyses, 37 clusters for Pietrain and 35 clusters for Duroc were detected. Gene set enrichment analyses revealed common and varying pathways among the identified clusters of both breeds.

This is the first comprehensive study that described the transcriptome profile of respiratory cells of two different breeds post PRRSV infection, especially of infected lung DCs. The investigations showed that the virus-host interaction was different for the various respiratory cell-types and that the expression trends proceeded contrarily for both breeds during the first time points after infection. Additionally, key clusters, key pathways and specific gene transcripts were identified. The main findings were the clearly different reactions of Duroc and Pietrain respiratory cells during the first hours post infection, the capacity of PRRSV to infect lung DCs and to replicate extremely there as well as the different responses of respiratory cells after PRRSV infection.

7 References

Abada PB, Larson CA, Manorek G, Adams P, Howell SB (2012): Sec61beta controls sensitivity to platinum-containing chemotherapeutic agents through modulation of the copper-transporting ATPase ATP7A. Mol Pharmacol 82, 510-520

Abbas AK, Lichtman AH, Pillai S (2012): Cellular and Molecular Immunology 7th edition. Saunders an imprint of Elsevier Inc. 1-35, 37-53, 55-88, 139-171, 203-224, 243-268, 293-317

Adler M, Murani E, Brunner R, Ponsuksili S, Wimmers K (2013): Transcriptomic response of porcine PBMCs to vaccination with tetanus toxoid as a model antigen. PLoS One 8, e58306

Ait-Ali T, Wilson AD, Carre W, Westcott DG, Frossard JP, Mellencamp MA, Mouzaki D, Matika O, Waddington D, Drew TW, Bishop SC, Archibald AL (2011): Host inhibits replication of European porcine reproductive and respiratory syndrome virus in macrophages by altering differential regulation of type-I interferon transcriptional response. Immunogenetics 63, 437-448

Akira S, Takeda K, Kaisho T (2001): Toll-like receptors: critical proteins linking innate and acquired immunity. Nat Immunol 2, 675-680

Alberts B, Johnson A, Lewis J, Raff M, Roberts K, Walter P (2008): Molecular biology of the cell 5th edition. Garland Science, Taylor & Francis Group, LLC. 921-944, 1417-1601

Allende R, Lewis TL, Lu Z, Rock DL, Kutish GF, Ali A, Doster AR, Osorio FA (1999): North American and European porcine reproductive and respiratory syndrome viruses differ in non-structural protein coding regions. J Gen Virol 80 (Pt 2), 307-315

Anders S, Huber W (2010): Differential expression analysis for sequence count data. Genome Biol 11, R106

Austyn JM, Hankins DF, Larsen CP, Morris PJ, Rao AS, Roake JA (1994): Isolation and characterization of dendritic cells from mouse heart and kidney. J Immunol 152, 2401-2410

Badaoui B, Grande R, Calza S, Cecere M, Luini M, Stella A, Botti S (2013): Impact of genetic variation and geographic distribution of porcine reproductive and respiratory syndrome virus on infectivity and pig growth. BMC Vet Res 9, 58

Badaoui B, Rutigliano T, Anselmo A, Vanhee M, Nauwynck H, Giuffra E, Botti S (2014): RNA-Sequence Analysis of Primary Alveolar Macrophages after In Vitro Infection with Porcine Reproductive and Respiratory Syndrome Virus Strains of Differing Virulence. PLoS One 9, e91918

Balasuriya UB (2013): Coronaviridae; arteriviridae and roniviridae, In: McVey DS, Kennedy M, Chengappa MM, editors. Veterinary Microbiology 3rd edition, John Wiley & Sons, Inc. 456-486

Banchereau J, Steinman RM (1998): Dendritic cells and the control of immunity. Nature 392, 245-252

Bautista EM, Faaberg KS, Mickelson D, McGruder ED (2002): Functional properties of the predicted helicase of porcine reproductive and respiratory syndrome virus. Virology 298, 258-270

Benfield DA, Nelson E, Collins JE, Harris L, Goyal SM, Robison D, Christianson WT, Morrison RB, Gorcyca D, Chladek D (1992): Characterization of swine infertility and respiratory syndrome (SIRS) virus (isolate ATCC VR-2332). J Vet Diagn Invest 4, 127-133

Beura LK, Sarkar SN, Kwon B, Subramaniam S, Jones C, Pattnaik AK, Osorio FA (2010): Porcine reproductive and respiratory syndrome virus nonstructural protein 1beta modulates host innate immune response by antagonizing IRF3 activation. J Virol 84, 1574-1584

Beutler B (2004): Innate immunity: an overview. Mol Immunol 40, 845-859

Biffani S, Botti S, Bishop SC, Stella A, Giuffra E (2011): Using SNP array data to test for host genetic and breed effects on Porcine Reproductive and Respiratory Syndrome Viremia. BMC Proc 5 Suppl 4, S28

Bizargity P, Bonney EA (2009): Dendritic cells: a family portrait at mid-gestation. Immunology 126, 565-578

BMEL (2011): DART Deutsche Antibiotika-Resistenzstrategie. Bundesministerium für Ernährung, Landwirtschaft und Verbraucherschutz

BMEL (2014): http://www.bmel.de/SharedDocs/Pressemitteilungen/2014/083-SC-AMG-Novelle.html, Pressemitteilung Nr. 83 vom 31.03.14.

Boddicker N, Waide EH, Rowland RR, Lunney JK, Garrick DJ, Reecy JM, Dekkers JC (2012): Evidence for a major QTL associated with host response to porcine reproductive and respiratory syndrome virus challenge. J Anim Sci 90, 1733-1746

Bonjardim CA (2005): Interferons (IFNs) are key cytokines in both innate and adaptive antiviral immune responses--and viruses counteract IFN action. Microbes Infect 7, 569-578

Brockmeier SL, Halbur PG, Thacker EL (2002): Porcine respiratory disease complex, In: Brogden KA, Guthmiller JM, editors. Polymicrobial Diseases. Washington (DC): ASM Press, Chapter 13. Available from: http://www.ncbi.nlm.nih.gov/books/NBK2481/

Calvert JG, Slade DE, Shields SL, Jolie R, Mannan RM, Ankenbauer RG, Welch SK (2007): CD163 expression confers susceptibility to porcine reproductive and respiratory syndrome viruses. J Virol 81, 7371-7379

Charerntantanakul W, Platt R, Roth JA (2006): Effects of porcine reproductive and respiratory syndrome virus-infected antigen-presenting cells on T cell activation and antiviral cytokine production. Viral Immunol 19, 646-661

Chase CCL, Lunney JK (2012): Immune system, In: Zimmerman JJ, Karriker LA, Ramirez A, Schwartz KJ, Stevenson GW, editors. Diseases of Swine 10th edition, John Wiley & Sons, Inc. 227-250

Chen XX, Quan R, Guo XK, Gao L, Shi J, Feng WH (2014): Up-regulation of pro-inflammatory factors by HP-PRRSV infection in microglia: implications for HP-PRRSV neuropathogenesis. Vet Microbiol 170, 48-57

Chen Y, Jiang G, Yang HR, Gu X, Wang L, Hsieh CC, Chou HS, Fung JJ, Qian S, Lu L (2009): Distinct response of liver myeloid dendritic cells to endotoxin is mediated by IL-27. J Hepatol 51, 510-519

Chen Z, Lawson S, Sun Z, Zhou X, Guan X, Christopher-Hennings J, Nelson EA, Fang Y (2010): Identification of two auto-cleavage products of nonstructural protein 1 (nsp1) in porcine reproductive and respiratory syndrome virus infected cells: nsp1 function as interferon antagonist. Virology 398, 87-97

Cho JG, Dee SA (2006): Porcine reproductive and respiratory syndrome virus. Theriogenology 66, 655-662

Cho JG, Dee SA, Deen J, Guedes A, Trincado C, Fano E, Jiang Y, Faaberg K, Collins JE, Murtaugh MP, Joo HS (2006a): Evaluation of the effects of animal age, concurrent bacterial infection, and pathogenicity of porcine reproductive and respiratory syndrome virus on virus concentration in pigs. Am J Vet Res 67, 489-493

Cho JG, Dee SA, Deen J, Trincado C, Fano E, Jiang Y, Faaberg K, Murtaugh MP, Guedes A, Collins JE, Joo HS (2006b): The impact of animal age, bacterial coinfection, and

isolate pathogenicity on the shedding of porcine reproductive and respiratory syndrome virus in aerosols from experimentally infected pigs. Can J Vet Res 70, 297-301

Collins JE, Benfield DA, Christianson WT, Harris L, Hennings JC, Shaw DP, Goyal SM, McCullough S, Morrison RB, Joo HS, et al. (1992): Isolation of swine infertility and respiratory syndrome virus (isolate ATCC VR-2332) in North America and experimental reproduction of the disease in gnotobiotic pigs. J Vet Diagn Invest 4, 117-126

Conzelmann KK, Visser N, Van Woensel P, Thiel HJ (1993): Molecular characterization of porcine reproductive and respiratory syndrome virus, a member of the arterivirus group. Virology 193, 329-339

Corzo CA, Mondaca E, Wayne S, Torremorell M, Dee S, Davies P, Morrison RB (2010): Control and elimination of porcine reproductive and respiratory syndrome virus. Virus Res 154, 185-192

Costers S, Lefebvre DJ, Delputte PL, Nauwynck HJ (2008): Porcine reproductive and respiratory syndrome virus modulates apoptosis during replication in alveolar macrophages. Arch Virol 153, 1453-1465

Das PB, Dinh PX, Ansari IH, de Lima M, Osorio FA, Pattnaik AK (2010): The minor envelope glycoproteins GP2a and GP4 of porcine reproductive and respiratory syndrome virus interact with the receptor CD163. J Virol 84, 1731-1740

De Baere MI, Van Gorp H, Delputte PL, Nauwynck HJ (2012): Interaction of the European genotype porcine reproductive and respiratory syndrome virus (PRRSV) with sialoadhesin (CD169/Siglec-1) inhibits alveolar macrophage phagocytosis. Vet Res 43, 47

Dea S, Sawyer N, Alain R, Athanassious R (1995): Ultrastructural characteristics and morphogenesis of porcine reproductive and respiratory syndrome virus propagated in the highly permissive MARC-145 cell clone. Adv Exp Med Biol 380, 95-98

Dee S, Otake S, Oliveira S, Deen J (2009): Evidence of long distance airborne transport of porcine reproductive and respiratory syndrome virus and Mycoplasma hyopneumoniae. Vet Res 40, 39

DeFranco AL, Locksley RM, Robertson M (2007): Immunity: The Immune Response in Infectious and Inflammatory Disease (Primers in Biology). Oxford University Press. 2-153

Delputte PL, Vanderheijden N, Nauwynck HJ, Pensaert MB (2002): Involvement of the matrix protein in attachment of porcine reproductive and respiratory syndrome virus to a heparinlike receptor on porcine alveolar macrophages. J Virol 76, 4312-4320

Dewey C, Charbonneau G, Carman S, Hamel A, Nayar G, Friendship R, Eernisse K, Swenson S (2000): Lelystad-like strain of porcine reproductive and respiratory syndrome virus (PRRSV) identified in Canadian swine. Can Vet J 41, 493-494

Diebold SS, Kaisho T, Hemmi H, Akira S, Reis e Sousa C (2004): Innate antiviral responses by means of TLR7-mediated recognition of single-stranded RNA. Science 303, 1529-1531

Dimmock NJ, Easton AJ, Leppard KN (2007): Introduction to modern virology 6th edition. Blackwell Publishing Ltd. 1-17, 214-225, 394-395

Do DN, Ostersen T, Strathe AB, Mark T, Jensen J, Kadarmideen HN (2014): Genome-wide association and systems genetic analyses of residual feed intake, daily feed consumption, backfat and weight gain in pigs. BMC Genet 15, 27

Duan X, Nauwynck HJ, Favoreel HW, Pensaert MB (1998): Identification of a putative receptor for porcine reproductive and respiratory syndrome virus on porcine alveolar macrophages. J Virol 72, 4520-4523

Duan X, Nauwynck HJ, Pensaert MB (1997): Virus quantification and identification of cellular targets in the lungs and lymphoid tissues of pigs at different time intervals after inoculation with porcine reproductive and respiratory syndrome virus (PRRSV). Vet Microbiol 56, 9-19

Eckerle I, Ehlen L, Kallies R, Wollny R, Corman VM, Cottontail VM, Tschapka M, Oppong S, Drosten C, Muller MA (2014): Bat airway epithelial cells: a novel tool for the study of zoonotic viruses. PLoS One 9, e84679

Edfors-Lilja I, Wattrang E, Marklund L, Moller M, Andersson-Eklund L, Andersson L, Fossum C (1998): Mapping quantitative trait loci for immune capacity in the pig. J Immunol 161, 829-835

Fang Y, Kim DY, Ropp S, Steen P, Christopher-Hennings J, Nelson EA, Rowland RR (2004): Heterogeneity in Nsp2 of European-like porcine reproductive and respiratory syndrome viruses isolated in the United States. Virus Res 100, 229-235

Fang Y, Snijder EJ (2010): The PRRSV replicase: exploring the multifunctionality of an intriguing set of nonstructural proteins. Virus Res 154, 61-76

Fitzgerald KA, Palsson-McDermott EM, Bowie AG, Jefferies CA, Mansell AS, Brady G, Brint E, Dunne A, Gray P, Harte MT, McMurray D, Smith DE, Sims JE, Bird TA,

O'Neill LA (2001): Mal (MyD88-adapter-like) is required for Toll-like receptor-4 signal transduction. Nature 413, 78-83

Flori L, Gao Y, Laloe D, Lemonnier G, Leplat JJ, Teillaud A, Cossalter AM, Laffitte J, Pinton P, de Vaureix C, Bouffaud M, Mercat MJ, Lefevre F, Oswald IP, Bidanel JP, Rogel-Gaillard C (2011a): Immunity traits in pigs: substantial genetic variation and limited covariation. PLoS One 6, e22717

Flori L, Gao Y, Oswald IP, Lefevre F, Bouffaud M, Mercat MJ, Bidanel JP, Rogel-Gaillard C (2011b): Deciphering the genetic control of innate and adaptive immune responses in pig: a combined genetic and genomic study. BMC Proc 5 Suppl 4, S32

Fogg DK, Sibon C, Miled C, Jung S, Aucouturier P, Littman DR, Cumano A, Geissmann F (2006): A clonogenic bone marrow progenitor specific for macrophages and dendritic cells. Science 311, 83-87

Gack MU (2014): Mechanisms of RIG-I-like receptor activation and manipulation by viral pathogens. J Virol 88, 5213-5216

Gao J, Xiao S, Liu X, Wang L, Ji Q, Mo D, Chen Y (2014): Inhibition of HSP70 reduces porcine reproductive and respiratory syndrome virus replication in vitro. BMC Microbiol 14, 64

Garrett WS, Chen LM, Kroschewski R, Ebersold M, Turley S, Trombetta S, Galan JE, Mellman I (2000): Developmental control of endocytosis in dendritic cells by Cdc42. Cell 102, 325-334

Geissmann F, Manz MG, Jung S, Sieweke MH, Merad M, Ley K (2010): Development of monocytes, macrophages, and dendritic cells. Science 327, 656-661

Geissmann F, Prost C, Monnet JP, Dy M, Brousse N, Hermine O (1998): Transforming growth factor beta1, in the presence of granulocyte/macrophage colony-stimulating factor and interleukin 4, induces differentiation of human peripheral blood monocytes into dendritic Langerhans cells. J Exp Med 187, 961-966

Genini S, Delputte PL, Malinverni R, Cecere M, Stella A, Nauwynck HJ, Giuffra E (2008): Genome-wide transcriptional response of primary alveolar macrophages following infection with porcine reproductive and respiratory syndrome virus. J Gen Virol 89, 2550-2564

Gimeno M, Darwich L, Diaz I, de la Torre E, Pujols J, Martin M, Inumaru S, Cano E, Domingo M, Montoya M, Mateu E (2011): Cytokine profiles and phenotype regulation of antigen presenting cells by genotype-I porcine reproductive and respiratory syndrome virus isolates. Vet Res 42, 9

Goldman AS, Prabhakar BS (1996): Immunology overview. In: Baron S, editor. Medical Microbiology 4th edition. Galveston (TX): University of Texas Medical Branch at Galveston; Chapter 1. Available from: http://www.ncbi.nlm.nih.gov/books/NBK7795/

Gong JL, McCarthy KM, Telford J, Tamatani T, Miyasaka M, Schneeberger EE (1992): Intraepithelial airway dendritic cells: a distinct subset of pulmonary dendritic cells obtained by microdissection. J Exp Med 175, 797-807

Gordon S, Martinez FO (2010): Alternative activation of macrophages: mechanism and functions. Immunity 32, 593-604

Grayson MH, Holtzman MJ (2007): Emerging role of dendritic cells in respiratory viral infection. J Mol Med (Berl) 85, 1057-1068

Grayson MH, Ramos MS, Rohlfing MM, Kitchens R, Wang HD, Gould A, Agapov E, Holtzman MJ (2007): Controls for lung dendritic cell maturation and migration during respiratory viral infection. J Immunol 179, 1438-1448

Guermonprez P, Valladeau J, Zitvogel L, Thery C, Amigorena S (2002): Antigen presentation and T cell stimulation by dendritic cells. Annu Rev Immunol 20, 621-667

Halbur PG, Rothschild MF, Thacker BJ, Meng X-J, Paul PS (1998): Differences in susceptibility of Duroc, Hampshire, and Meishan pigs to infection with a high virulence strain (VR2385) of porcine reproductive and respiratory syndrome virus (PRRSV). J Anim Breed Genet 115. 181-189

Heidt H, Cinar MU, Uddin MJ, Looft C, Jungst H, Tesfaye D, Becker A, Zimmer A, Ponsuksili S, Wimmers K, Tholen E, Schellander K, Grosse-Brinkhaus C (2013): A genetical genomics approach reveals new candidates and confirms known candidate genes for drip loss in a porcine resource population. Mamm Genome 24, 416-426

Herzog P, Drosten C, Muller MA (2008): Plaque assay for human coronavirus NL63 using human colon carcinoma cells. Virol J 5, 138

Hewitt CJ, Isailovic B, Mukwena NT, Nienow AW (2006): Insect and mammalian cell culture, In: Ratledge C, Kristiansen B, editors. Basic Biotechnology 3rd edition. Cambridge University Press 523-548

Hinton A, Bond S, Forgac M (2009): V-ATPase functions in normal and disease processes. Pflugers Arch 457, 589-598

Hu R, Lemonnier G, Bourneuf E, Vincent-Naulleau S, Rogel-Gaillard C (2011): Transcription variants of SLA-7, a swine non classical MHC class I gene. BMC Proc 5 Suppl 4, S10

Huang YW, Meng XJ (2010): Novel strategies and approaches to develop the next generation of vaccines against porcine reproductive and respiratory syndrome virus (PRRSV). Virus Res 154, 141-149

Janeway CA, Jr., Medzhitov R (2002): Innate immune recognition. Annu Rev Immunol 20, 197-216

Jiang Z, Zhou X, Michal JJ, Wu XL, Zhang L, Zhang M, Ding B, Liu B, Manoranjan VS, Neill JD, Harhay GP, Kehrli ME, Jr., Miller LC (2013): Reactomes of porcine alveolar macrophages infected with porcine reproductive and respiratory syndrome virus. PLoS One 8, e59229

Jungsoo G, Taesung P (2012): Identifying differential expression for RNA-seq data with no replication. Bioinformatics and Biomedicine Workshops (BIBMW), 2012 IEEE International Conference on, 847-851

Kaiser P (2010): The immune system. In: Bishop SC, Axford RFE, Nicholas FW, Owen JB, editors. Breeding for disease resistance in farm animals 3rd edition, CAB International. 15-37

Kamentsky LA, Melamed MR, Derman H (1965): Spectrophotometer: new instrument for ultrarapid cell analysis. Science 150, 630-631

Karlskov-Mortensen P, Bruun CS, Braunschweig MH, Sawera M, Markljung E, Enfalt AC, Hedebro-Velander I, Josell A, Lindahl G, Lundstrom K, von Seth G, Jorgensen CB, Andersson L, Fredholm M (2006): Genome-wide identification of quantitative trait loci in a cross between Hampshire and Landrace I: carcass traits. Anim Genet 37, 156-162

Karniychuk UU, Saha D, Geldhof M, Vanhee M, Cornillie P, Van den Broeck W, Nauwynck HJ (2011): Porcine reproductive and respiratory syndrome virus (PRRSV) causes apoptosis during its replication in fetal implantation sites. Microb Pathog 51, 194-202

Khatoon Z, Figler B, Zhang H, Cheng F (2014): Introduction to RNA-Seq and its applications to drug discovery and development. Drug Develop Res 75, 324-330

Kimman TG, Cornelissen LA, Moormann RJ, Rebel JM, Stockhofe-Zurwieden N (2009): Challenges for porcine reproductive and respiratory syndrome virus (PRRSV) vaccinology. Vaccine 27, 3704-3718

Kindt TJ, Goldsby RA, Osborne BA (2007): Kuby Immunology sixth edition, W. H. Freeman and Company. 1-75, 302-370, 447-474

King AM, Lefkowitz E, Adams MJ, Carstens EB (2011): Virus Taxonomy: Ninth Report of the International Committee on Taxonomy of Viruses, Elsevier Inc. 796-814

Kreutz LC, Ackermann MR (1996): Porcine reproductive and respiratory syndrome virus enters cells through a low pH-dependent endocytic pathway. Virus Res 42, 137-147

Kristensen CS, Botner A, Takai H, Nielsen JP, Jorsal SE (2004): Experimental airborne transmission of PRRS virus. Vet Microbiol 99, 197-202

Langmead B, Trapnell C, Pop M, Salzberg SL (2009): Ultrafast and memory-efficient alignment of short DNA sequences to the human genome. Genome Biol 10, R25

Laskin DL, Weinberger B, Laskin JD (2001): Functional heterogeneity in liver and lung macrophages. J Leukocyte Biol 70, 163-170

Lewis CR, Ait-Ali T, Clapperton M, Archibald AL, Bishop S (2007): Genetic perspectives on host responses to porcine reproductive and respiratory syndrome (PRRS). Viral Immunol 20, 343-358

Lewis CR, Torremorell M, Galina-Pantoja L, Bishop SC (2009): Genetic parameters for performance traits in commercial sows estimated before and after an outbreak of porcine reproductive and respiratory syndrome. J Anim Sci 87, 876-884

Li H, Handsaker B, Wysoker A, Fennell T, Ruan J, Homer N, Marth G, Abecasis G, Durbin R (2009): The Sequence Alignment/Map format and SAMtools. Bioinformatics 25, 2078-2079

Li H, Zheng Z, Zhou P, Zhang B, Shi Z, Hu Q, Wang H (2010): The cysteine protease domain of porcine reproductive and respiratory syndrome virus non-structural protein 2 antagonizes interferon regulatory factor 3 activation. J Gen Virol 91, 2947-2958

Li J, Yin Y, Guo B, Zhou S, Zhang Y, Liu X, Sun T (2012): Sequence analysis of the NSP2, ORF5, and ORF7 genes of 11 PRRS virus isolates from China. Virus Genes 45, 256-264

Liu CH, Chaung HC, Chang HL, Peng YT, Chung WB (2009a): Expression of Toll-like receptor mRNA and cytokines in pigs infected with porcine reproductive and respiratory syndrome virus. Vet Microbiol 136, 266-276

Liu K, Victora GD, Schwickert TA, Guermonprez P, Meredith MM, Yao K, Chu FF, Randolph GJ, Rudensky AY, Nussenzweig M (2009b): In vivo analysis of dendritic cell development and homeostasis. Science 324, 392-397

López A (2001): Respiratory system, thoracic cavity and pleura. In: McGavin MD, Carlton WW, Zachary JF, editors. Thomson's Special Veterinary Pathology third edition, Mosby, Inc. St. Louis. 125-195

Loving CL, Brockmeier SL, Sacco RE (2007): Differential type I interferon activation and susceptibility of dendritic cell populations to porcine arterivirus. Immunology 120, 217-229

Lu T, Liang H, Li H, Wu H (2011a): High Dimensional ODEs Coupled with Mixed-Effects Modeling Techniques for Dynamic Gene Regulatory Network Identification. J Am Stat Assoc 106, 1242-1258

Lu X, Gong YF, Liu JF, Wang ZP, Hu F, Qiu XT, Luo YR, Zhang Q (2011b): Mapping quantitative trait loci for cytokines in the pig. Anim Genet 42, 1-5

Lu X, Liu J, Fu W, Zhou J, Luo Y, Ding X, Liu Y, Zhang Q (2013): Genome-wide association study for cytokines and immunoglobulin G in swine. PLoS One 8, e74846

Lund J, Sato A, Akira S, Medzhitov R, Iwasaki A (2003): Toll-like receptor 9-mediated recognition of Herpes simplex virus-2 by plasmacytoid dendritic cells. J Exp Med 198, 513-520

Lund JM, Alexopoulou L, Sato A, Karow M, Adams NC, Gale NW, Iwasaki A, Flavell RA (2004): Recognition of single-stranded RNA viruses by Toll-like receptor 7. Proc Natl Acad Sci 101, 5598-5603

Lunney JK, Chen H (2010): Genetic control of host resistance to porcine reproductive and respiratory syndrome virus (PRRSV) infection. Virus Res 154, 161-169

Luo R, Xiao S, Jiang Y, Jin H, Wang D, Liu M, Chen H, Fang L (2008): Porcine reproductive and respiratory syndrome virus (PRRSV) suppresses interferon-beta production by interfering with the RIG-I signaling pathway. Mol Immunol 45, 2839-2846

Ma P, Castillo-Davis CI, Zhong W, Liu JS (2006): A data-driven clustering method for time course gene expression data. Nucleic Acids Res 34, 1261-1269

Ma P, Zhong W (2008): Penalized Clustering of Large-Scale Functional Data With Multiple Covariates. J Am Stat Assoc, 103:482 625-636

MacPherson G, Austyn J (2012): Exploring Immunology. Wiley-VCH Verlag & Co. KGaA. 1-48, 99-216

Mamo S, Mehta JP, McGettigan P, Fair T, Spencer TE, Bazer FW, Lonergan P (2011): RNA sequencing reveals novel gene clusters in bovine conceptuses associated with maternal recognition of pregnancy and implantation. Biol Reprod 85, 1143-1151

Mantovani A, Cassatella MA, Costantini C, Jaillon S (2011): Neutrophils in the activation and regulation of innate and adaptive immunity. Nat Rev Immunol 11, 519-531

Marioni JC, Mason CE, Mane SM, Stephens M, Gilad Y (2008): RNA-seq: an assessment of technical reproducibility and comparison with gene expression arrays. Genome Res 18, 1509-1517

Martelli MP, Bierer BE (2003): Cellular and molecular biology of lymphoid cells, In: Handin RI, Lux, SE, Stossel, TP, editors. Blood: Principles and Practice of Hematology 2nd edition. Lippincott Williams & Wilkins 589-620

Martin M (2011): Cutadapt removes adapter sequences from high-throughput sequencing reads. EMBnet.journal, 17, 10-12

Mateu E, Diaz I (2008): The challenge of PRRS immunology. Vet J 177, 345-351

Mateu E, Martin M, Vidal D (2003): Genetic diversity and phylogenetic analysis of glycoprotein 5 of European-type porcine reproductive and respiratory virus strains in Spain. J Gen Virol 84, 529-534

Matrosovich M, Matrosovich T, Garten W, Klenk HD (2006): New low-viscosity overlay medium for viral plaque assays. Virol J 3, 63

Medzhitov R, Janeway CA, Jr. (1997): Innate immunity: the virtues of a nonclonal system of recognition. Cell 91, 295-298

Medzhitov R, Preston-Hurlburt P, Kopp E, Stadlen A, Chen C, Ghosh S, Janeway CA, Jr. (1998): MyD88 is an adaptor protein in the hToll/IL-1 receptor family signaling pathways. Mol Cell 2, 253-258

Mercer J, Greber UF (2013): Virus interactions with endocytic pathways in macrophages and dendritic cells. Trends Microbiol 21, 380-388

Meulenberg JJ, Hulst MM, de Meijer EJ, Moonen PL, den Besten A, de Kluyver EP, Wensvoort G, Moormann RJ (1993): Lelystad virus, the causative agent of porcine epidemic abortion and respiratory syndrome (PEARS), is related to LDV and EAV. Virology 192, 62-72

Miller DM, Thornley TB, Greiner DL, Rossini AA (2008): Viral infection: a potent barrier to transplantation tolerance. Clin Dev Immunol 2008, 742810

Miller LC, Neill JD, Harhay GP, Lager KM, Laegreid WW, Kehrli ME, Jr. (2010): In-depth global analysis of transcript abundance levels in porcine alveolar macrophages

following infection with porcine reproductive and respiratory syndrome virus. Adv Virol 2010, 864181

Modrow S, Falke D, Truyen U, Schätzl H (2010): Viren mit einzelsträngigem RNA-Genom in Plusstrangorientierung. In: Molekulare Virologie 3. Auflage. Spektrum Akademischer Verlag Heidelberg. 145-262

Mortensen S, Stryhn H, Sogaard R, Boklund A, Stark KD, Christensen J, Willeberg P (2002): Risk factors for infection of sow herds with porcine reproductive and respiratory syndrome (PRRS) virus. Prev Vet Med 53, 83-101

Mosayebi G, Moazzeni SM (2011): Spleen and liver dendritic cells differ in their tolerogenic and cytokine induction potential. Iran J Allergy Asthm 10, 163-170

Murphy K, Travers P, Walter P (2008): Janeway's Immunobiology, Seventh Edition Interactive, Garland Science, Taylor & Francis Group, LLC. 1-38, 39-108, 323-377, 421-495

Murtaugh MP, Stadejek T, Abrahante JE, Lam TT, Leung FC (2010): The ever-expanding diversity of porcine reproductive and respiratory syndrome virus. Virus Res 154, 18-30

Murtaugh MP, Xiao Z, Zuckermann F (2002): Immunological responses of swine to porcine reproductive and respiratory syndrome virus infection. Viral Immunol 15, 533-547

Nauwynck HJ, Duan X, Favoreel HW, Van Oostveldt P, Pensaert MB (1999): Entry of porcine reproductive and respiratory syndrome virus into porcine alveolar macrophages via receptor-mediated endocytosis. J Gen Virol 80 (Pt 2), 297-305

Nedialkova DD, Gorbalenya AE, Snijder EJ (2010): Arterivirus Nsp1 modulates the accumulation of minus-strand templates to control the relative abundance of viral mRNAs. PLoS Pathog 6, e1000772

Neumann EJ, Kliebenstein JB, Johnson CD, Mabry JW, Bush EJ, Seitzinger AH, Green AL, Zimmerman JJ (2005): Assessment of the economic impact of porcine reproductive and respiratory syndrome on swine production in the United States. J Am Vet Med Assoc 227, 385-392

Nicod LP (1999): Pulmonary defence mechanisms. Respiration 66, 2-11

Niggemeyer H (2012): Antibiotika bleibt ein Reizthema. SUS Nr. 1, 16-17

Okwan-Duodu D, Umpierrez GE, Brawley OW, Diaz R (2013): Obesity-driven inflammation and cancer risk: role of myeloid derived suppressor cells and alternately activated macrophages. Am J Cancer Res 3, 21-33

Pabst T (2010): Bei der PRRS-Bekämpfung am Ball bleiben. Top agrar 10, 8-11

Palzer A (2013): Neue PRRS-Varianten bringen Gefahr SUS Nr. 6, 26-27

Park JY, Kim HS, Seo SH (2008): Characterization of interaction between porcine reproductive and respiratory syndrome virus and porcine dendritic cells. J Microbiol Biotechn 18, 1709-1716

Pejsak Z, Markowska-Daniel I (1997): Losses due to porcine reproductive and respiratory syndrome in a large swine farm. Comp Immunol Microb 20, 345-352

Petry DB, Holl JW, Weber JS, Doster AR, Osorio FA, Johnson RK (2005): Biological responses to porcine respiratory and reproductive syndrome virus in pigs of two genetic populations. J Anim Sci 83, 1494-1502

Petry DB, Lunney J, Boyd P, Kuhar D, Blankenship E, Johnson RK (2007): Differential immunity in pigs with high and low responses to porcine reproductive and respiratory syndrome virus infection. J Anim Sci 85, 2075-2092

Piras V, Selvarajoo K (2014): Beyond MyD88 and TRIF Pathways in Toll-Like Receptor Signaling. Front Immunol 5, 70

Pol JM, van Dijk JE, Wensvoort G, Terpstra C (1991): Pathological, ultrastructural, and immunohistochemical changes caused by Lelystad virus in experimentally induced infections of mystery swine disease (synonym: porcine epidemic abortion and respiratory syndrome (PEARS)). Vet Quart 13, 137-143

Ponsuksili S, Jonas E, Murani E, Phatsara C, Srikanchai T, Walz C, Schwerin M, Schellander K, Wimmers K (2008): Trait correlated expression combined with expression QTL analysis reveals biological pathways and candidate genes affecting water holding capacity of muscle. BMC Genomics 9, 367

Quinlan AR, Hall IM (2010): BEDTools: a flexible suite of utilities for comparing genomic features. Bioinformatics 26, 841-842

Reiner G, Willems H, Pesch S, Ohlinger VF (2010): Variation in resistance to the porcine reproductive and respiratory syndrome virus (PRRSV) in Pietrain and Miniature pigs. J Anim Breed Genet 127, 100-106

Reis e Sousa C (2001): Dendritic cells as sensors of infection. Immunity 14, 495-498

Rodriguez-Gomez IM, Gomez-Laguna J, Carrasco L (2013): Impact of PRRSV on activation and viability of antigen presenting cells. World J Virol 2, 146-151

Rossow KD (1998): Porcine reproductive and respiratory syndrome. Vet Pathol 35, 1-20

Rowland RR, Kervin R, Kuckleburg C, Sperlich A, Benfield DA (1999): The localization of porcine reproductive and respiratory syndrome virus nucleocapsid protein to the

nucleolus of infected cells and identification of a potential nucleolar localization signal sequence. Virus Res 64, 1-12

Sallusto F, Lanzavecchia A (1994): Efficient presentation of soluble antigen by cultured human dendritic cells is maintained by granulocyte/macrophage colony-stimulating factor plus interleukin 4 and downregulated by tumor necrosis factor alpha. J Exp Med 179, 1109-1118

Schlee M (2013): Master sensors of pathogenic RNA - RIG-I like receptors. Immunobiology 218, 1322-1335

Schmid MA, Takizawa H, Baumjohann DR, Saito Y, Manz MG (2011): Bone marrow dendritic cell progenitors sense pathogens via Toll-like receptors and subsequently migrate to inflamed lymph nodes. Blood 118, 4829-4840

Schroder K, Hertzog PJ, Ravasi T, Hume DA (2004): Interferon-gamma: an overview of signals, mechanisms and functions. J Leukocyte Biol 75, 163-189

Sertl K, Takemura T, Tschachler E, Ferrans VJ, Kaliner MA, Shevach EM (1986): Dendritic cells with antigen-presenting capability reside in airway epithelium, lung parenchyma, and visceral pleura. J Exp Med 163, 436-451

Shapiro H (2003): Practical Flow Cytometry. New York: Wiley-Liss

Shortman K, Liu YJ (2002): Mouse and human dendritic cell subtypes. Nat Rev Immunol 2, 151-161

Shortman K, Naik SH (2007): Steady-state and inflammatory dendritic-cell development. Nat Rev Immunol 7, 19-30

Shuai K, Liu B (2003): Regulation of JAK-STAT signalling in the immune system. Nat Rev Immunol 3, 900-911

Sieg S, King C, Huang Y, Kaplan D (1996): The role of interleukin-10 in the inhibition of T-cell proliferation and apoptosis mediated by parainfluenza virus type 3. J Virol 70, 4845-4848

Snijder EJ, Kikkert M, Fang Y (2013): Arterivirus molecular biology and pathogenesis. J Gen Virol 94, 2141-2163

Snijder EJ, Meulenberg JJ (1998): The molecular biology of arteriviruses. J Gen Virol 79 (Pt 5), 961-979

Snijder EJ, van Tol H, Pedersen KW, Raamsman MJ, de Vries AA (1999): Identification of a novel structural protein of arteriviruses. J Virol 73, 6335-6345

Sørensen V, Jorsal SE, Mousing J (2006): Diseases of the respiratory system. In: Straw BE, Zimmerman JJ, D'Allaire S, Taylor DJ, editors. Diseases of Swine 9th edition. Blackwell Publishing Company, Ames Iowa. 149-178

Soudi S, Zavaran-Hosseini A, Muhammad Hassan Z, Soleimani M, Jamshidi Adegani F, Hashemi SM (2013): Comparative study of the effect of LPS on the function of BALB/c and C57BL/6 peritoneal macrophages. Cell J 15, 45-54

Statistisches-Bundesamt (2010): Land- und Forstwirtschaft, Fischerei; Rinder- und Schweinebestand. Statistisches Bundesamt, Wiesbaden, Fachserie 3, Reihe 4.1

Statistisches-Bundesamt (2014): Land- und Forstwirtschaft, Fischerei; Viehbestand. Statistisches Bundesamt, Wiesbaden, Fachserie 3 Reihe 4.1, 4-5

Stockert JC, Blazquez-Castro A, Canete M, Horobin RW, Villanueva A (2012): MTT assay for cell viability: Intracellular localization of the formazan product is in lipid droplets. Acta Histochem 114, 785-796

Stumbles PA, Upham JW, Holt PG (2003): Airway dendritic cells: co-ordinators of immunological homeostasis and immunity in the respiratory tract. APMIS 111, 741-755

Sun D, Ding A (2006): MyD88-mediated stabilization of interferon-gamma-induced cytokine and chemokine mRNA. Nat Immunol 7, 375-381

Sur JH, Doster AR, Christian JS, Galeota JA, Wills RW, Zimmerman JJ, Osorio FA (1997): Porcine reproductive and respiratory syndrome virus replicates in testicular germ cells, alters spermatogenesis, and induces germ cell death by apoptosis. J Virol 71, 9170-9179

Tang F, Barbacioru C, Wang Y, Nordman E, Lee C, Xu N, Wang X, Bodeau J, Tuch BB, Siddiqui A, Lao K, Surani MA (2009): mRNA-Seq whole-transcriptome analysis of a single cell. Nat Methods 6, 377-382

Thanawongnuwech R, Thacker B, Halbur P, Thacker EL (2004): Increased production of proinflammatory cytokines following infection with porcine reproductive and respiratory syndrome virus and Mycoplasma hyopneumoniae. Clin Diagn Lab Immun 11, 901-908

Tian K, Yu X, Zhao T, Feng Y, Cao Z, Wang C, Hu Y, Chen X, Hu D, Tian X, Liu D, Zhang S, Deng X, Ding Y, Yang L, Zhang Y, Xiao H, Qiao M, Wang B, Hou L, Wang X, Yang X, Kang L, Sun M, Jin P, Wang S, Kitamura Y, Yan J, Gao GF (2007): Emergence of fatal PRRSV variants: unparalleled outbreaks of atypical PRRS in China and molecular dissection of the unique hallmark. PLoS One 2, e526

Tijms MA, Nedialkova DD, Zevenhoven-Dobbe JC, Gorbalenya AE, Snijder EJ (2007): Arterivirus subgenomic mRNA synthesis and virion biogenesis depend on the multifunctional nsp1 autoprotease. J Virol 81, 10496-10505

Tizard IR (2013): Veterinary Immunology 9th edition, Saunders an imprint of Elsevier Inc. 1-164, 209-310

Trapnell C, Pachter L, Salzberg SL (2009): TopHat: discovering splice junctions with RNA-Seq. Bioinformatics 25, 1105-1111

Tsunetsugu-Yokota Y, Muhsen M (2013): Development of human dendritic cells and their role in HIV infection: antiviral immunity versus HIV transmission. Front Microbiol 4, 178

Uddin MJ, Cinar MU, Grosse-Brinkhaus C, Tesfaye D, Tholen E, Juengst H, Looft C, Wimmers K, Phatsara C, Schellander K (2011): Mapping quantitative trait loci for innate immune response in the pig. Int J Immunogenet 38, 121-131

Van Gorp H, Van Breedam W, Delputte PL, Nauwynck HJ (2008): Sialoadhesin and CD163 join forces during entry of the porcine reproductive and respiratory syndrome virus. J Gen Virol 89, 2943-2953

Vanderheijden N, Delputte PL, Favoreel HW, Vandekerckhove J, Van Damme J, van Woensel PA, Nauwynck HJ (2003): Involvement of sialoadhesin in entry of porcine reproductive and respiratory syndrome virus into porcine alveolar macrophages. J Virol 77, 8207-8215

Vincent AL, Thacker BJ, Halbur PG, Rothschild MF, Thacker EL (2005): In vitro susceptibility of macrophages to porcine reproductive and respiratory syndrome virus varies between genetically diverse lines of pigs. Viral Immunol 18, 506-512

Wang R, Nan Y, Yu Y, Yang Z, Zhang YJ (2013): Variable interference with interferon signal transduction by different strains of porcine reproductive and respiratory syndrome virus. Vet Microbiol 166, 493-503

Wang X, Eaton M, Mayer M, Li H, He D, Nelson E, Christopher-Hennings J (2007): Porcine reproductive and respiratory syndrome virus productively infects monocyte-derived dendritic cells and compromises their antigen-presenting ability. Arch Virol 152, 289-303

Weber M, Gawanbacht A, Habjan M, Rang A, Borner C, Schmidt AM, Veitinger S, Jacob R, Devignot S, Kochs G, Garcia-Sastre A, Weber F (2013): Incoming RNA virus nucleocapsids containing a 5'-triphosphorylated genome activate RIG-I and antiviral signaling. Cell Host Microbe 13, 336-346

Weesendorp E, Stockhofe-Zurwieden N, Popma-De Graaf DJ, Fijten H, Rebel JM (2013): Phenotypic modulation and cytokine profiles of antigen presenting cells by European subtype 1 and 3 porcine reproductive and respiratory syndrome virus strains in vitro and in vivo. Vet Microbiol 167, 638-650

Wensvoort G, Terpstra C, Pol JM, ter Laak EA, Bloemraad M, de Kluyver EP, Kragten C, van Buiten L, den Besten A, Wagenaar F, et al. (1991): Mystery swine disease in The Netherlands: the isolation of Lelystad virus. Vet Quart 13, 121-130

Wills RW, Zimmerman JJ, Yoon KJ, Swenson SL, Hoffman LJ, McGinley MJ, Hill HT, Platt KB (1997): Porcine reproductive and respiratory syndrome virus: routes of excretion. Vet Microbiol 57, 69-81

Wimmers K, Murani E, Schellander K, Ponsuksili S (2009): QTL for traits related to humoral immune response estimated from data of a porcine F2 resource population. Int J Immunogenet 36, 141-151

Wolf JB (2013): Principles of transcriptome analysis and gene expression quantification: an RNA-seq tutorial. Mol Ecol Resour 13, 559-572

Wu S, Wu H (2013): More powerful significant testing for time course gene expression data using functional principal component analysis approaches. BMC Bioinformatics 14, 6

Xiao S, Jia J, Mo D, Wang Q, Qin L, He Z, Zhao X, Huang Y, Li A, Yu J, Niu Y, Liu X, Chen Y (2010a): Understanding PRRSV infection in porcine lung based on genome-wide transcriptome response identified by deep sequencing. PLoS One 5, e11377

Xiao S, Mo D, Wang Q, Jia J, Qin L, Yu X, Niu Y, Zhao X, Liu X, Chen Y (2010b): Aberrant host immune response induced by highly virulent PRRSV identified by digital gene expression tag profiling. BMC Genomics 11, 544

Yamamoto M, Sato S, Hemmi H, Hoshino K, Kaisho T, Sanjo H, Takeuchi O, Sugiyama M, Okabe M, Takeda K, Akira S (2003): Role of adaptor TRIF in the MyD88-independent toll-like receptor signaling pathway. Science 301, 640-643

Zhang X, Wang C, Schook LB, Hawken RJ, Rutherford MS (2000): An RNA helicase, RHIV -1, induced by porcine reproductive and respiratory syndrome virus (PRRSV) is mapped on porcine chromosome 10q13. Microb Pathogenesis 28, 267-278

Zhao W, Pahar B, Borda JT, Alvarez X, Sestak K (2007): A decline in CCL3-5 chemokine gene expression during primary simian-human immunodeficiency virus infection. PLoS One 2, e726

Zhou A, Zhang S (2012): Regulation of cell signaling and porcine reproductive and respiratory syndrome virus. Cell Signal 24, 973-980

Zhou P, Zhai S, Zhou X, Lin P, Jiang T, Hu X, Jiang Y, Wu B, Zhang Q, Xu X, Li JP, Liu B (2011a): Molecular characterization of transcriptome-wide interactions between highly pathogenic porcine reproductive and respiratory syndrome virus and porcine alveolar macrophages in vivo. Int J Biol Sci 7, 947-959

Zhou Y, Zheng H, Gao F, Tian D, Yuan S (2011b): Mutational analysis of the SDD sequence motif of a PRRSV RNA-dependent RNA polymerase. Sci China Life Sci 54, 870-879

Zimmerman J, Benfield DA, Murtaugh MP, Osorio F, Stevenson GW, Torremorell M (2006): Porcine reproductive and respiratory syndrome virus (Porcine arterivirus). In: Straw BE, Zimmerman JJ, D'Allaire S, Taylor DJ, editors. Diseases of Swine 9th edition. Blackwell Publishing Company, Ames Iowa. 387-406

Zimmerman JJ, Benfield DA, Dee SA, Murtaugh MP, Stadejek T, Stevenson GW, Torremorell M (2012): Porcine reproductive and respiratory syndrome virus (Porcine arterivirus). In: Zimmerman JJ, Karriker LA, Ramirez A, Schwartz KJ, Stevenson GW, editors. Diseases of Swine 10th edition, John Wiley & Sons, Inc. 461-486

8 Appendix

Table A1: Abbreviations of gene transcripts and proteins

gene transcripts and proteins	
ACTB	Actin, beta
ADM	Adrenomedullin
APR-1	Apoptosis-related protein 1
ATP6V0C	ATPase, H+ transporting, lysosomal 16kDa, V0 subunit c
ATP6V0D1	ATPase, H+ transporting, lysosomal 38kDa, V0 subunit d1
ATP6V1F	ATPase, H+ transporting, lysosomal 14kDa, V1 subunit F
ATP6V1C1	ATPase, H+ transporting, lysosomal 42kDa, V1 subunit C1
ATP6V1E1	ATPase, H+ transporting, lysosomal 31kDa, V1 subunit E1
ATP6V1G1	ATPase, H+ transporting, lysosomal 13kDa, V1 subunit G1
ATP6V1B2	ATPase, H+ transporting, lysosomal 56/58kDa, V1 subunit B2
BFL-1	Bcl-2-related protein A1
CANX	Calnexin
CCL4	Chemokine (C-C motif) ligand 4
CCL8	Chemokine (C-C motif) ligand 8
CCL20	Chemokine (C-C motif) ligand 20
CCL23	Chemokine (C-C motif) ligand 23
CCL3L1	Chemokine (C-C motif) ligand 3-like 1
CD80	CD80 molecule
CD86	CD86 molecule
C-JUN	C-JUN protein
CTSL	Cathepsin L1

CXCL2	Chemokine (C-X-C motif) ligand 2
CXCL10	Chemokine (C-X-C motif) ligand 10
DDX58/RIG-I	DEAD (Asp-Glu-Ala-Asp) box polypeptide 58
EEA1	Early endosome antigen 1
FLT1	Fms-related tyrosine kinase 1 (vascular endothelial growth factor/vascular permeability factor receptor)
GAPDH	Glyceraldehyde-3-phosphate dehydrogenase
HPRT1	Hypoxanthine phosphoribosyltransferase 1
HSPG2	Heparan sulfate proteoglycan 2
IFNβ1	Interferon, beta 1, fibroblast
IFN-γ	Interferon, gamma
IL-1	Interleukin 1
IL-1α	Interleukin 1, alpha
IL-1β	Interleukin-1 beta
IL-4	Interleukin 4
IL-5	Interleukin 5
IL-6	Interleukin-6
IL-8/CXCL8	Interleukin 8
IL-10	Interleukin 10
IL-12	Interleukin 12
IL-12p40	Interleukin 12B (natural killer cell stimulatory factor 2, cytotoxic lymphocyte maturation factor 2, p40)
IL-13	Interleukin 13
IL-18	Interleukin 18
IRAK4	Interleukin-1 receptor-associated kinase 4
IRF3	Interferon regulatory factor 3
IRF7	Interferon regulatory factor 7
ITGB1	Integrin, beta 1 (fibronectin receptor, beta polypeptide, antigen CD29 includes MDF2, MSK12)
ITGA5	Integrin, alpha 5 (fibronectin receptor, alpha polypeptide)

ITGB2	Integrin, beta 2 (complement component 3 receptor 3 and 4 subunit)
JAK2	Janus kinase 2
LGP2	Laboratory of genetics and physiology-2
LOC733646	Lysosomal 9kDa H+ transporting ATPase V0 subunit e
LOC100153940	Thrombospondin-2-like
MAL	MyD88-adapter-like
MAVS/IPS-1	Mitochondrial antiviral signaling protein
MCL1	Myeloid cell leukemia sequence 1
MDA5	Melanoma differentiation factor-5
MyD88	Myeloid differentiation primary response gene (88)
NF-$_K$B	Nuclear factor-$_K$B
RAB5C	RAB5C, member RAS oncogene family
RELA	V-rel reticuloendotheliosis viral oncogene homolog A (avian)
RIG-I	Retinoic acid inducible gene I
SIGLEC-1/CD169	Sialoadhesin
SEC61B	Sec61 beta subunit
SEC61G	Sec61 gamma subunit
SEC61A1	Sec61 alpha 1 subunit (S. cerevisiae)
SLA-1/MHC I	MHC class I antigen 1
SLA-2	MHC class I antigen 2
SLA-5	MHC class I antigen 5
SLA-6	MHC class I antigen 6
SLA-7	MHC class I antigen 7
SLA-DMB	MHC class II, DM beta
SLA-DRA	SLA-DRA MHC class II DR-alpha
SLA-DRB1	MHC class II histocompatibility antigen SLA-DRB1
SLA-DQA1	MHC class II histocompatibility antigen SLA-DQA
SLA-DQB1	SLA-DQ beta1 domain

STAT1	signal transducer and activator of transcription 1, 91kDa
STAT3	Signal transducer and activator of transcription 3 (acute-phase response factor)
TCIRG1	T-cell, immune regulator 1, ATPase, H+ transporting, lysosomal V0 subunit A3
TFRC	Transferrin receptor (p90, CD71)
THBS1	Thrombospondin 1
TLR2	Toll-like receptor 2
TLR3	Toll-like receptor 3
TLR4	Toll-like receptor 4
TLR7	Toll-like receptor 7
TLR8	Toll-like receptor 8
TLR9	Toll-like receptor 9
TLR10	Toll-like receptor 10
TNF-α	Tumor necrosis factor
TRIF	TIR domain-containing adaptor inducing IFN-β
VEGFA	Vascular endothelial growth factor A
VEGFB	Vascular endothelial growth factor B

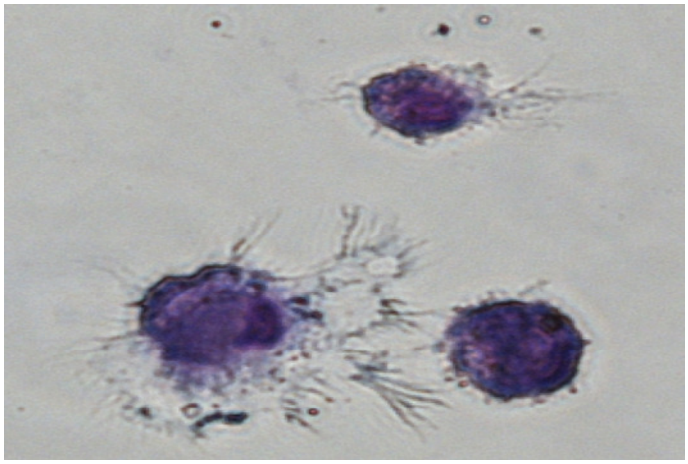

Figure A1: PAMs, after staining with REASTAIN® Quick-Diff Kit (Nikon, 40 x)

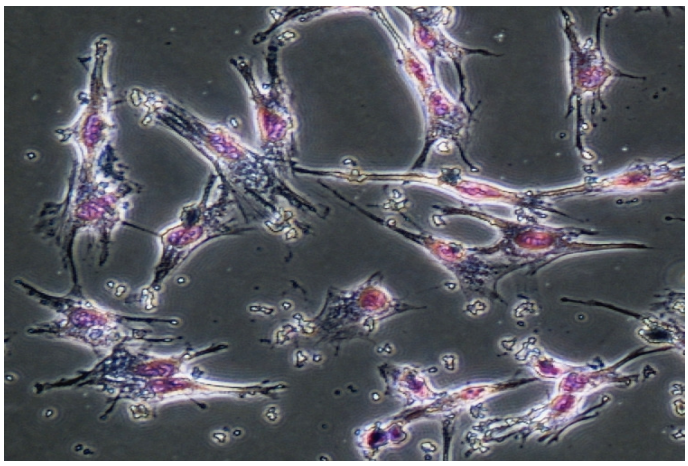

Figure A2: lung DCs, after staining with REASTAIN® Quick-Diff Kit (Nikon, 20 x)

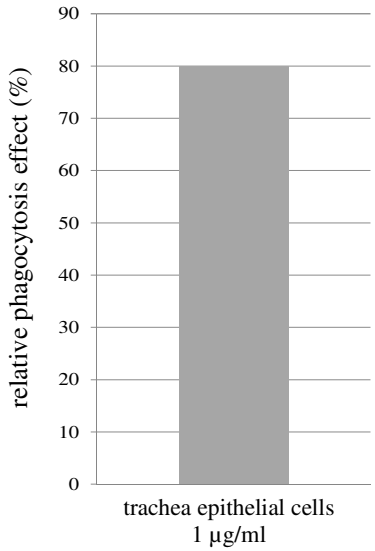

Figure A3: Relative phagocytosis effect (%) of LPS (dose: 1 µg/ml) infected trachea epithelial cells

Expression profiles of TNF-α and IL-12p40 (compare chapter 4.2)

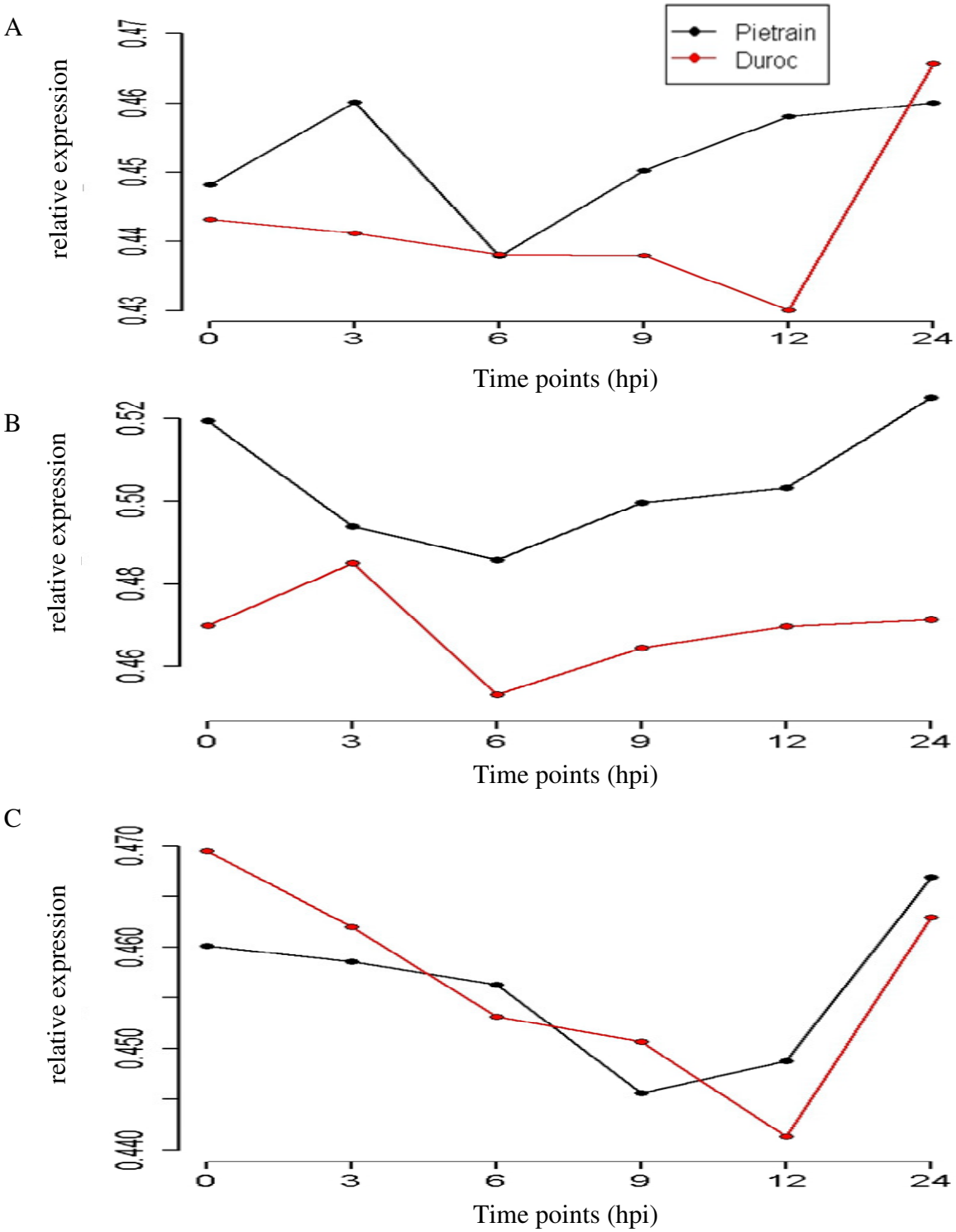

Figure A4: Gene expression levels of TNF-α in non-infected (0 h) and infected (3, 6, 9, 12, 24 hpi) lung DCs (A), PAMs (B) and trachea epithelial cells (C) of Pietrain and Duroc, detected by real-time PCR

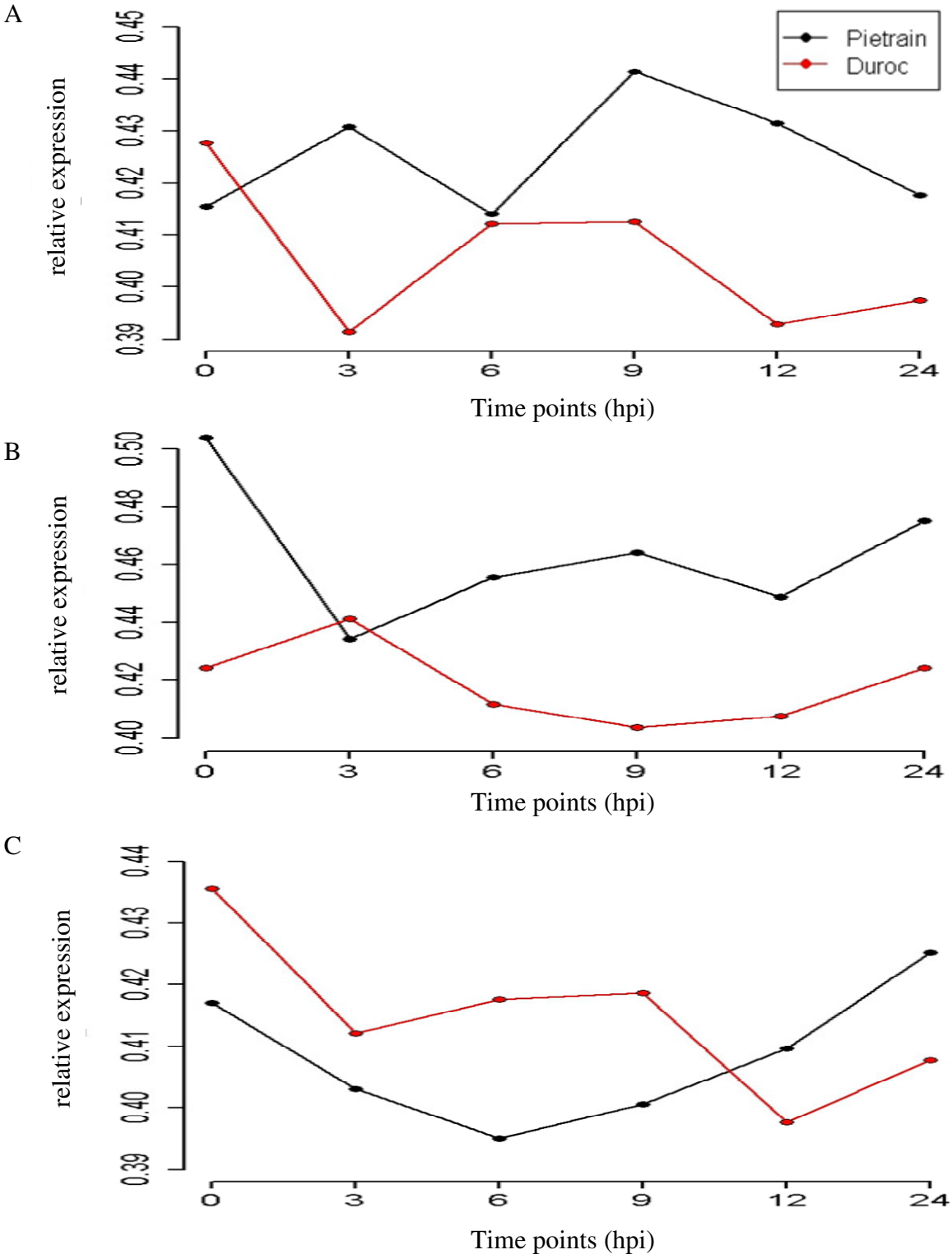

Figure A5: Gene expression levels of IL-12p40 in non-infected (0 h) and infected (3, 6, 9, 12, 24 hpi) lung DCs (A), PAMs (B) and trachea epithelial cells (C) of Pietrain and Duroc, detected by real-time PCR

Table A2: Read counts of Pietrain lung DCs before and after filtration as well as mapping statistics, detected by RNA-Seq

	0 h	3 hpi	6 hpi	9 hpi	12 hpi	24 hpi
Total number of reads before filtration	24,053,167	13,339,563	26,335,005	23,764,179	22,940,461	20,933,383
Read length (bp) before filtration	101	101	101	101	101	101
Total number of reads after filtration	23,717,404	12,971,915	25,801,906	23,369,340	22,279,166	20,391,529
Read length (bp) after filtration	50 - 86	50 - 86	50 - 86	50 - 86	50 - 86	50 - 86
Reads mapped	18,701,018 (78.9 %)	10,222,722 (78.8 %)	19,304,549 (74.8 %)	18,346,271 (78.5 %)	17,409,655 (78.2 %)	15,724,439 (77.1 %)
Reads unmapped	5,012,073 (21.1 %)	2,749,133 (21.2 %)	6,492,538 (25.2 %)	5,018,589 (21.5 %)	4,865,667 (21.8 %)	4,663,647 (22.9 %)

Table A3: Read counts of Duroc lung DCs before and after filtration as well as mapping statistics, detected by RNA-Seq

	0 h	3 hpi	6 hpi	9 hpi	12 hpi	24 hpi
Total number of reads before filtration	28,877,319	23,008,410	23,964,835	23,011,180	30,230,707	26,345,601
Read length (bp) before filtration	101	101	101	101	101	101
Total number of reads after filtration	28,466,825	22,700,565	23,461,003	22,558,620	29,565,956	25,336,902
Read length (bp) after filtration	50 - 86	50 - 86	50 - 86	50 - 86	50 - 86	50 - 86
Reads mapped	22,653,491 (79.6 %)	18,449,177 (81.3 %)	18,398,910 (78.4 %)	17,723,212 (78.6 %)	22,982,092 (77.8 %)	19,109,408 (75.4 %)
Reads unmapped	5,808,047 (20.4 %)	4,247,089 (18.7 %)	5,057,839 (21.6 %)	4,831,044 (21.4 %)	6,574,532 (22.2 %)	6,227,285 (24.6 %)

Table A4: Cluster description of Pietrain lung DCs after RNA-Seq

Breed	Cluster number	Total number of gene transcripts	Minimum read count	Maximum read count	Mean read count	Standard deviation
Pi	1	863	0	0.91537053	0.02828491	0.15840183
Pi	2	812	0	6.19251625	0.31579132	0.64907889
Pi	3	314	0	3.05572091	0.35407897	0.69482009
Pi	4	752	0	12.3850325	1.02253584	1.35811138
Pi	5	679	0	17.9350677	1.47784386	1.89031132
Pi	6	628	0	21.3900463	3.31068742	3.07105856
Pi	7	555	0	19.3528991	3.09081278	2.87941681
Pi	8	720	0	43.3476137	5.96615067	4.78686277
Pi	9	339	0	38.2864669	7.07647317	6.04036205
Pi	10	778	0	55.7979883	10.9386301	7.78226339
Pi	11	577	0	64.170139	17.0999682	10.4353287
Pi	12	587	0	90.4952853	21.4750095	13.7052117
Pi	13	559	0	108.988286	25.2037138	16.0470372
Pi	14	497	0	148.795133	40.3733222	22.8429996
Pi	15	616	0	168.06465	53.7707231	29.8622814
Pi	16	564	0	161.005422	58.3673345	28.4848062
Pi	17	367	1.23850325	222.930585	71.3898629	35.086972
Pi	18	583	0	372.789478	105.254502	52.0594309
Pi	19	266	1.23850325	275.004371	102.295483	48.7184557
Pi	20	642	1.23850325	363.630788	129.617898	57.4791541
Pi	21	738	1.9927853	506.547829	172.229673	72.2444302
Pi	22	308	0	547.322447	192.682155	96.7298299
Pi	23	635	11.9567118	546.974042	247.414722	92.54614
Pi	24	348	3.71550975	797.287732	279.655901	118.474172
Pi	25	438	7.4310195	912.776895	292.836537	120.830718
Pi	26	450	21.9688927	880.588738	355.601921	145.166052
Pi	27	417	26.0085682	1244.69577	414.45876	168.408515
Pi	28	701	13.6235357	1275.25419	484.91804	174.612957
Pi	29	628	7.4310195	1530.79002	610.824675	242.973891
Pi	30	663	15.6626455	1989.03622	736.230596	275.449502
Pi	31	722	0	3066.92522	991.301219	412.503863
Pi	32	449	1.23850325	3143.3824	1346.48074	542.181936
Pi	33	742	16.1005422	4374.39348	1421.19365	584.200883
Pi	34	853	49.54013	8678.19227	2965.72128	1304.47705
Pi	35	406	13.0522046	27639.932	7525.60929	4066.5676
Pi	36	177	1299.18991	97251.908	25397.2643	15962.6523
Pi	37	23	11950.1623	608534.856	141870.815	111783.284

Table A5: Cluster description of Duroc lung DCs after RNA-Seq

Breed	Cluster number	Total number of gene transcripts	Minimum read count	Maximum read count	Mean read count	Standard deviation
Du	1	1131	1.38998696	352.361693	113.775597	46.1731227
Du	2	374	2.99068026	352.361693	125.901716	55.6190106
Du	3	318	0	229.632261	81.2702057	40.2650816
Du	4	639	0.86004592	174.340634	62.5512027	27.6596326
Du	5	432	0	177.447028	60.1831765	25.0035072
Du	6	1085	0	156.150233	33.6210159	18.1617715
Du	7	581	0	90.468653	26.8797638	14.8469444
Du	8	1016	0	53.8144869	11.8261107	7.7277743
Du	9	900	0	52.3427567	11.7154964	7.31239897
Du	10	876	0	19.0337297	4.25407735	3.15275855
Du	11	1023	0	17.6440941	3.34197555	2.70980731
Du	12	845	0	10.5864564	1.17725216	1.32223405
Du	13	629	0	8.56517837	0.94570336	1.12811443
Du	14	577	0	1.90337297	0.27902183	0.50424272
Du	15	801	0	0.9423818	0.04673877	0.1909431
Du	16	510	0	4.41102352	0.35334174	0.64910825
Du	17	275	6.88036736	597.731915	179.831788	80.387099
Du	18	615	8.82204704	445.513375	198.104409	69.8456502
Du	19	765	4.3002296	679.297622	219.707788	92.5049197
Du	20	254	28.2305505	549.408591	247.862352	93.6124819
Du	21	713	44.7223879	699.217333	330.833759	103.033228
Du	22	602	21.501148	868.046853	378.209362	131.188954
Du	23	484	67.5697405	1276.55021	455.866559	173.43611
Du	24	317	0.86004592	1291.06307	481.307533	195.117839
Du	25	336	7.74041328	1472.00038	589.300823	265.713602
Du	26	698	52.9322822	1487.87944	677.23956	207.239894
Du	27	563	110.258671	2039.65728	791.41894	267.680744
Du	28	518	47.3025256	3027.72654	1238.17687	419.926149
Du	29	738	114.386107	2522.51469	1209.70575	392.703631
Du	30	353	20.6411021	4837.7583	1700.2442	768.083661
Du	31	406	44.7223879	4926.23107	2252.4431	693.549059
Du	32	558	8.97204076	9984.79284	3798.58711	1520.95237
Du	33	290	165.128817	25552.177	8846.09184	3705.83905
Du	34	141	1186.56533	67427.6002	22124.4407	10588.5271
Du	35	33	10964.0401	762300.734	110382.108	108376.963

Validation of RNA-Sequencing data of SLA-1, CD86 and IFNβ1

A

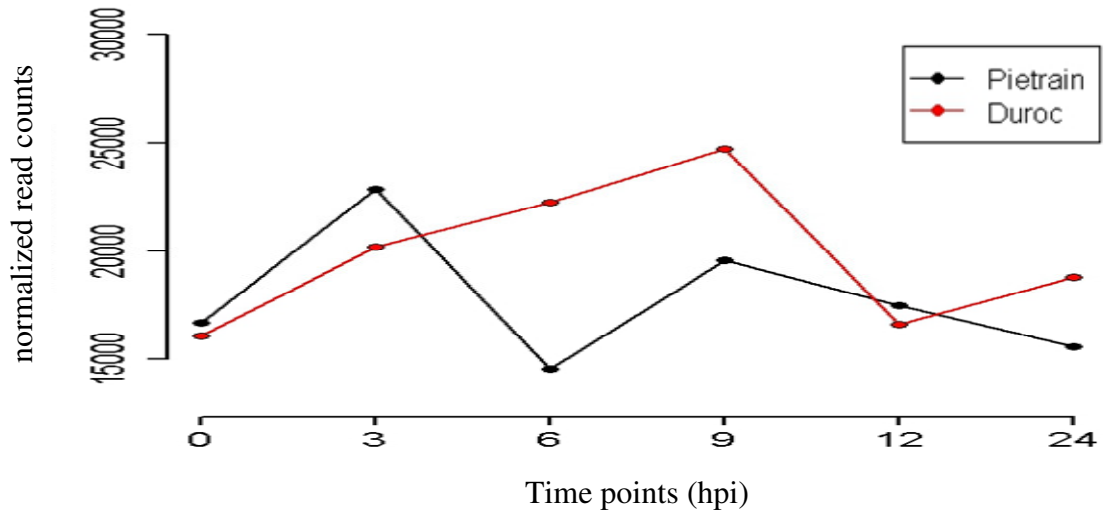

B

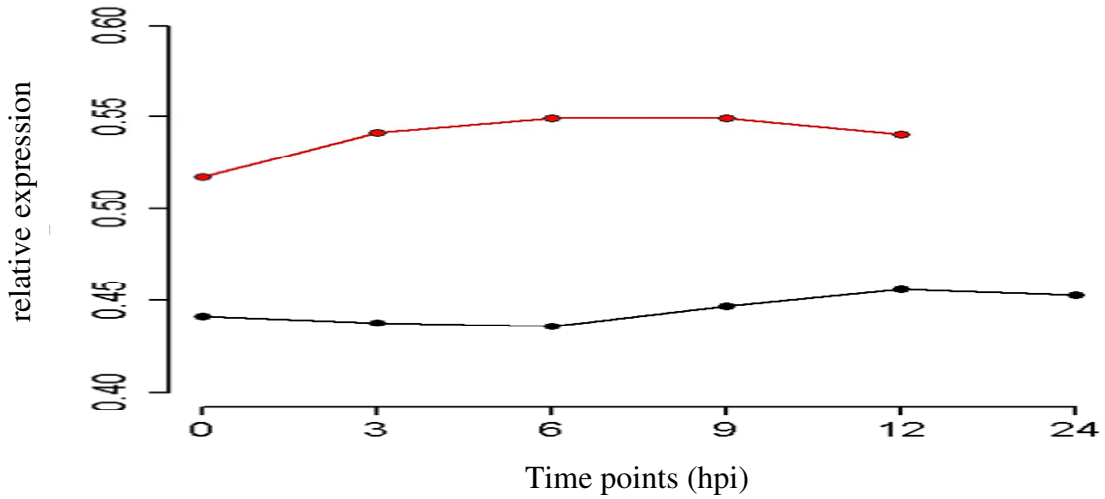

C

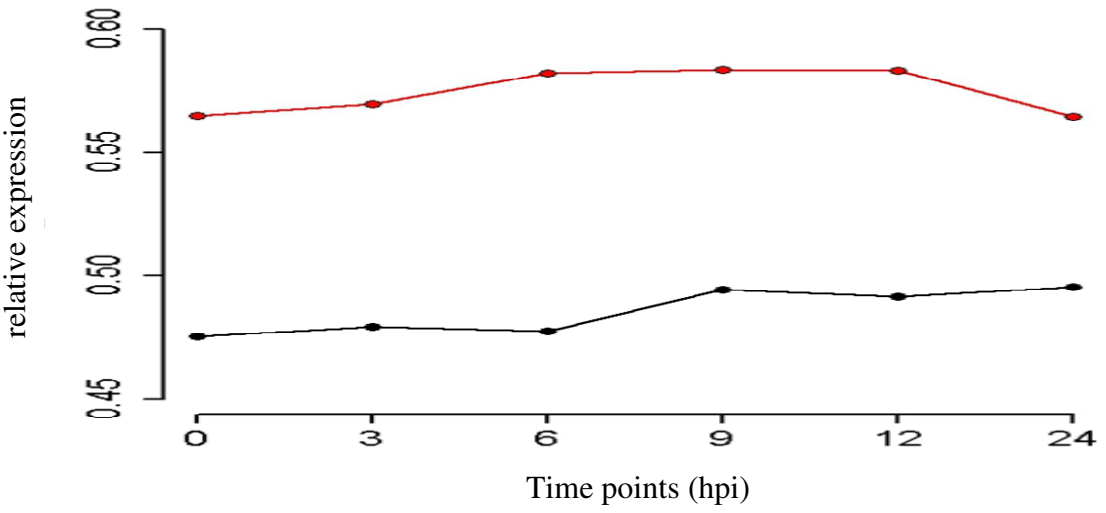

D

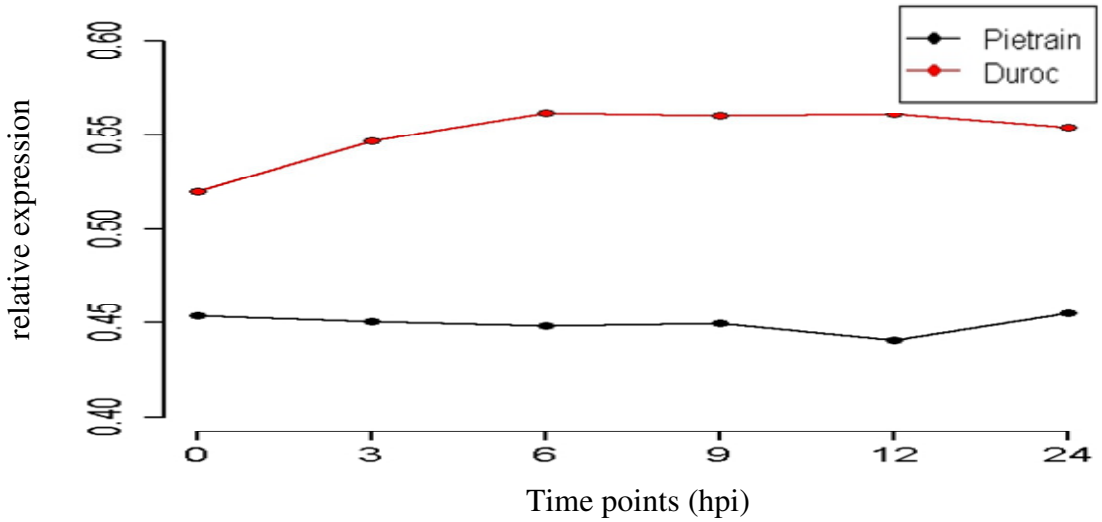

Figure A6: Gene expression profile of SLA-1 in infected and non-infected lung DCs, detected by RNA-Seq (A) and by real-time PCR (B), gene expression profile of SLA-1 in infected and non-infected PAMs, detected by real-time PCR (C) and gene expression profile of SLA-1 in infected and non-infected trachea epithelial cells, detected by real-time PCR (D) of Pietrain (black line) and of Duroc (red line). All measurements were done at 0 h and at 3, 6, 9, 12, 24 hpi

A

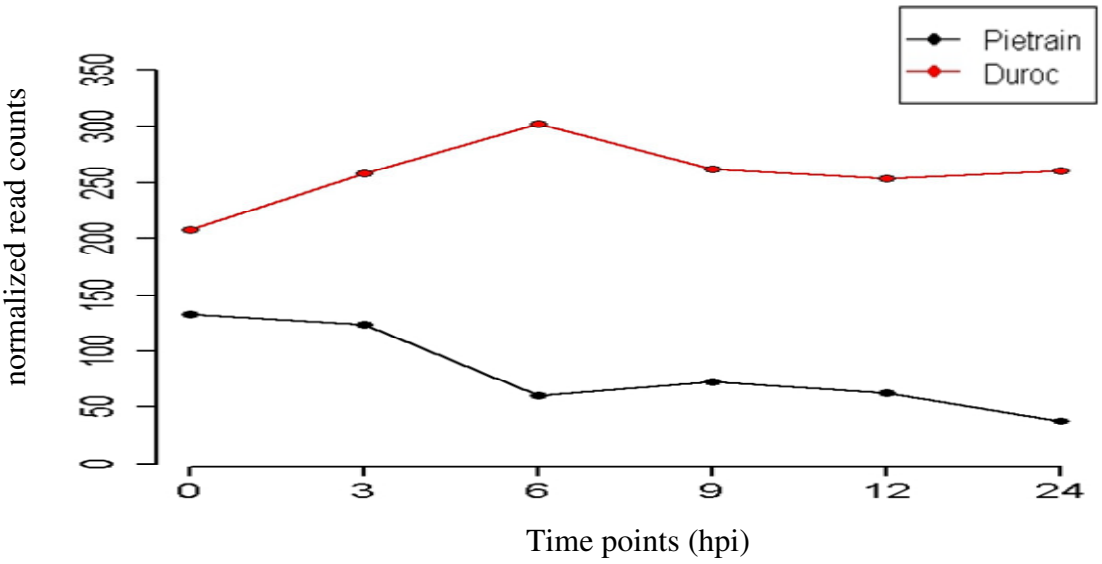

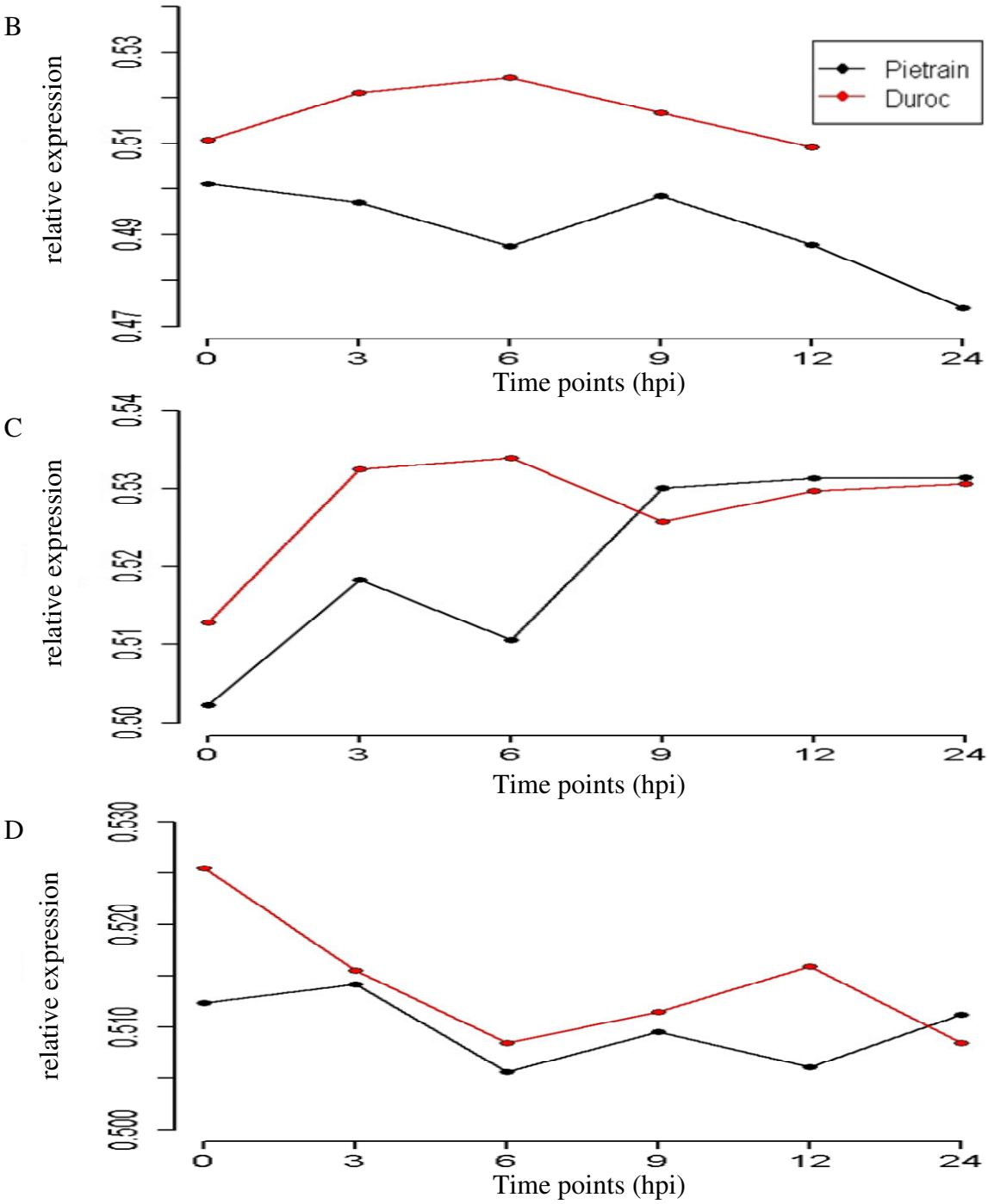

Figure A7: Gene expression profile of CD86 in infected and non-infected lung DCs, detected by RNA-Seq (A) and by real-time PCR (B), gene expression profile of CD86 in infected and non-infected PAMs, detected by real-time PCR (C) and gene expression profile of CD86 in infected and non-infected trachea epithelial cells, detected by real-time PCR (D) of Pietrain (black line) and of Duroc (red line). All measurements were done at 0 h and at 3, 6, 9, 12, 24 hpi

A

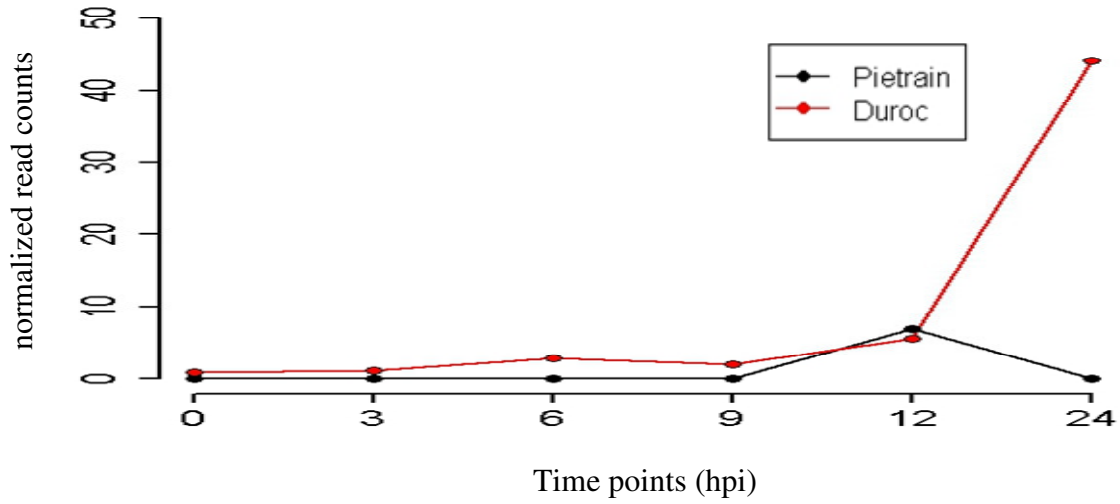

Time points (hpi)

B

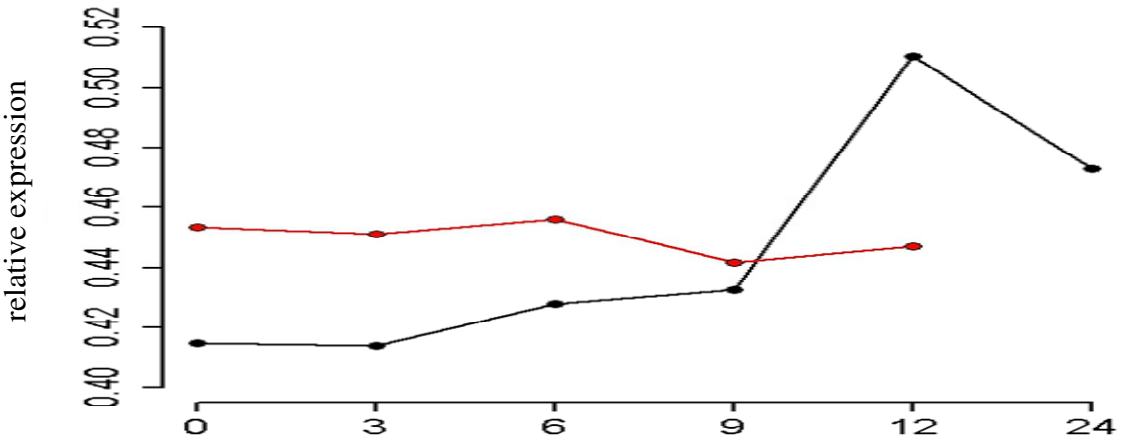

Time points (hpi)

C

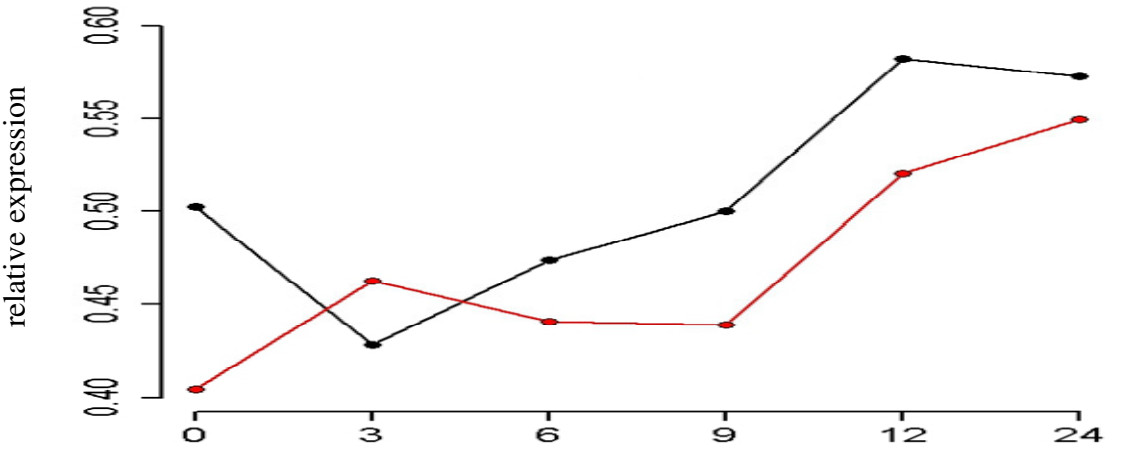

Time points (hpi)

D

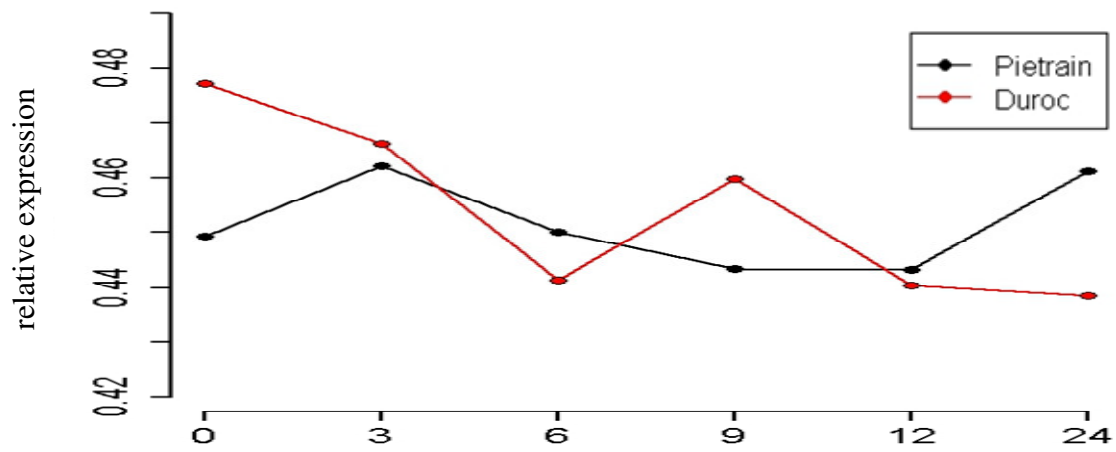

Time points (hpi)

Figure A8: Gene expression profile of IFN1ß in infected and non-infected lung DCs, detected by RNA-Seq (A) and by real-time PCR (B), gene expression profile of IFN1ß in infected and non-infected PAMs, detected by real-time PCR (C) and gene expression profile of IFN1ß in infected and non-infected trachea epithelial cells, detected by real-time PCR (D) of Pietrain (black line) and of Duroc (red line). All measurements were done at 0 h and 3, 6, 9, 12, 24 hpi

Thank you - Dankeschön!

Folgenden Personen, die mich während meiner Doktorarbeit begleitet und unterstützt haben, danke ich besonders:

Meinem Doktorvater, Herrn Prof. Dr. Karl Schellander, für die Überlassung des Themas und seinen fachlichen Rat; Herrn Prof. Dr. Heinz-Wilhelm Dehne für die Übernahme des Korreferates

Den ehemaligen und aktiven Mitarbeitern der *Abteilungen Tierzucht und Tierhaltung sowie Haustiergenetik des Instituts für Tierwissenschaften* der Rheinischen Friedrich-Wilhelms-Universität Bonn:

> Herrn Prof. Dr. Looft, Herrn PD Dr. Dawit Tesfaye, Herrn PD Dr. med. vet. Michael Hölker, Herrn Dr. Ulas Cinar, Herrn Dr. Jasim Uddin, Frau Dr. Christiane Neuhoff, Herrn Dr. Ernst Tholen, Frau Dr. Christine Große-Brinkhaus für die fachlichen Diskussionen und Ratschläge
>
> Frau Helga Brodeßer, Frau Nadine Leyer, Frau Bianca Peters, Frau Birgit Koch-Fabritius, Frau Stephanie Fuchs, Herrn Peter Müller, Herrn Stephan Knauf und den Azubis für die Hilfe im Labor und bei der Regelung von bürokratischen, organisatorischen, technischen und administrativen Angelegenheiten
>
> Frau Dr. Simret Weldenegodguad, Herrn Dr. Munir Hossain, Frau Dr. Hanna Heidt, Herrn Dr. Luc Frieden, Frau Sarah Bergfelder, Frau Xueqi Qu, Herrn Ahmed Amin und Herrn Ijaz Ahmad für ein gutes Arbeitsklima

Dem Leiter und den Mitarbeitern des *Instituts für Virologie* des Universitätsklinikums Bonn:

> Herrn Prof. Dr. Christian Drosten und Herrn Dr. Marcel A. Müller für die Ermöglichung der Durchführung der Versuche an Ihrem Institut
>
> Frau Dr. med. Isabella Eckerle und Herrn Stephan Kallies für die Einarbeitung in den virologischen Forschungsbereich und die Hilfe bei virologischen Fragestellungen

Meiner Familie und meinen Freunden für Ihre Kraft, Energie und Rückhalt.

Publications

Pröll M, Neuhoff C, Große-Brinkhaus C, Sahadevan S, Qu X, Cinar M U, Müller M A, Drosten C, Uddin M J, Tesfaye D, Tholen E, Looft C, Schellander K (2014): RNA-Seq analysis of respiratory cells infected with porcine reproductive and respiratory syndrome virus (PRRSV). Animal Immunogenetic and Molecular Immunology Workshop, 30./31.10.2014, Kayseri, Turkey, Proceedings (Abstr)

Yang Q, Neuhoff C, Zhang R, **Pröll M**, Große-Brinkhaus C, Uddin M J, Cinar M U, Fan H, Tesfaye D, Islam M A, Qu X, Tholen E, Hoelker M, Islam M A, Schellander K (2014): Sulforaphane inhibits CD14 gene expression in LPS stimulated alveolar macrophages of German Landrace pigs. DGfZ/GfT-Gemeinschaftstagung, 17./18.9.2014, Dummerstorf, Deutschland, Tagungsband: A21 (Proc)

Qu X, Cinar MU, Fan H, **Pröll M**, Tesfaye D, Tholen E, Looft C, Holker M, Schellander K, Uddin MJ (2014): Comparison of the innate immune responses of porcine monocyte-derived dendritic cells and splenic dendritic cells stimulated with LPS. Innate Immun

Hossain M, Tesfaye D, Salilew-Wondim D, Held E, **Pröll M**, Rings F, Kirfel G, Looft C, Tholen E, Uddin M J, Schellander K, Hoelker M (2014): Massive deregulation of miRNAs from nuclear reprogramming errors during trophoblast differentiation for placentogenesis in cloned pregnancy. BMC Genomics 15(1): 43

Pröll M, Große-Brinkhaus C, Sahadevan S, Qu X, Islam M A, Müller M A, Drosten C, Cinar M U, Uddin M J, Tesfaye D, Tholen E, Looft C, Schellander K (2013): RNA-Seq Analyse von porcinen dendritischen Zellen nach experimenteller Infektion mit PRRSV. DGfZ/GfT-Gemeinschaftstagung, 4./5.9.2013, Göttingen, Deutschland, Tagungsband: B1 (Proc)

Qu X, Cinar M U, Fan H, **Pröll M**, Tesfaye D, Tholen E, Looft C, Hoelker M, Schellander K, Uddin M J (2013): Comparison of the porcine monocytederived dendritic cells and spleenic dendritic cells immune responses to lipopolysaccharide stimulation. DGfZ/GfT-Gemeinschaftstagung, 4./5.9.2013, Göttingen, Deutschland, Tagungsband: C7 (Proc)

Islam MA, **Pröll M**, Hölker M, Tholen E, Tesfaye D, Looft C, Schellander K, Cinar MU (2013): Alveolar macrophage phagocytic activity is enhanced with LPS priming, and combined stimulation of LPS and lipoteichoic acid synergistically induce pro-inflammatory cytokines in pigs. Innate Immunity; (6):631-43

Cinar MU, Islam MA, **Pröll M**, Kocamis H, Tholen E, Tesfaye D, Looft C, Schellander K, Uddin MJ (2013): Evaluation of suitable reference genes for gene expression studies in porcine PBMCs in response to LPS and LTA. BMC Research Notes; 6:56

Neuhoff C, **Pröll M**, Grosse-Brinkhaus C, Frieden L, Becker A, Zimmer A, Tholen E, Looft C, Schellander K, Cinar MU (2012b): Global gene expression analysis of liver for androstenone and skatole production in the young boars using microarray. 63rd Annual Meeting of the European Federation of Animal Science (EAAP), 27.-31.8.2012, Bratislava, Slovakia. Abstract book (Abstr)

Neuhoff C, **Pröll M**, Grosse-Brinkhaus C, Heidt H, Tesfaye D, Tholen E, Looft C, Schellander K, Cinar MU (2012): Proteome analysis of skeletal muscle in high and low drip loss Duroc × Pietrain F2 pigs. 33rd Conference of the International Society for Animal Genetics (ISAG), 15.-20.7.2012, Cairns, Australia (Poster)

Neuhoff C, **Pröll M**, Grosse-Brinkhaus C, Frieden L, Becker A, Zimmer A, Cinar MU, Tholen E, Looft C, Schellander K (2011): Identifizierung von relevanten Genen des Metabolismus von Androstenon und Skatol in der Leber von Jungebern mit Hilfe von Transkriptionsanalysen. Vortragstagung der Deutschen Gesellschaft für Züchtungskunde e.V. (DGfZ) und der Gesellschaft für Tierzuchtwissenschaften e.V. (GfT), 6./7.9.2011, Freising-Weihenstephan, Deutschland, Tagungsband: D07 (Proc)

Hossain MM, Tesfaye D, **Pröll M**, Cinar MU, Rings F, Tholen E, Schellander K, Hoelker M (2010a): Massive deregulation of miRNAs from nuclear reprogramming errors affecting redifferentiation for placentogenesis in bovine SCNT pregnancy. 26th Scientific Meeting of the European Embryo Transfer Association (AETE), Proc, 10./11.9.2010, Kuopio, Finland (Abstr)

Hossain MM, Tesfaye D, **Pröll M**, Cinar MU, Rings F, Tholen E, Schellander K, Hoelker M (2010b): Massive deregulation of miRNAs in day-50 bovine placenta derived from SCNT pregnancy. Vortragstagung der Deutschen Gesellschaft für Züchtungskunde e.V. (DGfZ) und der Gesellschaft für Tierzuchtwissenschaften e.V. (GfT), Tagungsband, 15./16.9.2010, Kiel, Deutschland, C03 (Proc)

Pröll M, Tesfaye D, Hossain MM, Cinar MU, Hoelker M, Tholen E, Looft C, Schellander K (2010): Expressionsanalyse von miRNA-Prozessgenen in Rinderplazenten am Tag 50 der Trächtigkeit aus klonierten, künstlich besamten und in vitro erzeugten Embryonen. Vortragstagung der Deutschen Gesellschaft für Züchtungskunde e.V. (DGfZ) und der Gesellschaft für Tierzuchtwissenschaften e.V. (GfT), Tagungsband, 15./16.9.2010, Kiel, Deutschland, C04 (Proc)